



UNIVERSITY OF PRISTINA-KOSOVSKA MITROVICA
REPUBLIC OF SERBIA

THE
UNIVERSITY
THOUGHT
PUBLICATION IN NATURAL SCIENCES

VOL. 6, N° 2, 2016.

PUBLISHED BY UNIVERSITY OF PRISTINA-FACULTY OF SCIENCES
KOSOVSKA MITROVICA-REPUBLIC OF SERBIA

ISSN 1450-7226 (Print)

ISSN 2560-3094 (Online)

UNIVERSITY OF PRISTINA-KOSOVSKA MITROVICA, SERBIA
UNIVERSITY THOUGHT
PUBLICATION IN NATURAL SCIENCES

Aims and Scope

The University Thought - Publication in Natural Sciences (Univ. thought, Publ. nat. sci.) is a scientific journal founded in 1994. by the University of Priština, and was published semi annually until 1998.

Today, the University Thought - Publication in Natural Sciences is an international, peer reviewed, Open Access journal, published semi annually in the online and print version by the University of Priština, temporarily settled in Kosovska Mitrovica, Serbia. The Journal publishes articles on all aspects of research in Biology, Chemistry, Geography, Information technologies, Mathematics and Physics in the form of original papers, short communications and reviews (invited) by authors from the country and abroad.

The University Thought - Publication in Natural Sciences serves as an interdisciplinary forum covering a wide range of topics for a truly international audience. Journal is endeavor of the University of Priština to acquaint the scientific world with its achievements and wish to affirm the intellectual potential and natural resources of own region. Our aim is to put forward attitude of principle that science is universal and we invite all scientists to cooperate wherever their scope of research may be. We are convinced that shall contribute to do victory of science over barriers of all kinds erected throughout the Balkans.

Director

Srećko P. Milačić, PhD, Serbia

Editor in Chief

Nebojša V. Živić, PhD, Serbia

Deputy Editor in Chief

Vidoslav S. Dekić, PhD, Serbia

Associate Editors

Ljubiša Kočinac, PhD, Serbia, Ranko Simonović, PhD, Serbia, Stefan Panić, PhD, Serbia, Branko Drljača, PhD, Serbia, Aleksandar Valjarević, PhD, Serbia

Editorial Board

Gordan Karaman, PhD, Montenegro, Gerhard Tarmann, PhD, Austria, Predrag Jakšić, PhD, Serbia, Slavica Petović, PhD, Montenegro, Momir Paunović, PhD, Serbia, Bojan Mitić, PhD, Serbia, Stevo Najman, PhD, Serbia, Zorica Svirčev, PhD, Serbia, Ranko Simonović, PhD, Serbia, Miloš Đuran, PhD, Serbia, Radosav Palić, PhD, Serbia, Snežana Mitić, PhD, Serbia, Slobodan Marković, PhD, Serbia, Milivoj Gavrilov, PhD, Serbia, Jelena Golijanin, PhD, Bosnia and Herzegovina, Dragoljub Sekulović, PhD, Serbia, Dragica Živković, PhD, Serbia, Stefan Panić, PhD, Serbia, Petros Bithas, PhD, Greece, Zoran Hadzi-Velkov, PhD, The Former Yugoslav Republic Of, Ivo Kostić, PhD, Montenegro, Petar Spalević, PhD, Serbia, Marko Petković, PhD, Serbia, Gradimir Milovanovic, PhD, Serbia, Ljubiša Kočinac, PhD, Serbia, Ekrem Savas, PhD, Turkey, Zoran Ognjanović, PhD, Serbia, Donco Dimovski, PhD, The Former Yugoslav Republic Of, Nikita Šekutkovski, PhD, The Former Yugoslav Republic Of, Leonid Chubarov, PhD, Russian Federation, Žarko Pavićević, PhD, Montenegro, Miloš Arsenović, PhD, Serbia, Svetislav Savović, PhD, Serbia, Slavoljub Mijović, PhD, Montenegro, Saša Kočinac, PhD, Serbia

Technical Secretary

Danijel Došić, Serbia

Editorial Office

Ive Lola Ribara 29; 38220, Kosovska Mitrovica, Serbia, e-mail: editor.utnsjournal@pr.ac.rs, office.utnsjournal@pr.ac.rs, office.utnsjournal@gmail.com; fax: +381 28 425 397

Available Online

This journal is available online. Please visit <http://www.utnsjournal.pr.ac.rs> to search and download published articles.

CONTENTS

BIOLOGY

Predrag Jakšić

NEW CONTRIBUTIONS TO THE KNOWLEDGE OF LEPIDOPTERA FAUNA OF KOSOVO AND METOHIA (REPUBLIC OF SERBIA) 1

Predrag Vasić, Tatjana Jakšić, Nikola Đukić

THE EFFECT OF ALTITUDE ON THE PRESENCE OF PLANT SPECIES IN STANDS FOR JUNIPERUS L. PLANT SPECIES ON KOPAONIK 5

CHEMISTRY

Ružica Micić, Snežana Mitić, Ranko Simonović, Dragana Sejmanović

KINETIC DETERMINATION OF GOLD(III) BASED ON ITS INHIBITORY EFFECT IN OXIDIZING HOMOGENEOUS REACTION SYSTEM 11

GEOGRAPHY

Danijela Vukoičić, Milena Nikolić, Jelena Raičević

CONTEMPORARY DEMOGRAPHIC CHANGES IN SETTLEMENTS ALONG THE ADMINISTRATIVE LINE IN SERBIA TOWARDS AUTONOMOUS PROVINCE OF KOSOVO AND METOHIJA 17

INFORMATION TECHNOLOGIES

Marko Smilić, Stefan Panić, Milan Savić, Petar Spalević, Dejan Milić

HK DISTRIBUTION MODEL FOR ATMOSPHERIC TURBULENCE CHANNEL UNDER THE INFLUENCE OF POINTING ERRORS 27

Časlav Stefanović, Danijel Došić

THE LCR OF WIRELESS MACRODIVERSITY SSC RECEIVER IN THE PRESENCE OF GAMMA SHADOWED KAPPA-MU FADING 32

MATHEMATICS

Stojan Radenović, Sumit Chandok, Wasfi Shatanawi

SOME CYCLIC FIXED POINT RESULTS FOR CONTRACTIVE MAPPINGS 38

Jelena Vujaković, Miloje Rajović

THE NUMBER OF ZERO SOLUTIONS FOR COMPLEX CANONICAL DIFFERENTIAL EQUATION OF SECOND ORDER WITH CONSTANT COEFFICIENTS IN THE FIRST QUADRANT 41

Eugen Ljajko, Vladica Stojanović, Dragana Valjarević, Tanja Jovanović

CAN THE TRANSFORMATION OF INSTRUCTION PROCESS INTO A VIRTUAL PLACE INDUCE A SHIFT IN BEHAVIORAL PATTERNS OF TEACHERS AND STUDENTS? 47

PHYSICS

Tijana Kevkić, Vladica Stojanović, Dragan Petković

MODIFICATION OF TRANSITION'S FACTOR IN THE COMPACT SURFACE POTENTIAL- BASED MOSFET MODEL 55

Slavica Kuzmanović, Marija Stojanović Krasić, Ana Mančić, Branko Drljača and Milutin Stepić

THE INFLUENCE OF NONLINEAR AND LINEAR DEFECTS ON THE LIGHT PROPAGATION THROUGH LINEAR ONE-DIMENSIONAL PHOTONIC LATTICE..... 61

Branko Drljača, Slavica Jovanović, Svetislav Savović

CALCULATION OF THE FREQUENCY RESPONSE AND BANDWIDTH IN LOW NUMERICAL APERTURE STEP-INDEX PLASTIC OPTICAL FIBER USING TIME DEPENDENT POWER FLOW EQUATION 67

NEW CONTRIBUTIONS TO THE KNOWLEDGE OF LEPIDOPTERA FAUNA OF KOSOVO AND METOHIA (REPUBLIC OF SERBIA)

Predrag Jakšić^{1*}

¹Faculty of Sciences and Mathematics, University of Niš, Niš, Serbia.

ABSTRACT

Seven species of Lepidoptera - *Triodia sylvina* (Linnaeus, 1761), *Trichiura crataegi* (Linnaeus, 1758), *Eriogaster lanestris* (Linnaeus, 1758), *Endromis versicolora* (Linnaeus, 1758), *Caradrina clavipalpis* (Scopoli, 1763), *Polymixis rufocincta* (Gayer, 1828) and *Oria musculosa* (Hübner, 1808) were recorded for the first time in Kosovo and Metohia, Republic of Serbia. The next seven

species - *Trichiura crataegi* (Linnaeus, 1758), *Lycia graecarius* (Staudinger, 1861), *Biston strataria* (Hufnagel, 1767), *Agriopis aurantiaria* (Hübner, 1799), *Erannis defoliaria* (Clerck, 1759), *Parasemia plantaginis* (Linnaeus, 1758) and *Euplagia quadripunctaria* (Poda, 1761) were confirmed for the same area. Besides detailed faunistic data, illustrations of some adults are given.

Key words: Lepidoptera, Kosovo and Metohia.

1. INTRODUCTION

The initial papers on Lepidoptera for Kosovo and Metohia were published at beginning of the XX Century by Dr. Hans Rebel, one of the leading European lepidopterist from Nat. Hist. Museum in Wien. Rebel published four papers in the German language on the Lepidoptera of Metohia ((Rebel, 1910), (Rebel 1914), (Rebel 1917a) and (Rebel 1917b)).

Rebel for the first time describe a new taxa from Kosovo and Metohia: *Zygaena exulans apfelbecki* (Rebel, 1910) from Ljuboten, Šar-Planina Mt. In few last decades new contributions were given by Djordjije Djorović ((Djorović, 1974a; 1974b), (Djorović, 1975), (Djorović 1992) and Predrag Jakšić (Jakšić, 1987; 1999; 2003), (Jakšić & Ristić, 1999), (Jakšić & Dimović, 2000).

2. MATERIAL AND METHODS

Specimens were collected using butterfly net and Philips 250 W mercury light bulb trap. The positions and coordinates at which the Lepidoptera were caught were determined using Garmin e-Trex Vista Gps device (Table 1).

The photos of specimens were taken by Nikon Camera with AF-S Micro Nikkor Lens (Table 2). Genitalia from few moth specimens were dissected and microscope slides were used for reliable identification of a specific taxa.

((Fibiger et al., 1990–2010), (Fibiger & Lafontaine, 2005), (Forster & Wohlfahrt's, 1960–1981), as well as (Hausmann et al., 2001–2015) were used for species identification. The taxonomic order and nomenclature were done according to ((Karsholt & Razowski, 1996) and (Van Nieukerken et al., 2011) for high level taxa.

3. RESULTS AND DISCUSSION

Fam. Hepialide

63. *Triodia sylvina* (Linnaeus, 1761)

Material examined: Šar-Planina Mt, Stojkova kuća, 1750 m, 1.VIII 1973., 1♂, Jakšić P. leg.; Priština, Grmija Mt., 700 m., 30.VIII 1973., 2♂♂, 3♀♀, Jakšić P. leg.; 20.IX 1986., 1♀, Jakšić P. leg. This is a new distribution records in Kosovo and Metohia. Species is distributed in Serbia.

This larva feeds on various plants roots, including *Echium vulgare*, *Taraxacum*, *Pteridium* and *Rumex*. This species overwinters twice as a larva.

Fam. Lasiocampidae

6731. *Trichiura crataegi* (Linnaeus, 1758)









The literature data (Djorović, 1992): Mojstir, Crnoljevo.

Material examined: Novo Brdo, Bostane, 800 m, 20.IX 1984, 1♂, Jakšić P. leg. (Tab. 2:1).

Table 1. List of sampling sites.

SAMPLING SITES	ELEVATION (m)	UTM	COORDINATES	
			Latitude ϕ (N)	Longitude λ (E)
Novo Brdo, Bostane	850	EN31	42° 36' 00"	21° 25' 38"
Peć, Miliševac	500-600	DN32	42° 39' 40"	20° 15' 10"
Priština, Babin Most	580	EN03	42° 44' 47"	21° 04' 58"
Priština, Grmija Mt.	700	EN12	42° 40' 30"	21° 11' 54"
Priština, town	600	EN12	42° 39' 48"	21° 09' 28"
Šar-Planina Mt, Blateštičko Jezero	2200	EM07	42° 11' 28"	21° 04' 24"
Šar-Planina Mt, Dovedenica	1550	EM07	42° 10' 08"	20° 57' 49"
Šar-Planina Mt, Mekuš Bor	1700	DM96	42° 12' 23"	21° 04' 11"
Šar-Planina Mt, Rudoka	2400	DM73	41° 56' 35"	20° 47' 59"
Šar-Planina Mt., Stojkova Kuća	1750	EM07	42° 10' 51"	21° 02' 01"

Table 2. Examined species.

		
1. <i>Trichiura crataegi</i> (Linnaeus, 1758)	2. <i>Eriogaster lanestris</i> (Linnaeus, 1758)	3. <i>Endromis versicolora</i> (Linnaeus, 1758)
		
4. <i>Lycia graecarius</i> (Staudinger, 1861);	5. <i>Biston strataria</i> (Hufnagel, 1767)	6. <i>Erannis defoliaria</i> (Clerck, 1759)
		
7. <i>Euplagia quadripunctaria</i> (Poda, 1761)	8. <i>E. quadripunctaria</i> forma <i>lutescens</i> Staudinger, 1861	

Species is distributed in Serbia. The larval foodplants are *Betula verrucosa*, *Betula pubescens*, *Betula nana*, *Alnus incana*, *Salix* species, *Populus tremula*, *Sorbus aucuparia*, *Crataegus* species, *Prunus padus*, and *Vaccinium* species

6738. *Eriogaster lanestris* (Linnaeus, 1758)

Material examined: Priština, Grmija 700 m, 20.III 1980., 1♂, Jakšić P. leg. Tab. 2:2). This is a new faunistic record from Kosovo and Metohia. Species is distributed in Serbia. The larvae feed on *Prunus spinosa* and *Crataegus*. This plant species are present in the area (Krivošej, 2013).The pupae may stay unhatched for years.

6769. *Cosmotriche lobulina* ([Denis & Schiffermüller], 1775) [syn.: *lunigera* (Esper.), 1784]

Material examined: Priština, Grmija Mt., 700 m, 22.VI 1974., 1♂, Jakšić P. leg. This is a new faunistic record from Kosovo and Metohia. Species is distributed in Serbia. The caterpillars feed on different conifer species: *Abies*, *Pinus*, *Picea*.

Fam. Endromidae

6784. *Endromis versicolora* (Linnaeus, 1758)

Material examined: Novo Brdo, Bostane, 800 m, 6.IV 1982, 1♂, Jakšić P. leg. (Tab. 2:3). This is a new faunistic record from Kosovo and Metohia.

Species is distributed in Serbia.

The caterpillars food plants is *Betula*, as well as *Alnus*, *Corylus*, and *Tilia*.

Fam. Geometridae

7676. *Lycia graecarius* (Staudinger, 1861)

The literature data: (Jakšić & Ristić, 1999) are this species incorrectly listed under the name *Lycia zonaria* (Denis & Schiffermüller, 1775).

Material examined: Priština, Grmija, 700 m, 15.III 1979., 1♂, Jakšić P. leg. (Tab. 2:5).

Species is distributed in Serbia. This species is polyphagous on deciduous trees.

7685. *Biston strataria* (Hufnagel, 1767)

The literature data: (Djorović, 1992): Birač, Garačevo, Mojstir, Crnoljevo.

Material examined: Priština, Grmija, 700 m, 15.III 1979., 1♂, Jakšić P. leg. (Tab. 2:5). Species is distributed in Serbia. This species is polyphagous on deciduous trees.

7695. *Agriopis aurantiaria* (Hübner, 1799)

The literature data: (Djorović, 1992): Birač (Suva Reka), Garačevo, Mojstir.

Material examined: Priština, Grmija, 700 m, 15.X 1979., 1♂, Jakšić P. leg. Species is distributed in Serbia. Foodplant(s): Betalaceae and Rosaceae: polyphagous on deciduous trees.

7699. *Erannis defoliaria* (Clerck, 1759)

The literature data: (Djorović, 1992): Birač (Suva Reka), Garačevo, Mojstir, Crnoljevo.

Material examined: Novo Brdo, Bostane, 800 m, 27.XI 1982., 2♂♂, Jakšić P. leg. (Tab. 2:6). Species is distributed in Serbia. Caterpillars are recorded on more than 20 plant species.

8274. *Epirrhoe tristata* (Linnaeus, 1758)

Material examined: Šar-Planina Mt, Devedenica, 1300 m 21.VI 1995., 1♂, Jakšić P. leg ; Šar-Planina Mt., Blateštičko Jezero, 2200 m, 25.VI 1997., 6♂♂, Jakšić P. leg. This is a new distributional record in Kosovo and Metohia. Species is distributed in Serbia.

Larva monophagous on *Gallium* (Rubiaceae), (Janković, 1982) reported *Galium silvaticum*, *G. erectum* and *G. anisophyllum* on Šar-Planina Mt.

Fam. Noctuidae

9433. *Caradrina clavipalpis* (Scopoli, 1763)

Material examined: Priština, Grmija Mt., 700 m 1♂, 22.VIII 1973.: 1♂, 1.IX 1978 and Novo Brdo, Bostane, 800 m, 1♂, 8. VI 1982., Jakšić P. leg. Genitalia slides SR-1918, SR-1933 and SR-6209. Genitalia patern is identical to the one presented by (Rezbanyai-Reser, 1986). This is a new distributional records in Kosovo and Metohia. Species is distributed in Serbia. The larvae feed on *Plantago* and various grasses.

9726. *Polymixis rufocincta* (Geyer, 1828)

Material examined: Priština, Babin Most, 580 m, 4.VI 1982., Jakšić P. leg. 1 Novo Brdo, Bostane, 800 m, 17.X 1982., 1♂, Jakšić P. leg. This is the first faunistic records from Kosovo and Metohia. Species is distributed in Serbia

This species is polyphag on *Hieracium*, *Silene*, *Dianthus*, *Asplenium*, and *Lamium*.

9885. *Oria musculosa* (Hübner, 1808)

Material examined: Priština, 600 m, 30.VII 1991., 1♂, Jakšić P. leg. This is a new faunistic records from Kosovo and Metohia. Species is distributed in Serbia. The larvae feed internally in the stems of cereal crops (fam Poaceae).

Fam. Erebiidae: Arctiinae

10557. *Parasemia plantaginis* (Linnaeus, 1758)

The literature data: (Rebel, 1917a): Žljeb Mt., 1400-1700 m, f. *lutea* Tutt, *hospital* Schiff. and *bicolor* Rätz.

Material examined: Šar-Planina Mt., Rudoka, 2400 m, 27.VII 1995., 2♂♂, Jakšić P. leg.; Šar-Planina Mt., Mekuš Bor, 1700 m, 23.VI 1997., 1♂, Jakšić P. leg. Species is distributed in Serbia. The species is polyphagous, on herbaceous plants: *Rubus idaeus*, *Plantago*, *Leontodon* and *Hieracium*.

10605. *Euplagia quadripunctaria* (Poda, 1761)

The literature data: (Rebel, 1917a): Novo Selo; (Djorović, 1974); Birač (Suva Reka); Djorović, Miliševac, 600 m, 9.-10.VIII 1987., 1♂, the yellow wing form *lutescens* Staudinger, 1861. (Tab. 2:7 and 8). The caterpillars are polyphagous on *Lamium*, *Urtica*, *Glechoma*, *Rubus*, *Taraxacum*, *Plantago* and others.

(Liebert & Brakefield, 1990) pointed out that:... "the colour polymorphism in the warningly-coloured moth *Callimorpha quadripunctaria* (Lepidoptera: Arctidae) involves three major phenotypes with bright

red, orange and yellow hindwings. These are controlled by two unlinked gene loci, each with a pair of alleles exhibiting complete dominance. Once locus, when homozygous recessive, is epistatic to the other.”

4. CONCLUSION

Moths representatives of the following six families have been reported: Hepialidae, Lasiocampida, Endromidae, Geometridae, Noctuidae and Arctiidae. Obtained results of fourteen species contribute to the more complete faunistic knowledge of the distribution of Lepidoptera species in Kosovo and Metohia and Serbia generally

REFERENCES

- Djorović, Dj. 1974. Neke važnije vrste defolijatora hrasta iz familije Tortricidae. Šumarski pregled, Skoplje, 5-6, pp. 35-43.
- Djorović, Dj. 1974. Prilog poznavanju nekih vrsta defolijatora hrasta iz familije Arctiidae na Kosovu. Šumarstvo, Beograd, 10-12, pp. 19-23.
- Djorović, Dj. 1975. Prilog poznavanju moljaca u hrastovim šumama na Kosovu. Zaštita bilja, 26(133), pp. 229-233.
- Djorović, Dj. 1992. Biocenotički kompleks gusenica hrasta. Priština: Udruženje "Nauka i društvo" AP Kosova i Metohije., pp. 1-191.
- Forster, W., & Wohlfahrt, T. 1960. Die Schmetterlinge Mitteleuropas. Stuttgart: Franckh'sche Verlagshandlung. 1960-1981.
- Jakšić, P. 1987. Specifični elementi faune Lepidoptera nekih kosovskih klisura. Priroda Kosova, Priština, 6, pp. 93-107.
- Jakšić, P. 1999. Distribution of butterfly communities (Lepidoptera: Hesperioidea and Papilionoidea) in plant communities over the Jažinačko jezero lake region on Šar-planina Mt. / Distribucija zajednica dnevnih leptira (Lepidoptera: Hesperioidea & Papilionoidea) u biljnim zajednicama na širem području Jažinačkih jezera na Šar-planini. The University Thought, Nat. Sci., Priština, 5(2), pp. 71-75.
- Jakšić, P., & Dimović, D. 2000. Pregled utvrđenih vrsta rodova Eilema Hübner, (1804) i Lithosia Fabricius, 1798 Bora i susednih područja (Lepidoptera: Arctiidae, Lithosiinae) / The Review of the examined species of genera Eilema Hübner, 1819 and Lithosia Fabricius, 1798 in Bor town and surrounding area (Lepidoptera: Arctiidae, Lithosiinae). Zaštita prirode, Beograd, 52(1), pp. 47-63.
- Jakšić, P. 2016. Tentative Check List of Serbian Microlepidoptera. Ecologica Montenegrina, Podgorica, 7, pp. 33-258.
- Jakšić, P., & Ristić, G. 1999. New and rare species of Lepidoptera in Yugoslavia. Acta entomologica serbica, Beograd, 4(1/2), pp. 63-74. 2001.
- Janković, M.M. 1982. Prilog poznavanju vegetacije Šarplanine sa posebnim osvrtom na neke značajne reliktnne vrste biljaka / Contribution to the study of the vegetations of the Šarplanina Mountain with particular reference to some conspicuous relict plant species. Glasnik Instituta za botaniku i Botaničke bašte Univerziteta u Beogradu, 15(1-3), pp. 75-129. (XIII).
- Karsholt, O., & Razowski, J. 1996. The Lepidoptera of Europe. A Distributional Checklist. Stenstrup: Apollo Books.
- Krivošej, Z. 2013. Flora planine Grmija kod Prištine. Univerzitet u Prištini.
- Liebert, T.G., & Brakefield, P.M. 1990. The genetics of colour polymorphism in the aposematic Jersey Tiger Moth Callimorpha quadripunctaria. Heredity, 64(1), pp. 87-92. doi:10.1038/hdy.1990.11
- Rebel, H. 1910. Bericht der Sektion für Lepidopterologie. II. Derselbe gibt die Beschreibung zweier neuer Lepidopterenformen aus Albanien bekannt. Verhandlungen der zoologisch-botanischen Gesellschaft in Wien, 60(4-6). fig 1.
- Rebel, H. 1914. Lepidopteren aus dem Nordalbanisch-Montenegrinischen Granzgebiete. Sitzungsberichte der Kaiserlichen Akademie der Wissenschaften in Wien, 23(1), pp. 1111-1128.
- Rebel, H. 1917. Lepidopteren aus Neumontenegro. Sitzungsberichte, Abteilung 1, Kaiserliche Akademie der Wissenschaften in Wien. Mathematisch-naturwissenschaftliche Klasse, 126, pp. 765-813.
- Rebel, H. 1917. Neue Lepidopterenfunde in Nordalbanien, Mazedonien und Serbien. Jahresbericht des Naturwissenschaftlichen Orientvereins, 21, pp. 17-24.
- Rezbanyai-Reser, L. 1986. Caradrina ingrate Staudinger, 1897, eine schwer erkennbare neue Wanderfalterart in Mitteleuropa. Atalanta, 17(1-4), pp. 151-156.

* E-mail: jaksicpredrag@gmail.com

THE EFFECT OF ALTITUDE ON THE PRESENCE OF PLANT SPECIES IN STANDS FOR JUNIPERUS L. PLANT SPECIES ON KOPAONIK

Predrag Vasić^{1*}, Tatjana Jaksić¹, Nikola Đukić¹

¹Faculty of Natural Sciences and Mathematics, University of Piština, Kosovska Mitrovica, Serbia.

ABSTRACT

In this paper we present an assessment of the altitude effect on the plant species presence in different plant communities – the species of *Juniperus* genus (*Juniperus communis* L., *Juniperus oxycedrus* L. and *Juniperus sibirica* Burgsdorf) on Kopaonik Mountain. Two juniper species (*Juniperus communis* and *Juniperus oxycedrus*) were recorded at altitudes ranging from 420 m to 1420 m, while the third species *Juniperus sibirica* was found at an altitude of 2100 m. It was

determined that the plant communities with the presence of species of the *Juniperus* genus differ in botanical terms at different altitudes. It was found that there are plant species in certain communities that are present only at some altitudes, while others were present at almost all altitudes. The species of *Hypericum perforatum* L. is recorded in all of plant communities surveyed that proves its best adaptation to the conditions at different altitudes.

Keywords: Kopaonik Mountain, altitude, botanical composition, plant communities, *Juniperus* L., *Hypericum perforatum* L.

1. INTRODUCTION

Mountain regions are ideal for describing and studying the environmental responses of plant communities (Naqinezhad et al., 2009).

Kopaonik Mountain is located in the central part of the Balkan Peninsula and extends from northwest to southeast (NW-SE), between 20° 35' and 21° 18' of east longitude and 42° 43' and 43° 23' of north latitude. On the western side, Kopaonik massif is separated from geologically similar Rogozna and Golija with the valleys of the Ibar and Sitnica rivers. From the north, Kopaonik is separated with the valley of Jošanica River from the identical geological massif of Željina Mountain, and the whole area (Kopaonik-Željin) is bounded with the depression of the Morava River basin. From the South and Southwest the Lab River separates Kopaonik from Kosovo depression basin. The upper parts of the Rasina and Toplica rivers can be geographically regarded as the eastern border of Kopaonik massif (Gavrilović, 1979).

In terms of structure and morphology, the largest part of Kopaonik, especially its western part belongs to the so-called zone of internal Dinarides that was formed during the Alpine orogeny. The eastern parts of the Kopaonik massif are integral parts of the Serbian-Macedonian mass, and their basic geomorphological characteristics originated from

hercin orogenesis, which means that they were morphologically shaped before the western part (Vasović, 1988).

Kopaonik mountain is extremely complex in geological terms. It is composed of three basic types of rocks: sediments, igneous and metamorphic rocks.

Kopaonik is characterized by multiple types of soil resulting by interaction of the relief, climate and vegetation over a longer period of time.

At lower altitudes, up to 1000 m, siorezem, organogenic and siliceous soil, as well as Hum siliceous soil dominate. Siorezems are extremely shallow soil up to 20 inches deep. It can be found on steep slopes of sparse forests or poor pastures. Humus siliceous soil is a special type of fertile soil and it is formed at neutral, basic and acidic siliceous rocks. This type of soil is of relatively low productivity. Forests and pastures develop on it.

Brown and sour brown soils are dominant at altitudes above 1000 m. They are formed on acid silicate rocks, slightly inclined slopes and plateaus. Acid brown soil can be relatively deep, while on the prominent ridges and slopes it can be more shallow and prone to erosion. Kopaonik land is suitable for forests and pastures development.

Kopaonik has great elevation gradient, starting from the base, to its highest peaks. It can be divided into six high altitude climatic zones:

1. The first zone is dominated by thermophilic oak forests of *Quercum frainetto* species. This is the zone with dry, warm and mountain climate of sub-Mediterranean character. It stretches from the foothills up to 750m on the northern, and up to 1050 m on the southern exposures. The average temperature of this zone is about 11°C, and the average annual precipitation is about 787mm of rainfall.
2. The second zone is a zone of gradual transformation into mountain climate. The presence of sessile oak forests, ie. vegetation type *Quercum petrae-cerris* is characteristic. It is located at an altitude of 1050 -1150 m in the southern and 750-1000 m in the northern exposures. The average annual temperature of this zone is about 7.2 °C, and the average annual precipitation is about 800 mm of rainfall.
3. The third zone is a zone of lower and middle temperate mountain climate. Vegetation is represented by beech and beech-fir forests of *Fagion moesiaca* type. The zone extends at an altitude of 1150-1550 m, on the southern and 1000-1500 m on the northern exposures. The average annual temperature of this zone is about 5°C, the mean annual precipitation is about 827 mm of rainfall.
4. The fourth zone represents the area where the mountain climate is sharper and vegetation is dominated by pure spruce forests from *Vaccinio-Piceion* type. It stretches between 1550 and 1750 m above sea level on the southern and 1500 and 1700 m on the northern exposure.
The annual average temperature is around 4°C and the average annual precipitation is about 857 mm of rainfall.
5. The fifth zone is in the zone of harsh subalpine climate. The vegetation type is made of communities of subalpine bushes of *Juniperion Vaccinion myrtilli*. They are located in the area between 1750-1950 m on the southern and 1700-1950 m on the northern exposures. The temperature of this

zone on average is 3°C, and the annual precipitation is 870 mm.

6. The sixth zone is a zone that is covered by pre alpine harsh climate. The vegetation of this pre alpine climate consists of the high mountain pastures and mountain pastures, from *Poion violaceae* type. They are located in the zone above 1950 m above the sea level. Annual temperatures prevailing in these areas rarely rise above 2°C, while the average amount of annual precipitation is about 883 mm of rainfall.

2. THEORETICAL PART

Vegetation distribution in mountain landscapes is characterized by spatially heterogeneous environmental conditions concerning climate, soil and geology as well as frequency and intensity of disturbance (Karkaj et al., 2012).

One important factor is altitude which has a strong influence on the vegetation structure. Impact of altitude to floristic composition have been considered as the subject of numerous studies ((Lomolino, 2001), (Naqinezhad et al., 2009), (Karkaj et al., 2012)). Altitudinal gradients are regarded as the most powerful ecological element which affects the natural vegetation structure.

Altitude presents an important orographic factor that affects the modification of various climates and soils, (Vasić et al., 2008) and therefore the species richness and the vegetation structure.

Temperature and relative humidity are the most important factors that determine the extent to which plants are present.

With increasing altitude the air becomes less thin and fresh, reflecting the solar radiation and temperature regime habitats. Proper temperature drops (for every 100 m above sea level, the temperature drops to 0,58°C) (Vasić et al., 2008).

With altitude increase the air becomes less thin and fresher, reflecting the solar radiation and temperature regime of a habitat. The temperature drops (for every 100 m above the sea level, the temperature drops to 0,58°C) (Vasić et al., 2008).

With the sea level increase, the relative humidity also rises due to the ascending air currents that send water vapor high into the air (Vasić, 2012).

Plants that inhabit different altitudes are extremely efficient and cost-effectively customized to survive in a changing climate.

3. EXPERIMENTAL PART

3.1. Material and methods

The research in this paper was done in the period from 2015 to 2016. The list of flora is made up of the species given in an alphabetical order. The species presented in this paper include the plant communities in which species of *Juniperus* genus (*Juniperus communis*, *J. and J. oxycedrus sibirica*) were recorded at different altitudes (470 m, 630 m, 830 m, 1030 m, 1230 m, 1430 m, and 2100 m).

The plant material was determined using a Serbian flora key (Josifović, 1970-1986), and a nomenclature of plant species is customized to a flora of Europe

(Tutin, 1964-1980, 1993) and IOPI databases (International Organisation for Plant Information).

3.1.1. Synthesis

The subject of study in this paper is the presence of plants at different altitudes in the plant communities with the appearance of the genus *Juniperus* species (*J. communis*, *J. oxycedrus* and *J. sibirica*). Two species of juniper (*Juniperus communis* and *Juniperus oxycedrus*) were found at altitudes from 420 m to 1420 m, while the third species, *Juniperus sibirica*, was found at an altitude of 2100 m. It should be noted that the species *Juniperus communis* and *Juniperus oxycedrus* could be found together up to 1420 m above sea level, but as the altitude increased these two species were less present because of the increasing negative anthropogenic impact on them (logging and deforestation).

Table 1. The presence of plant species in the plant communities with a dominance of species of the *Juniperus* genus.

	470m	630m	830m	1030m	1230m	1430m	2100m
<i>Achillea millefolium</i> L.	+	-	+	+	+	+	-
<i>Acinos alpinus</i> (L.) Moench	-	-	+	-	-	-	-
<i>Agrimonia eupatoria</i> Ledeb.	-	+	-	-	-	-	-
<i>Agrostis stolonifera</i> L.	-	-	-	-	-	+	+
<i>Anagallis foemina</i> Miller	-	-	+	-	-	-	-
<i>Artemisia vulgaris</i> L.	-	+	-	-	-	-	-
<i>Asperula cynanchica</i> L.	+	-	+	-	-	-	-
<i>Astragalus onobrychis</i> L.	-	-	+	-	-	-	-
<i>Bupleurum veronense</i> Turra	+	-	-	-	-	-	-
<i>Calamintha vulgaris</i> (L.) Druce	-	+	-	-	-	-	-
<i>Campanula patula</i> L.	-	-	-	-	-	+	-
<i>Carduus acanthoides</i> L.	-	+	-	-	-	-	-
<i>Carlina vulgaris</i> L.	-	-	-	+	-	+	-
<i>Centaurea jacea</i> L.	-	-	-	-	+	-	-
<i>Centaurea scabiosa</i> L.	-	+	-	-	-	-	-
<i>Centaurea alba</i> L. subsp. <i>splendens</i> (L.) Arcangeli	-	-	+	-	-	-	-
<i>Centaurea biebersteinii</i> DC.	+	+	-	+	-	-	-
<i>Centaureum erythraea</i> Rafin.	-	-	-	+	-	-	-
<i>Cerastium caespitosum</i> Gilib.	-	-	-	-	-	-	+
<i>Chamaespartium sagittale</i> (L.) P. Gibbs	-	-	-	-	+	-	-
<i>Cirsium eriophorum</i> (L.) Scop.	-	+	-	+	+	+	+
<i>Cornus mas</i> L.	-	+	-	-	-	-	-
<i>Coronilla varia</i> L.	+	+	-	-	-	-	-
<i>Crataegus monogyna</i> Jacq.	+	-	-	-	-	-	-
<i>Cuscuta</i> sp.	-	+	-	-	-	-	-

	470m	630m	830m	1030m	1230m	1430m	2100m
<i>Cytisus jankae</i> Velen.	-	-	+	-	-	-	-
<i>Dactylis glomerata</i> L.	-	-	-	-	-	-	+
<i>Daucus carota</i> L.	-	+	-	-	-	-	-
<i>Dianthus cruentus</i> Griseb.	-	-	+	-	-	-	-
<i>Digitalis laevigata</i> Waldst. & Kit.	-	+	-	-	-	-	-
<i>Dorycnium herbaceum</i> Vill.	-	+	-	+	-	-	-
<i>Eryngium campestre</i> L.	+	+	-	-	+	-	-
<i>Euphorbia amygdaloides</i> L.	-	-	-	+	-	-	-
<i>Euphorbia cyparissias</i> L.	+	-	-	-	+	-	-
<i>Euphrasia stricta</i> D. Wolff ex J. F. Lehm.	-	-	-	+	-	-	-
<i>Fagus moesiaca</i> (K.Maly) Czech.	-	-	-	-	-	+	-
<i>Fragaria vesca</i> L.	+	+	-	-	+	+	+
<i>Galium verum</i> L.	-	-	-	+	+	-	-
<i>Gentianella austriaca</i> (A. & J. Kerner) J. Holub	-	-	-	-	-	-	+
<i>Genista januensis</i> Viv.	-	-	-	-	-	+	+
<i>Geranium columbinum</i> L.	-	-	+	-	-	-	-
<i>Gnaphalium sylvaticum</i> L.	-	-	-	-	-	+	-
<i>Helianthemum nummularium</i> (L.) Miller	-	+	-	+	+	-	-
<i>Helleborus odorus</i> Waldst. & Kit.	-	+	-	+	-	+	-
<i>Hieracium hoppeanum</i> Schult.	-	-	-	+	+	+	-
<i>Hieracium pilosella</i> L.	+	-	+	-	-	-	-
<i>Hypericum perforatum</i> L.	+	+	+	+	+	+	+
<i>Juniperus communis</i> L.	+	+	+	+	+	+	-
<i>Juniperus oxycedrus</i> L.	+	+	+	+	+	+	-
<i>Juniperus sibirica</i> Burgsdorf.	-	-	-	-	-	-	+
<i>Lathyrus</i> sp.	-	+	-	-	-	-	-
<i>Leontodon hispidus</i> L.	-	-	+	+	+	+	-
<i>Linaria vulgaris</i> Miller	-	+	-	-	-	-	-
<i>Linum catharticum</i> L.	-	-	-	-	+	-	-
<i>Linum hologynum</i> Rchb.	-	-	-	-	+	-	-
<i>Lotus corniculatus</i> L.	-	+	-	-	-	+	-
<i>Luzula luzuloides</i> (Lam.) Dandy & Wilmott	-	-	-	-	-	+	-
<i>Medicago prostrata</i> Jacq.	-	-	+	-	-	-	-
<i>Nardus stricta</i> L.	-	-	-	-	-	+	-
<i>Onobrychis viciifolia</i> Scop.	+	-	-	-	-	-	-
<i>Ononis spinosa</i> L.	+	+	-	-	+	-	-
<i>Petrorhagia prolifera</i> (L.) P. W. Ball & Heywood	-	+	-	-	-	-	-
<i>Petrorhagia saxifraga</i> (L.) Link	+	-	+	+	-	-	-
<i>Phleum phleoides</i> (L.) Karsten	-	-	-	-	+	-	-
<i>Picris hieracioides</i> L.	+	+	-	-	-	-	-
<i>Pimpinella saxifraga</i> L.	-	-	-	-	+	-	-
<i>Plantago lanceolata</i> L.	+	-	-	-	+	-	-
<i>Plantago media</i> L.	-	+	-	+	+	-	-
<i>Poa cenisia</i> All.	-	+	-	-	-	-	-

	470m	630m	830m	1030m	1230m	1430m	2100m
<i>Polygala comosa</i> Schkuhr	-	+	-	+	+	-	-
<i>Potentilla arenaria</i> Borkh.	+	+	+	-	+	-	-
<i>Potentilla argentea</i> L.	+	-	-	-	-	-	-
<i>Potentilla heptaphylla</i> L. subsp. <i>australis</i> (Krašan ex Nyman) Gams	-	-	-	+	-	-	-
<i>Primula veris</i> L.	-	-	-	+	-	-	-
<i>Prunella laciniata</i> (L.) L	-	-	-	+	+	-	-
<i>Prunella vulgaris</i> L.	-	-	-	+	-	-	-
<i>Pteridium aquilinum</i> (L.) Kuhn.	-	-	-	+	-	-	-
<i>Ranunculus bulbosus</i> L.	-	-	-	-	+	-	-
<i>Rubus praecox</i> Bertol.	+	-	-	-	-	-	-
<i>Rubus ideaus</i> L.	-	+	-	-	-	-	-
<i>Rumex acetosella</i> L.	-	-	-	-	-	+	-
<i>Rumex crispus</i> L.	-	-	+	-	-	-	-
<i>Rumex sanguineus</i> L.	-	-	-	-	-	-	+
<i>Scabiosa argentea</i> L.	-	+	-	-	-	-	-
<i>Salvia amplexicaulis</i> Lam.	-	+	-	-	-	-	-
<i>Salvia verticillata</i> L.	+	-	+	-	-	-	-
<i>Sanguisorba minor</i> Scop.	+	+	-	+	-	-	-
<i>Scabiosa columbaria</i> L.	-	-	-	+	-	+	+
<i>Sedum sexangulare</i> L.	-	+	-	-	-	-	-
<i>Senecio squalidus</i> L. subsp. <i>rupestris</i> (Waldst. & Kit.) Greuter	-	-	-	-	+	+	-
<i>Silene sendtneri</i> Boiss.	-	-	-	-	-	+	-
<i>Stachys annua</i> (L.) L.	-	-	+	-	-	-	-
<i>Stachys recta</i> L.	-	-	+	-	-	-	-
<i>Stachys scardica</i> (Griseb.) Hayek	-	-	-	+	-	-	-
<i>Stellaria graminea</i> L.	-	-	-	-	-	+	+
<i>Taraxacum officinale</i> Weber	-	-	-	-	-	-	+
<i>Teucrium chamaedrys</i> L.	+	+	-	-	-	-	-
<i>Teucrium montanum</i> L.	+	-	+	+	-	-	-
<i>Thymus</i> sp.	+	+	-	+	+	-	+
<i>Trifolium ochroleucon</i> Hudson	-	-	-	+	-	-	-
<i>Trifolium patens</i> Schreber	-	-	-	+	-	+	-
<i>Trifolium pratense</i> L.	-	+	+	-	-	+	+
<i>Tussilago farfara</i> L.	-	-	-	-	-	-	+
<i>Verbascum</i> sp.	-	-	+	-	-	+	+
<i>Viola tricolor</i> L.	-	-	+	-	-	-	-
<i>Xeranthemum annuum</i> L.	+	+	-	-	-	-	-

4. RESULTS AND DISCUSSION

It was found that there are plants species present only at certain altitudes, while others are present at almost all altitudes as it can be observed from the table (Table. 1).

Plant species that occur only at one altitude are: *Acinos alpinus* (830 m), *Agrimonia eupatoria* (630 m), *Anagallis foemina* (830 m), *Artemisia vulgaris* (630 m), *Astragalus onobrychis* (830 m), *Calamintha vulgaris* (630 m), *Centaureum erythraea* (1030 m),

Comus mas (630 m), *Dactylis glomerata* (2100 m) and other.

Plant species that occur only at two altitudes: *Agrostis stolonifera* (1430 m and 2100 m), *Asperula cynanchica* (470 m and 830 m), *Carlina vulgaris* (1030 m and 1430 m), *Coronilla varia* (470 m and 630 m), *Dorycnium herbaceum* (630 m and 1030 m), *Euphorbia cyparissias* (470 m and 1230 m), *Prunella laciniata* (1030 m and 1230 m), *Salvia verticillata* (470 m and 630 m) and other.

Plant species that can be seen at more than two altitudes are: *Achillea millefolium* (470 m, 830 m, 1030 m, 1230 m and 1430 m), *Cirsium eriophorum* (470 m, 1030 m, 1230 m, 1430 m and 2100 m), *Fragaria vesca* (470 m, 630 m, 1230 m, 1430 m and 2100 m), *Leontodon hispidus* (830, m, 1030 m, 1230, m, 1430 m), *Ononis spinosa* (470 m, 630 m and 1230 m) and other.

It was noted that the plant species *Hypericum perforatum*, is recorded in all of plant communities surveyed that proves its best adaptation to the conditions at different altitudes.

5. CONCLUSION

In this paper we showed that plant species inhabit habitats of different altitudes and the plants respond differently related to various soil factors in investigated communities. Some plants are adapted on various types of land and climate, such as *Hypericum perforatum*. Other species have adapted to live in the narrow range of temperature and humidity, and therefore inhabit only small areas where they 'he been specialized on certain properties of the soil at different altitudes of the mountain. Plant as: *Acinos alpinus* (830), *Agrimonia eupatoria* (630), *Anagallis foemina Mili* (830) live in habitats on certain altitude, while *Agrostis alba* (1430 и 2100), *Carlina vulgaris* (130 and 1430) and *Achillea millefolium* (470, 1030, 1230 and 1430), *Cirsium eriophorum* (470, 1030, 1230 and 1430) can be found on two or more different altitudes.

ACKNOWLEDGEMENT

This paper was written under the project of the Ministry of Education, Science and Development of Republic of Serbia OI 171025.

REFERENCES

- Gavrilović С., 1979. Хипсонометрија површине рељефа Копаника. Зборник радова географског института ПМФ у Београду, 26. Београд.
- IOPI databases . Retrieved from <http://plantnet.rbgsyd.nsw.gov.au/iopi/iopihome.htm>
- Josifović, M., & ed., 1970. Flora of SR Serbia I-X. Belgrade, Serbia: SANU. In Serbian.
- Karkaj, E.S., Motamedi, J., Akbarlou, M., & Alijanpour, A. 2012. Floristic Structure and Vegetation Composition of Boralan Mountainous Rangelands in North-Western Azerbaijan, Iran., pp. 697-706.
- Lomolino, M.V. 2001. Elevation gradients of species-density: Historical and prospective views. *Global Ecology and Biogeography*, 10, pp. 3-13.
- Naqinezhad, A., Jalili, A., Attar, F., Ghahreman, A., Wheelerc, B.D., Hodgsonc, J.G., . . . Maassoumi, A. 2009. Floristic characteristics of the wetland sites on dry southern slopes of the Alborz Mts. Iran: The role of altitude in floristic composition. *Flora*, 204, pp. 254-269.
- Tutin, T.G., Heywood, V.H., Burges, N.A., Moore, D.M., Valentine, D.H., Walters, S.M., . . . eds., 1964. *Flora Europaea*, I-V. London: Cambridge University Press. 1964-1980.
- Vasić, P. 2012. Morfološko anatomska građa listova roda *Juniperus* sa različitih nadmorskih visina Kopaonika. Prirodno-matematički fakultet Univerziteta u Prištini sa privremenim sedištem u Kosovskoj Mitrovici. Doktorska disertacija.
- Vasić, P., Labus, N., Topuzović, M., & Dubal, D. 2008. Morphological-anatomical characteristics of Juniper (*Juniperus sibirica*) from the area of mountain Kopaonik. *Заштита природе*, 59(1-2), pp. 115-120.
- Vasić, P., Topuzović, M., Labus, N., & Dubak, D. 2008. Morphological-anatomical characteristics of Commun Juniper (*Juniperus communis*) from the area of mountain Kopaonik. *Natura Montenegrina*, 7(3), pp. 97-107.
- Vasović, M. 1988. Kopaonik. Београд: Стручна knjiga.
- Васовић М., 1988. Копаник. Београд: СГД. Посебно издање, књига 65.

* E-mail: predrag.vasic@pr.ac.rs

KINETIC DETERMINATION OF GOLD(III) BASED ON ITS INHIBITORY EFFECT IN OXIDIZING HOMOGENOUS REACTION SYSTEM

Ružica Micić^{1*}, Snežana Mitić², Ranko Simonović¹, Dragana Sejmanović¹

¹Faculty of Sciences and Mathematics, University of Pristina, Kosovska Mitrovica, Serbia.

²Faculty of Sciences and Mathematics, University of Niš, Niš, Serbia.

ABSTRACT

Development and application of a simple, fast, green analytical kinetic method for the determination of micro-amounts of gold(III) ions, were presented in this paper. The method was based on the inhibitory effect of traces of Au(III) ions on the redox reaction between disodium-6-hydroxy-5-[(4-sulfophenyl)azo]-2-naphtalenesulfonate (artificial azo-dye "Sunset Yellow FCF", E110 in further text selected as SY) and hydrogen-peroxide, in alkaline media of borate buffer. All experimental parameters affecting to the determination: reagent concentrations, pH and temperature were investigated and optimised. Working experimental conditions are set according to the highest sensitivity of the proposed kinetic

method for the determination of Au(III) ions. The linearity of the method was obtained within the range 1.97-59.07 µg/mL of Au(III) ions with relative standard deviation of 3.66- 0.43 %, respectively. The influence by possible interference effects by major ions on the determination of Au(III) and their limits are investigated, at the constant Au(III) concentration of 39.39 µg/mL. The results of Au(III) determination in samples obtained by proposed kinetic method and comparative ICP-OES method were statistically agreeable. Obtained results for Au(III) determination in analyzed samples, as well as the development and validation of the proposed analytical procedure have given and discussed.

Keywords: gold(III), kinetic method, sunset yellow.

1. INTRODUCTION

Chemistry of gold is still the subject of research in scientific articles, not only because of its beauty and rarity and usage in jewelry, coinage and economics. Many properties of a gold(III) and gold-nanoparticles as enzyme inhibitor, vehicles for delivery of cancer drugs, antirheumatics based on its coordination and valence state, in many electron transfer processes ((Chandrakant, et al., 2016), (Narkhede et al., 2016), (Yang et al., 2016), (Pyrzyńska et al., 2006). Modern sophisticated techniques such as inductively coupled plasma mass spectrometry (ICP-MS) (Juvonen et al., 2002), flame atomic absorption spectrometry (FAAS), electrothermal atomic absorption spectrometry (ETA-AAS), inductively coupled plasma atomic emission spectrometry (ICP-AES) (Bulut et al., 2011), and other spectrophotometric methods involving chromogenic reagents such as morin, quercetin (Balcerzak et al., 2006), Spheron (R) and (biphenyl) dimethanethiol, (Behpour et al., 2005) etc. and electroanalytical techniques (square wave voltammetry-SWV, differential pulse voltammetry-DPV etc.) (Bulut et al., 2011) are the most commonly

used techniques in the determination of gold at low levels. UV-Vis spectrophotometric methods ((Chen et al., 2006), (Kamble et al., 2010)) are remarkable for their simplicity and versatility. Other sensitive techniques such as neutron activation analysis (NAA) (Nat et al., 2004) or total reflection X-ray fluorescence spectrometry (TXRF) (Messerschmidt et al., 2000) are less often applied in gold determination due to the complexity and cost of the required instrumentation.

Despite the large number of modern analytical techniques, kinetic methods still are used in real samples in the context of the study of the mechanism and rate of the chemical reactions. Also kinetic methods are preferred in terms of cost the experiment.

In this study simple and fast kinetic-spectrophotometric method was developed, based on inhibitory effect of gold(III). Experimental conditions were optimized as follow: $C_{SY}=4 \cdot 10^{-5}$ mol/L; $CH_2O_2=0.4$ mol/L; pH=10.5; $t=25.0 \pm 0.1$ °C. Measurements were done at the wavelength of absorbance maximum of the indicator substance-

artificial color "Sunset Yellow FCF, at $\lambda_{max} = 478.4$ nm.

2. EXPERIMENTAL

2.1. Apparatus

Spectrophotometric measurements were performed on Perkin-Elmer Lambda 15 UV-Vis spectrophotometer, using cylindrical cell thermostated at $25.0 \pm 0.1^\circ\text{C}$. A Julabo MP-5A model thermostatic bath was used to maintain the reaction temperature at $25.0 \pm 0.1^\circ\text{C}$. A pH meter (Hanna pH-210) with a glass electrode was employed for measuring pH values in the aqueous solution. 01 and pH of 4.00 ± 0.01 , were used. iCAP 6000 ICP-OES, Thermo Scientific, Cambridge, United Kingdom.

2.2. Reagents and Solutions

Analytical grade chemicals and deionized water (MicroMed high purity water system, TKA Wasseraufbereitungssysteme GmbH) were used for the preparation all of solutions. The stock Au(III) solution (1×10^{-3} mol/L) was prepared by dissolving $\text{Au}[\text{HCl}_4]$ (Alfa Aesar, A Jonson Matthey Company) in demineralized water. A working solution (1×10^{-5} mol /L) was obtained by diluting the stock solution with water. A solution of SY (provided by the Pharmaceutical laboratory Zdravlje-Actavis, Leskovac, Serbia), of 1×10^{-3} mol/L, was prepared by measuring 0.0226g of substance of analytical grade, and dissolving with deionized water in a volumetric flask of 50 ml. A solution of H_2O_2 of 2 mol/L was prepared by appropriate dilution of 30% H_2O_2 , (Merck) of reagent in volumetric flask of 50 mL with deionized water. The solution of borate buffer was prepared by appropriate mixing a solution of $\text{Na}_2\text{B}_4\text{O}_7 \cdot 10\text{H}_2\text{O}$ (0.05 mol/L) and 0.1 mol/L solution of NaOH. All the glassware used was washed with aqueous solution of HCl (1:1) and then thoroughly rinsed with running, distilled water, and then, finally with deionized water.

2.3. Kinetic-Spectrophotometric procedure

Bouderin flask with a four compartment was used for preparing solution (working volume of 5ml) before the start of reaction; a series of standard solution of Au(III) were placed in the first compartment, 0.2 ml of 1×10^{-3} mol/L solution of SY in the second, 2 ml borate buffer pH of 10.5 in the

third and 1 ml of 2 mol/L H_2O_2 in the fourth compartment. The solution was kept at $25.0 \pm 0.1^\circ\text{C}$ in the thermostated bath, before the mixing and beginning of the reaction. After mixing the reaction mixture was put into the spectrophotometric cell with path-length of 1 cm, and the absorbance at 478.4 nm was measured every 30 s during the first period of 6 min from the beginning of the reaction. The reaction rate was monitored spectrophotometrically. Absorbance measurements have been performed at the wavelength of the absorption maximum of SY at 478.4 nm.

Sample preparation. After the preparation of the sample solution injections containing the Au (III) ions in a concentration of 50 mg/0.5mL, based on the weight of the salt of sodium thio-auro-maleate Na_2SAuO_4 , was transferred quantitatively to the volumetric flasks of 50 mL and diluted with demineralized water to line. The concentration of this solution, calculated with respect to the Au (III) ion was 58 mg/mL. From this solution were made series of four different concentrations of Au (III) which are located in the area of the calibration curve: 58.0, 29.1, 14.5, and 4.8 mg/mL.

3. RESULTS AND DISCUSSION

3.1. Optimization of Reaction Variables

Inhibiting effect of Au(III) ion on the rate of reaction oxidation of *di*-sodium-6-hydroxy-5-[(4-sulfophenyl)azo]-2-naphtalenesulfonic acid (artificial color Sunset Yellow FCF, E110) by hydrogen peroxide in borate buffer was observed during kinetic research of this indicator system (Micic et al. 2009, 2014). In order to determine the lowest possible deterable concentration of Au(III), the reaction conditions (the influence of the pH, SY, hydrogen-peroxide concentrations, buffer volume and temperature) were studied for both, non-inhibited and inhibited reactions. The method of tangents was used and the slope of the linear section absorbance-time curve, $dA/dt = tg\alpha$, was used as a measure of the reaction rate. In this study, for all parameters investigated, the rates of non-inhibited (indicator) and inhibited reaction were simultaneously measured.

Keeping all other experimental parameter constant, the influence of the pH in borate buffer on the rate of the reactions in the range of 8.0 – 11.5 were studied, under concentration of gold(III) of 39.4 $\mu\text{g/mL}$. The

influence of pH on the reaction rates were separately measured with the same method by varying the pH. The best results were obtained for the value pH of 10.5 (Fig. 1), and this value was selected for further work. the order for both reactions, are variable in investigated interval regarding to pH. In order to obtain the rate of reactions regarding to C_{H^+} the dependence $-\log \text{tg} \alpha / -\log C_{H^+}$ within interval of pH 9.5-10.5 were constructed. Based on the slope of this dependence the order of the reactions were calculated. Its value for non-inhibited reaction is -0.9 and for inhibited is -0.5. (Fig. 3 and 4). The dependence of the reaction rates for both reactions, on the volume of borate buffer was also studied. The optimum difference between the rate of the non-inhibited and inhibited reactions is for volume of 2.0 mL of borate buffer, Fig. 4. The dependence of the reaction rates on the concentration of H_2O_2 were investigated over the range 0.1–0.8 mol/L, Fig. 5. For further work, a concentration of H_2O_2 of 0.4 mol /L was selected as the suitable. The dependence of reaction rates on the concentration of SY was investigated over the range 1.0×10^{-5} – 6×10^{-5} mol/L. The optimum difference between the rates of the non-inhibited and inhibited reactions occurred for concentration of 4.0×10^{-5} mol/L of SY, Fig.6. At higher concentration of SY absorbance significantly increases ($A > 1.0$), when error of spectrophotometric measurement becomes higher (area of Beer's law validity). The influence of temperature on the reaction rate was studied in the range 22°C – 28°C . The rate of reaction as expected increases with temperature. Although higher sensitivity could be obtained at the higher reaction temperature, for practical reasons measurement were done at $25 \pm 0.1^\circ\text{C}$. On the basis of dependence of rates of reactions on the concentration of each reactant, kinetic equations for non-inhibited (1) and inhibited reactions can be derived as follows:

$$-\left(\frac{dC}{dt}\right) = k_0 \cdot C_{H^+}^{-0.9} \cdot C_{SY} \quad (1)$$

$$-\left(\frac{dC}{dt}\right) = k \cdot C_{H^+}^{-0.5} \cdot C_{SY} \cdot C_{Au(III)}^{-1} \quad (2)$$

Where k_0 is constant which is proportional to the constant rate of non-inhibited reaction, and k is constant which is proportional to the constant of inhibited reaction. Based on kinetic equations (1) and (2) rate constants were calculated for non-inhibitory

and inhibitory reactions in the temperature range of 22 – 25°C (295 – 301K), and obtained results are shown in Table 1.

Based on the Arrhenius's equation for non- inhibitory and inhibitory reactions Arrhenius's plot has obtained (Fig.7., 8.) the activation energy (E_a^*) were calculated by following equation, for both process, non-inhibited and inhibited:

$$E_a^* = -R \left[\frac{\partial \ln k}{\partial (1/T)} \right]_p \quad (3)$$

Based on its value and thermodynamics equations for change of Gibbs's energy, enthalpy (H) and entropy (S) can calculated for both processes. Based on this results mechanism of examined redox reactions can be discussed under given experimental conditions- concentration of reaction parameters, at room temperature and atmospheric pressure in examined redox system.

Table 1. Rate constants.

T(K)	$k_0 \cdot 10^8 (\text{mol/l})^{1-n} \text{S}^{-1}$	$k \cdot 10^8 (\text{mol/l})^{1-n} \text{S}^{-1}$
295	3.55	1.41
298	6.65	4.22
301	7.98	13.4

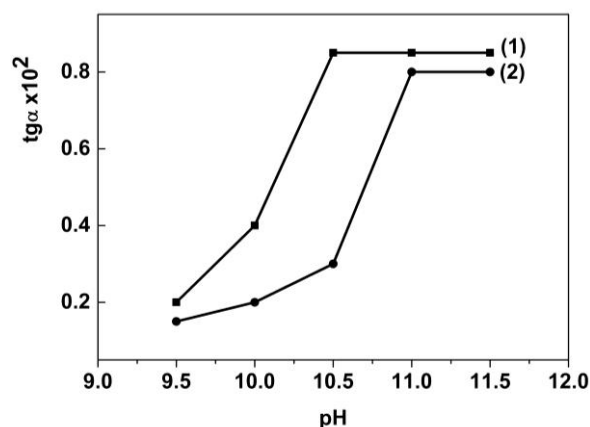


Fig. 1 The influence of pH.

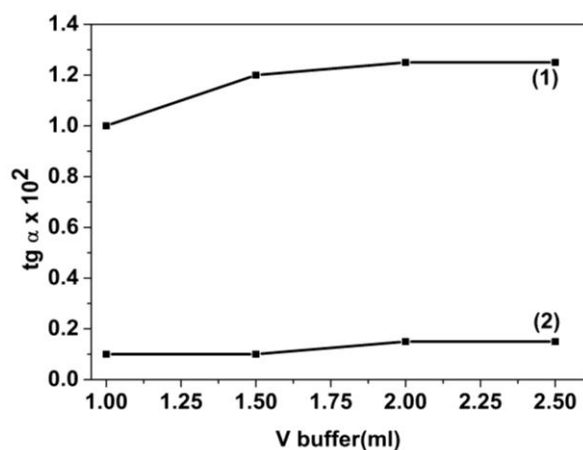


Fig. 2 The influence of borate buffer.

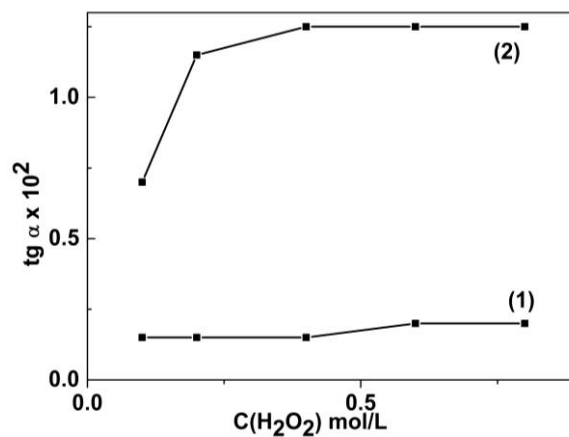


Fig. 5 The influence of H₂O₂.

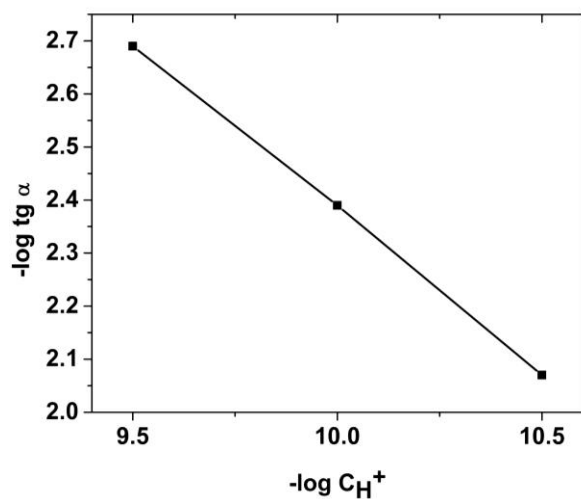


Fig. 3 Dependence $-\log \text{tg } \alpha / -\log C_{\text{H}^+}$ -non-inhibited.

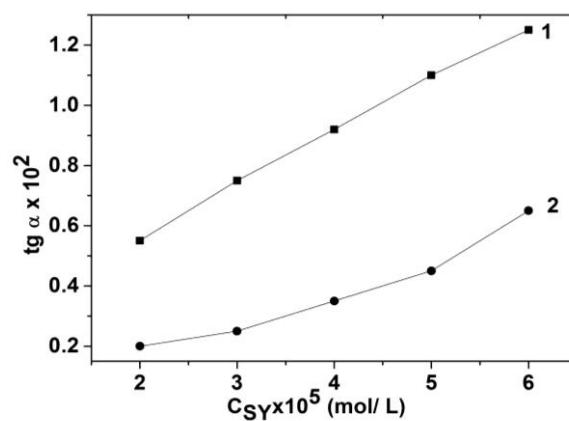


Fig. 6 The influence of SY.

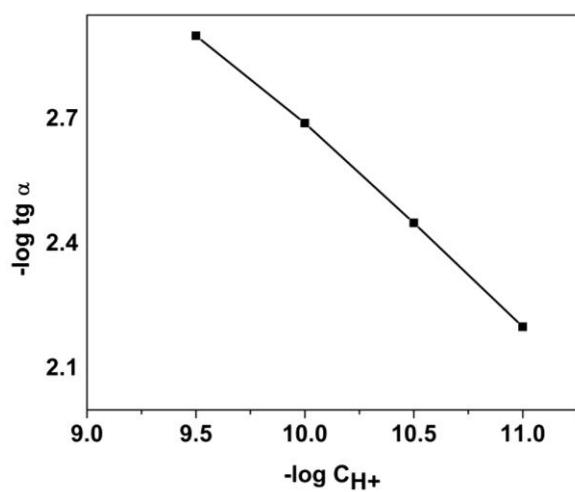


Fig. 4 Dependence $-\log \text{tg } \alpha / -\log C_{\text{H}^+}$ -inhibited.

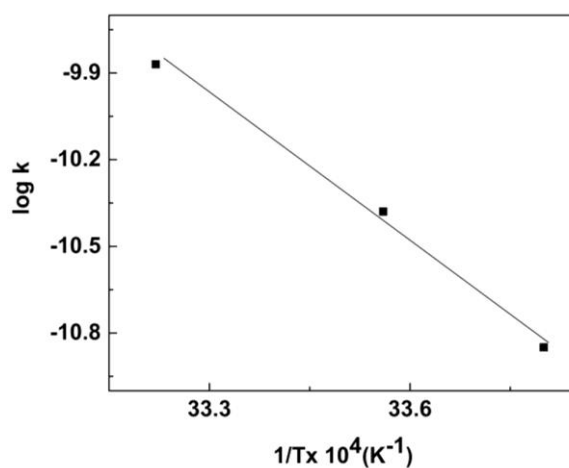


Fig. 7 Arrhenius' plot for inhibited reaction.

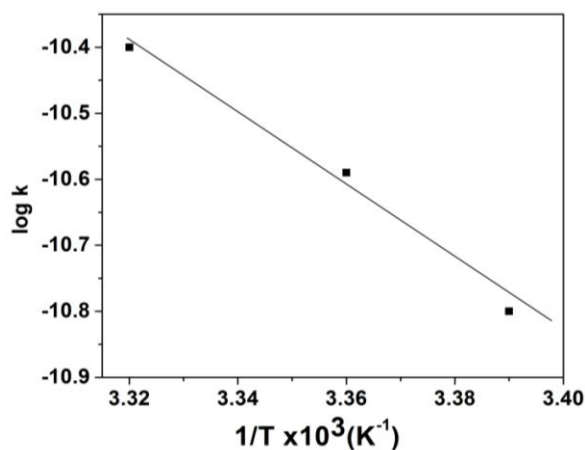


Fig. 8 Arrhenius' plot for non-inhibited reaction.

3.2. Validation of the proposed method

The calibration graph was constructed under the established optimal conditions regarding on sensitivity and reproducibility of the method as follows: $C_{SY}=4 \times 10^{-5} \text{ mol/L}$; $C_{H_2O_2}=0.4 \text{ mol/L}$; $\text{pH}=10.5$; $t=25.0 \pm 0.1^\circ\text{C}$, $\lambda_{\text{max}}=478.4 \text{ nm}$. The linearity was obtained within the range 1.97-59.07 $\mu\text{g/mL}$ of Au(III). Obtained analytical and statistical data of the calibration graph at $25.0 \pm 0.1^\circ\text{C}$ were presented in Table 2. In order to assess the precision and accuracy of the proposed kinetic method, measurements were done in five replicate determinations at each of four different Au(III) concentrations. Obtained results are shown in Table 3.

Table 2. Analytical and statistical data.

Analytical and Statistical Data	Temperature $25.0 \pm 0.1^\circ\text{C}$
	Dynamic range 1.97-59.07 ($\mu\text{g/mL}$)
Number of points	9
Limit of detection $\mu\text{g/mL}$	0.12
Limit of quantification $\mu\text{g mL}^{-1}$	0.36
Slope $\times 10^2$	-0.0126
Intercept $\times 10^2$	0.8948
Correlation Coefficient	-0.9997
Standard error of the slope	1.217×10^{-4}
Standard error of the intercept $\times 10^2$	0.00382
Standard deviation of the Fit $\times 10^2$	0.00382
Analytical frequency, h^{-1}	10

The robustness of proposed method is a measure of its capacity to remain unaffected by small, but deliberate variations in the method parameters and provides an indication of its reliability during usage. The most significant variables of the system (temperature and concentration of SY, hydrogen peroxide) were modified in range $\pm 10\%$ (excluding pH, which was modified in range $\pm 5\%$) from their optimum values. Errors lower than 5 % were observed in all cases.

Table 3. Accuracy and precision of the method.

Added ($\mu\text{g mL}^{-1}$)	Found ^a ($\mu\text{g mL}^{-1}$)	RSD ^b (%)	$(\bar{x}-\mu)/\mu \cdot 100^c$
1.9	1.9 ± 0.07	3.7	-3.1
19.7	19.9 ± 0.6	3.2	+1.1
39.4	38.8 ± 0.4	1.0	-1.5
59.1	58.8 ± 0.2	0.4	-0.4

^amean value \pm standard deviation ($n=5$) ^brelative standard deviation; ^c – accuracy.

To access the selectivity of the method, the influence of major foreign ions on the inhibited reaction rate was studied, under the reaction conditions mentioned above, at a constant Au(III) concentration of $C_{\text{Au(III)}}=39.39 \mu\text{g/mL}$. The results are summarized in Table 4.

Table 4. Selectivity of the proposed method.

Ratio $C_{\text{other ion}}/C_{\text{Au(III)}}$	Other ions
100	$\text{Na}^+, \text{K}^+, \text{Cl}^-$
10	$\text{F}^-, \text{Li}^+, \text{Zn}^{2+}, \text{Al}^{3+}, \text{Mg}^{2+}, \text{V}^{5+}, \text{As}^{3+}, \text{As}^{5+}, \text{SO}_3^{2-}, \text{NH}_4^+, \text{CH}_3\text{COOH}, \text{Sn}^{2+}, \text{Sr}^{2+}, \text{I}^-, \text{CO}_3^{2-}$
1	$\text{Mo}^{6+}, \text{Cr}^{6+}, \text{Ba}^{2+}, \text{Cd}^{2+}, \text{Ni}^{2+}, \text{Mn}^{2+}, \text{Al}^{3+}, \text{Ca}^{+2}, \text{NO}_3^-, \text{SO}_4^{2-}, \text{C}_2\text{O}_4^{2-}$
0.1	$\text{Fe}^{3+}, \text{Co}^{2+}, \text{Hg}^{2+}$

3.3 Application of the proposed method

In order to evaluate of proposed procedure this kinetic method was applied to the determination of Au(III) ions in pharmacological samples, ampoules Tauredon ® with Au(III) ions concentration of 50 mg/0.5 mL, (Na_2SAuO_4). Obtained results are given in

Table 5. As can see results obtained by proposed kinetic and comparable ICP-OES method are in good agreement.

Table 5. Application in ampules *Tauredon*®.

Added ($\mu\text{g/mL}$) <i>Tauredon</i> ®	Found ^a ($\mu\text{g/mL}$)	RSD ^b (%)	ICP-OES Found ^a ($\mu\text{g/mL}$)	F-test
4.8	4.8 \pm 0.2	3.1	4.8 \pm 0.2	1.0
14.5	14.4 \pm 0.5	3.6	14.5 \pm 0.4	1.6
29.1	28.8 \pm 0.6	2.2	29.0 \pm 0.3	0.4
58.1	57.2 \pm 0.8	1.3	59.1 \pm 0.3	0.7

4. CONCLUSION

In this work fast, simple cost-effective, green analytical kinetic method for gold(III) determination was given. Application of the method was demonstrated in pharmacological ampoules *Tauredon*®. Method has good analytical performance and could be useful for trace determination of Au(III) ions in different kind of real samples. Thus, the proposed method was found to be robust for routine determination of Au(III) in different real samples.

REFERENCES

- Balcerzak, M., Kosiorek, A., & Swiecicka, E. 2006. Morin as a spectrophotometric reagent for gold. *Journal of Analytical Chemistry*, 61, pp. 119-123.
- Behpour, M., Attaran, A.M., Ghoreishi, S.M., & Soltani, N. 2005. Column preconcentration of gold by adsorbing AuCl₄⁻ onto methyltrioctyl ammonium chloride-naphthalene and subsequent atomic absorption spectrometric determination. *Anal Bioanal Chem*, 382(2), pp. 444-7. pmid:15838616.
- Bulut, V.N., Duran, C., Boiyiklioglu, Z., Tufekci, M., & Soylak, M. 2011. Spectrophotometric determination of gold(II) after liquid-liquid extraction and selective pre-concentration with a novel dibenzo-18-crown-derivates. *Geostandards and Geoanalytical Research*, 35(4), pp. 471-483.
- Chen, Z., Huang, Z., Chen, J., Chen, J., Yin, J., Su, Q., & Yang, G. 2006. Spectrophotometric determination of gold in water and ore with 2-Carboxyl-1-

- Naphthalthiorhodanine. *Analytical Letters*, 39, pp. 579-587.
- Juvonen, R., Lakomaa, T., & Soikkeli, L. 2002. Determination of gold and the platinum group elements in geological samples by ICP-MS after nickel sulphide fire assay: Difficulties encountered with different types of geological samples. *Talanta*, 58(3), pp. 595-603. pmid:18968787.
- Kamble, G.S., Kolekar, S.S., Han, S.H., & Anuse, M.A. 2010. Synergistic liquid-liquid extractive spectrophotometric determination of gold(III) using 1-(2',4'-dinitro aminophenyl)-4,4,6-trimethyl-1,4-dihydropyrimidine-2-thiol. *Talanta*, 81(3), pp. 1088-95. pmid:20298898.
- Messerschmidt, J., von Bohlen, A., Alt, F., & Klockenkämper, R. 2000. Separation and enrichment of palladium and gold in biological and environmental samples, adapted to the determination by total reflection X-ray fluorescence. *Analyst*, 125(3), pp. 397-9. pmid:10829339.
- Micic, R.J., Mitić, S.S., & Simonovic, R.M. 2009. Analytical application of food dye Sunset Yellow for the rapid kinetic determination of traces of copper(II) by spectrophotometry. *Food Chemistry*, 117(3), pp. 461-465.
- Micic, R.J., Mitić, S.S., & Budimir, M. 2009. Highly Sensitive Determination of Traces of Co(II) in Pharmaceutical and Urine Samples Using Kinetic-Spectrophotometric Method. *Analytical Letters*, 42(7), pp. 935-947.
- Micic, R.J., Mitić, S.S., Pavlovic, A.N., Kostic, A.D., & Mitic, M.N. 2014. Application of tartrazine for sensitive and selective kinetic determination of Cu(II) traces. *Journal of Analytical Chemistry*, 69(12), pp. 1147-1152.
- Narkhede, C.P., Suryawanshy, R.K., Patil, C.D., Borase, H.P., & Patil, S.V. 2016. Use of protease inhibitory gold nanoparticles as a compatibility enhancer for Bt and deltamethrin: A novel approach for pest control. *Biocatalysis and Agricultural Biotechnology*, 8, pp. 8-12.
- Nat, A., Ene, A., & Lupu, R. 2004. Rapid determination of goLd in Romanian auriferous aLLuviaL sands, concentrates and rocks by 14 MeV NAA. *J Radional Nucl chem*, 261, pp. 179-188.
- Pyrzyńska, K. 2005. Recent developments in the determination of gold by atomic spectrometry techniques. *Spectrochimica Acta Part B*, 60, pp. 1316-1322.
- Yang, Y., Zeng, H., Zhang, Q., Bai, X., Liu, C., & Zhang, Y.H. 2016. Direct electron transfer and sensing performance for catechin nano-gold particles-polymer nano-composite with immobilized Laccase. *Chemical Physics Letters*, 658, pp. 259-269.

* E-mail: ruzica.micic@pr.ac.rs

CONTEMPORARY DEMOGRAPHIC CHANGES IN SETTLEMENTS ALONG THE ADMINISTRATIVE LINE IN SERBIA TOWARDS AUTONOMOUS PROVINCE OF KOSOVO AND METOHIJA

Danijela Vukoičić*, Milena Nikolić², Jelena Raičević³

¹Faculty of Natural Sciences and Mathematics, University of Pristina, Kosovska Mitrovica, Serbia.

²Belgrade Business School, Higher Education Institution for Applied Studies, Belgrade.

³Business school of applied studies-Blace, College of Professional Studies, Blace.

ABSTRACT

The settlements along the administrative line in Serbia towards Kosovo and Metohija had a very turbulent demographic changes in the past. These changes have influenced the present. In this paper we investigated the depopulation process of this area which is intensified with the political instability, social and economic changes. The main goal of this research was to analyze the causes and effects in the reduction of the number of

inhabitants, as well as the possibility of revitalizing the rural settlements of a given area. To obtain the desired results, we analyzed the existing literature and statistical data, used comparative and historical methods as well as implemented the field surveys. The application of the SWOT analysis to the researched area have showed us the strength, weakness, opportunities, and threats that can effect the process of revitalization of the village.

Key words: marginal areas, Kosovo and Metohija, demographic changes.

1. INTRODUCTION

Immigration in Europe from 1950 to the present day has increased by nearly two million people. Due to demographic changes many countries become ethnically diverse (Coleman, 2015). According to the political, economic and social changes during the 1990s and 2000s, population of the 29 former communist countries of Europe and Asia had a significant demographic changes. This includes a sudden drop in the birth rate, increased mortality and migration of large-scale, accompanied by large flows of refugees and internally displaced persons. In most countries in the region such demographic trends have led to the decrease and rapid aging of the population (Heleniak, 2015).

Mountain ranges on the Balkan Peninsula were appealing for a number of conquests from prehistory to the recent wars (Daras, 1995). In the last 550 years due to frequent wars, the Balkan peninsula remained the least developed area in Europe. In the 19th century the Balkan nations regained their independence, and after World War II until 1989, some countries of the Balkan peninsula were under the communist regime. During the 1990s, there was a civil war in the Balkan region, which led to the disintegration of the former

Yugoslavia (Skoulikidis et al., 2009). There have been frequent ethnic conflicts between Serbs and Albanians in Kosovo, (Bhaumik et al., 2006), which ended with NATO Alliance air strikes on the Federal Republic of Yugoslavia on the 24th March 1999. Alleged Albanian bullying, threats and intimidation of Serb school children and families meant thousands felt forced to sell their properties at depressed prices and migrate (Nelles, 2005). Thus, the beginning of the 21st century is marked by a large number of refugees and internally displaced persons from the territory of the autonomous province of Kosovo and Metohija (Marinović, 1999). Then from settlements along the administrative line between Serbia and Kosovo and Metohija have happened a sudden migration of the population towards the central parts of Serbia.

The administrative line in Serbia towards the province of Kosovo and Metohija is 352 km long and it includes 97 rural settlements. The natural, historical and political factors caused the demographic changes of these settlements, as well as geographic and traffic position. This area is isolated from the dynamic changes in other regions, because of its position in the southern part of the Republic, along the administrative

line to the province. In the past, the hilly and mountainous terrain of the area, with an altitude from 400 m to 2100 m served for harboring the population. Numerous archaeological studies indicate that the area was inhabited in late Neolithic and early Bronze Age. Serbs were the main population in the Middle Ages what testify numerous hill forts and Turkish census from the 15th and 16th century. The settling of the Turkish population in the region came after the Battle of Kosovo, and the rule of the Turks caused many population movements in Balkans. After 1833, the biggest part of today's administrative line area was the border between Serbia and Turkey (Jotić & Vukojičić, 2004). The turmoil of the 18th century changed the structure of the population. The unstable political and economic situation in these mountainous areas has caused migration of the Serbian population in the 19th century, which continued in the 20th and at the beginning of the 21st century (RZS). According to (Cvijić, 1922) in this area there were a crossing of the two migratory current from the Dinaric Alps and Kosovo-Metohija. The causes for migration were diverse, the population moved from Kosovo and Metohija due to the Turkish and Albanian terror, and

from the area of northern Montenegro and Eastern Herzegovina, because of arid land (Cvijić, 2010). The population were engaged in agriculture, livestock, mining (in the Kopaonik area) and timber harvesting.

2. RESEARCH AREA

The area along the administrative line of Serbia towards Kosovo and Metohija includes 11 municipalities (basic administrative-territorial units of the Republic of Serbia), divided into five districts. In the research area, there are 97 settlements, 21 of them are located in the municipality of Kursumlija, 15 settlements are on the territory of Novi Pazar, 12 belong to the municipality of Medvedja, 11 to Bujanovac, 10 to Raska and Presevo, 8 to Brus, 6 to Tutin, 2 to Leskovac and one settlement to municipalities of Lebane and Vranje.

Settlements in this area are of scattered type, mostly mountainous (above 1000 m), scattered around the valley sides of the river and high mountain meadows (Miletić et al., 2009). Settlements in the Preševo valley have the lowest altitude, about 400 m.

Table 1. Territorial expanse of border settlements.

Area/Region	Municipality /City	Total number of settl.	Number of border settlements	Area in hectares	Altitude zone in m
Raška region	Tutin	93	6	13693	700-2100
	Novi Pazar	99	15	11726.6	500-1400
	Raška	61	10	7774.1	420-1900
Rasinska region	Brus	58	8	8630.8	800-1900
Toplička region	Kuršumljija	90	21	26459.8	500-1700
Jablanička region	Medveđa	44	12	14947.8	500-1200
	Lebane	39	1	2602.2	600-1160
	Leskovac	144	2	3871	520-1100
	Vranje	84	1	1528.9	800-1200
Pčinjska region	Bujanovac	59	11	11457.4	400-1200
	Preševo	35	10	7140.2	460-1100
Total	11	806	97	102691.6	400-2100

Source of data: Statistical Office of the Republic of Serbia.

On the highest al On the highest altitude were a settlements in the municipality of Tutin (2100 m), Raska and Brus (up to 1900 m) and Kursumlija (1700 m). All settlements are divided into villages and mahalas (Table 1). Beside the investigation of the territorial expanse of settlements in the research area, we also analyzed the changes of population, size, number of households, the average number of members and the structure and density of households.

Based on all this, the aim of this paper is to point to the demographic changes in present time.

3. MATERIAL AND METHODS

The methodology in this paper is according to the subject, objectives and tasks of the research. Field studies are carried through direct and systematic observation, as well as conducting surveys and

interviews. The historical method contains the use of literature, written documents and other archive material and presents us knowledge about the past of this area, explains the current situation and helps to give a forecasts of future development. Data were collected in public institutions and in the Statistical Office of the Republic of Serbia. We used the cartographic method for representation of spatial distribution of settlements along the administrative line to Kosmet. The SWOT analysis is applied to identify key strengths and weaknesses, the opportunities for development of the research area, as well as the threats for the process of revitalization of these settlements.

4. RESEARCH RESULTS AND DISCUSSION

In most of the settlements (around 64) the majority of the population are Serbs, in six settlements the majority are Bosniaks, 25 settlements are populated by Albanians, and two by Montenegrins. Bosniak-Muslim settlements are at the territory of Tutin and Novi Pazar municipalities, Serbian are in the area of Raska, Bruce, Kursumlija, Leskovac, Lebane and Vranje, in Medvedja there are six settlements inhabited by Serbs, four by Albanians and two by Montenegrins. The Albanian settlements are in Bujanovac and Presevo ("see Fig. 1.").

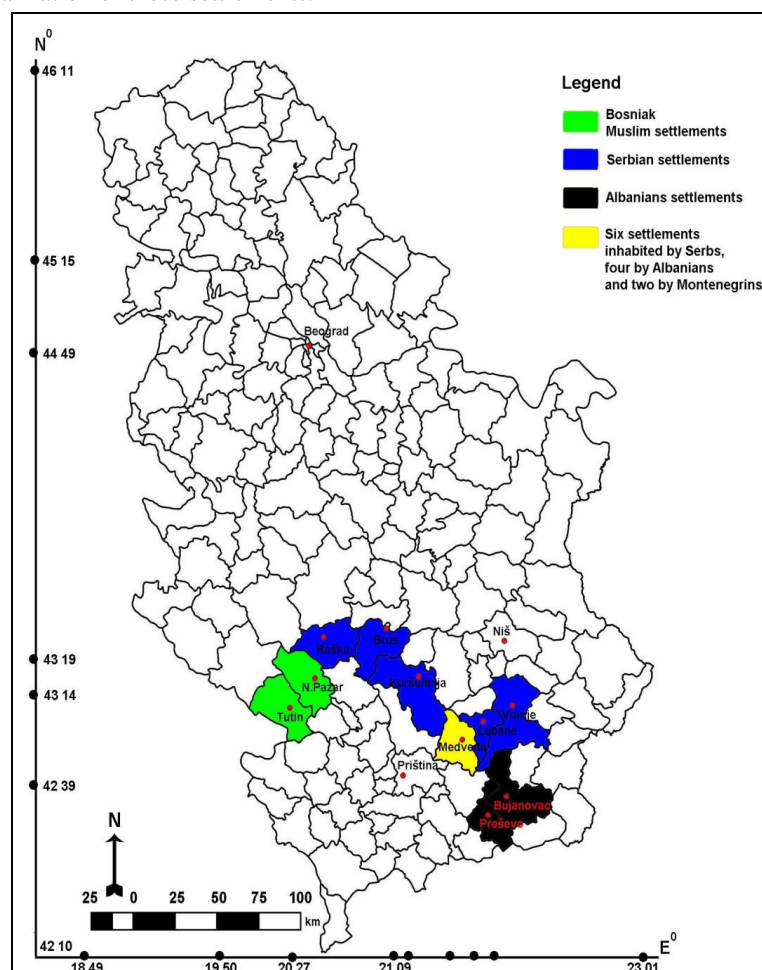


Fig.1. Distribution of majority population in settlements along the administrative line in Serbia towards Kosovo and Metohia; Source free GIS data DIVA (GIS) administrative areas and Statistical Office of the Republic Serbia. Scale 1:10,000,000 WGS 84.

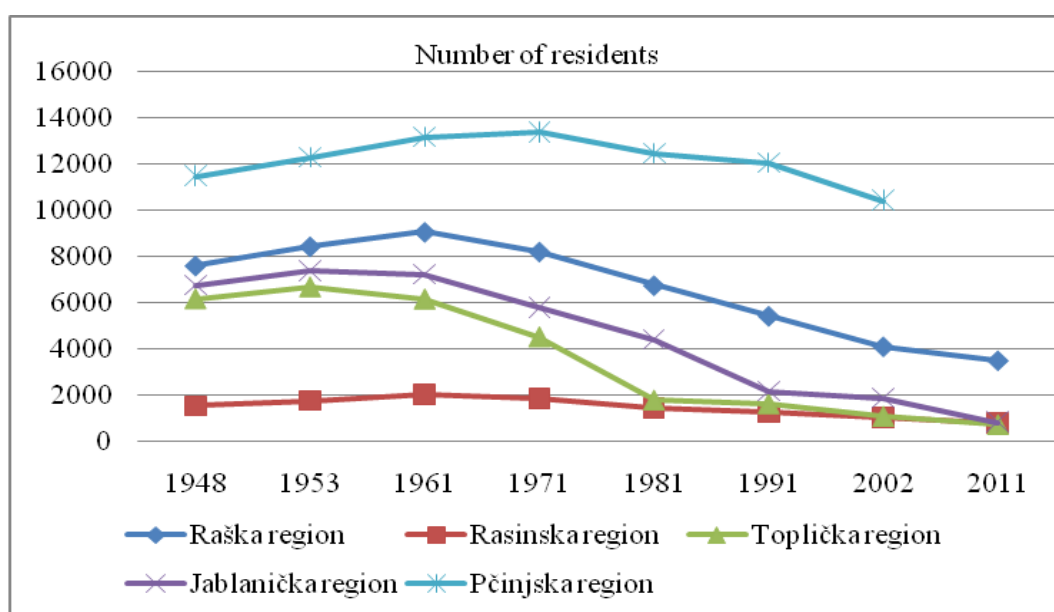
In the municipalities of Bujanovac and Presevo, the census in 2011. was not fully implemented because the residents refused to be registered. According to this list, in the 76 settlements along the administrative line lived 5802 inhabitants, 16,652 less than in 1948. During this period a big population decrease was registered, due to which large empty spaces were created along the administrative line toward the

province. The smallest decrease, of 19.3% was recorded in the villages of Tutin municipality and the largest in the municipality of Vranje, 90.8%, while in Lebane was recorded a decrease of 89.4%, in Medvedja 89.3%, and in Kursumlija 88.4%. The total number of population was increased after the World War II until 1961. (Table 2).

Table 2. Changes in number of residents in settlements along the administrative line

Indeksi	1948	1953/ 48	1961/ 53	1971/ 61	1981/ 71	1991/ 81	2002/ 91	2011/ 02	2011/ 48
Tutin	2512	110.5	109.8	93.5	95.7	98.2	76.9	98.4	80.7
Novi Pazar	2500	112.1	105.8	88	71.9	55.3	64.5	68.7	18.4
Raška	2581	110.3	106.7	90.1	77.9	79.4	80.5	73.2	38.6
Brus	1514	115	116	91.5	77.8	84.7	83.3	75.7	50.7
Kuršumlja	6148	108.3	92.2	73.3	39.4	91.4	66.3	66.4	11.6
Medveda	4866	109.3	97.2	82.4	81.3	43.5	96.4	35.8	10.7
Lebane	862	105.3	99.4	66.3	64.6	64.3	59	61.9	10.6
Leskovac	1005	113.7	99	79.7	59.4	71.8	65.4	73.3	18.3
Vranje	466	116.3	88.6	78.5	66.8	59.5	42	68.3	9.2
Bujanovac	7350	107.6	109	108.5	102.7	91.7	91.8	-	-
Preševo	3657	104.3	106.3	90.2	71.3	117.9	73.3	-	-
Total:	33461	109	103	89.7	79.5	83.7	82.2	-	-

Source of data: Statistical Office of the Republic of Serbia.

**Fig. 2.** Changes in population in the settlements along the administrative lines by region.

Source of data: Statistical Office of the Republic of Serbia.

Population in settlements at higher altitudes lives exclusively from animal husbandry and forest exploitation. In the valleys and valley extensions people mostly live from farming and wood processing (sawmills). Settlements have received electricity in the second half of the 20th century, they are supplied with water from the local springs. Most of the settlements remained without four-year schools, local communities and shops ((Milinčić, 2001), (Milinčić & Rosić, 2001), (Šaćirović, 2002)).

The development of the industry since the 60s of the last century caused the decrease of the population, and the last inter-census period marks the settlements without inhabitants (Smilov Laz - Novi Pazar, Tačevac and Vukojevac - Kursumlija and Gare - Preševo).

According to the census in 1953, only 13 settlements (13.4% of the total number of settlements) reduced the number of inhabitants compared to 1948 (Zlatare, Kasalj, Jova, Plavkovo, Mura, Bozoljin, Prevetica, Mali Trnovac, Letovica, Bercevac, Gare, Peceno and Porostica) while in 2002 compared to 1991, in 89 villages (91.8%) the number of inhabitants were reduced. Between the two census periods only eight settlements have recorded population growth (Brzece, Trn, Sponce, Grbavce, Konculj, Vrbani, Letovica and Peceno). Several settlements recorded a huge depopulation of over 90% (Vukojevac, Rastelica, Vasiljevac, Macja Stena, Vucja Lokva, Odojevice, Mala Braina, Gare). A significant population increase was recorded in three settlements in the municipality of Bujanovac, in the valley Binacka Morava and along

the main road Bujanovac - Gnjilane (transition Konculj, Vrbani and Letovica) (RZS).

There is a large number of small settlements along the administrative line of Serbia and the province, of up to 100 inhabitants, scattered and spilled type. The number of such settlements has increased 30 times

(from 2 to 61). Settlements without inhabitants were registered, too (4 settlements). The multiplication of such settlements, due to depopulation creates demographic voids (Miličić, 2003). The number of settlements with more than 1,000 residents in a given period declines (from 7 to 6) (Table 3).

Table 3. Number and size of settlements (by population) along the administrative line.

Year	Number of inhabitants					
	No Inhabitants	Up to 100	101-300	301-500	501-1000	over 1000
1961	-	2	52	24	12	7
%	0	2.1	53.6	24.7	12.4	7.2
2011	4	61	19	4	3	6
%	4.1	62.9	19.6	4.1	3.1	6.2

Source of data: Statistical Office of the Republic of Serbia.

The number of households from 4902 in 1948 dropped to 4331 in 2002. Population growth rate in this period is 3.8%. In the period 1953/1948, in 10 out of 11 municipalities, settlements had an population growth, and Presevo had a rate of natural decrease of 5%, while in the period 1961/1953 the rate of decrease of 0.3% was recorded only in settlements of the Kursumlija municipality. In the periods between the two census from 1961, trend of population decline is constantly increasing. Due to the lack of data on the

number of households in the 2011 census in the municipality of Bujanovac and Presevo, movements of households are unknown between 2011/2002. In the towns of other 9 municipalities the population decline were recorded. In the period 2011/1948, 6 municipalities recorded the rate of decrease (Novi Pazar, 47.4%, Kursumlija 67.4%, Medvedja 72.3%, 63% Lebane, Leskovac and Vranje 57.5%, 76.4%). Changes of the number of households in 63 different villages depends on their position.(Table 4).

Table 4. Changes of the number of households in the settlements along the administrative line.

Index	1948	1953 /48	1961/ 53	1971/ 61	1981/ 71	1991/ 81	2002/ 91	2011/ 02	2011/4 8
Tutin	351	109.4	113.5	123.2	82.3	103.4	94.1	94.2	115.4
Novi Pazar	344	107.0	113.6	103.1	90.0	82.2	81.2	69.9	52.6
Raška	372	109.7	126.5	107.0	96.7	104.5	89.6	75.0	100.8
Brus	209	112.4	139.6	100.0	102.4	104.8	101.4	81.5	139.2
Kursumlija	924	104.3	99.7	85.4	84.2	76.8	80.2	70.7	32.6
Medvedja	686	110.1	103.3	89.0	89.9	60.6	102.6	49.0	27.7
Lebane	127	102.4	106.2	88.4	83.6	79.4	71.6	81.0	37.0
Leskovac	146	106.2	108.4	95.8	81.4	88.5	72.4	73.8	42.5
Vranje	72	111.1	101.3	85.2	85.5	88.1	51.9	63.0	23.6
Bujanovac	1076	106.3	109.1	103.9	100.5	98.3	102.3	-	-
Presevo	595	95.0	103.2	91.8	71.4	99.0	129.9	-	-
Total	4902	105.8	109.0	98.1	90.0	90.2	96.2	-	-

Source of data: Statistical Office of the Republic of Serbia

Reducing the number of households, is followed with the reduce of the average number of members per household. In settlements along the administrative line towards Kosovo and Metohija average number of household members decrease from 1953 to 2002, from 7.0 to 4.3. The average number of household members is different in municipalities. In Tutin, in comparison to 1953, the average number of members decreased for 2.2 members till 2011, in Novi Pazar for 5.1, in Raska

for 4.3, in Brus for 4.8, in Kursumlija for 4.5, in Medvedja for 4.3, in Lebane for 5.1, in Leskovac, Vranje 4.4 and 4.3, and in 2002 in Bujanovac the number of members per household decreased for 0.7 compared to the year 1953 and for 2.4 members compared to 1961 in Presevo. he decrease from the average of 4 members per household indicates the disappearance of patriarchal families, the so-called family cooperatives (Table 5).

Geography

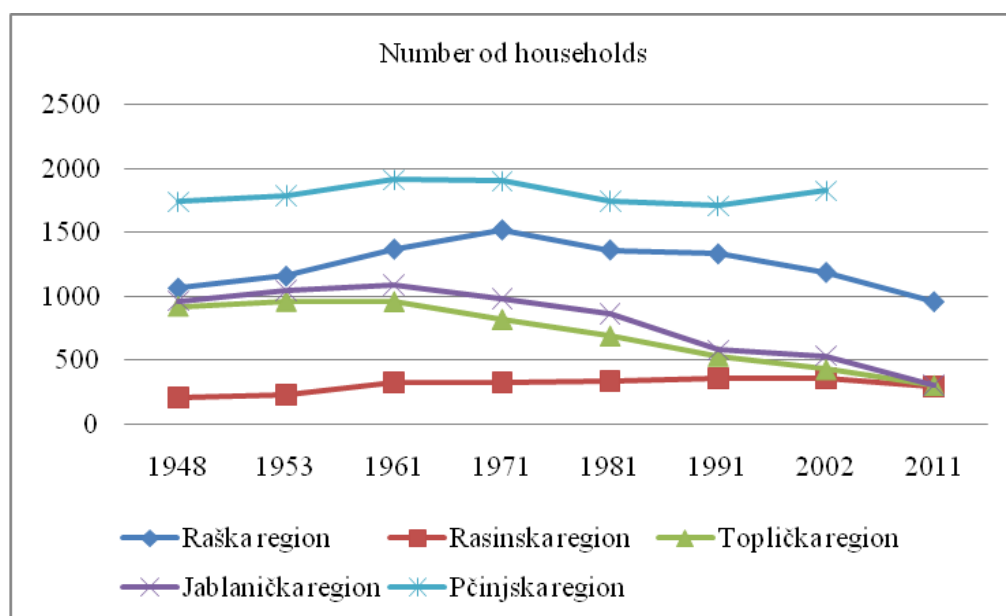


Fig. 3. Changes of the number of households in the settlements along the administrative lines by region.

Source of data: Statistical Office of the Republic of Serbia.

Table 5. The average number of household members in settlements along the administrative line.

Year	1948	1953	1961	1971	1981	1991	2002	2011
Tutin	7.1	7.2	7.0	5.3	6.2	5.9	4.8	5.0
Novi Pazar	7.3	7.6	7.1	6.1	4.8	3.3	2.6	2.5
Raška	6.9	7.0	5.9	5.0	4.0	3.0	2.7	2.7
Brus	7.2	7.4	6.2	5.6	4.3	3.5	2.8	2.6
Kuršumlija	6.7	6.9	6.4	5.5	2.6	3.1	2.5	2.4
Medveđa	7.1	7.0	6.6	6.1	5.6	4.0	3.7	2.7
Lebane	6.8	7.0	6.5	4.9	3.8	3.1	2.5	1.9
Leskovac	6.9	7.4	6.7	5.6	4.1	3.3	3.0	3.0
Vranje	6.5	6.8	5.9	5.5	4.3	2.9	2.3	2.5
Bujanovac	6.8	6.9	6.9	7.2	7.4	6.9	6.2	-
Preševo	6.1	6.8	7.0	6.8	6.8	8.1	4.6	-
Total	6.8	7.0	6.6	6.1	5.4	5.0	4.3	-

Source of data: Statistical Office of the Republic of Serbia

In 2002, the settlements in the research area were characterized by a family of six or more members (29.0%), 2 members (20.4%) and 1 member (13.9%). The largest number of settlements in 2011 is characterized by a family of 2 members (27.3%), 1 member (25.9%) and of 6 or more members (14.8%). The number of households of 1 member increased (by 12.0%) and of 2 members (by 6.9%), too. The number of members per household varies by municipality. Villages in Tutin (39.5%), Bujanovac (54.0%) and Preševo (29.0%), are dominating with 6 or more members per household, there were households of 2 members in Novi Pazar (33.5%), Bruce (30.9%),

Kursumlija (34.6%), Medveđa (32.6%), Leskovac (33.9%) and Vranje (35.3%), and 1 member in Raška (33.1%) and Lebane (42.6%). Changes in the structure of households (by number of members) is due to the movement of younger people to urban centers, where in search for the employee they established their own families, while in the countryside only elderly households remained (Vukoičić, 2014).

The process of change in population and number of households in the settlements along the administrative line of Serbia towards Kosovo and Metohija, was followed by the changes in population density.

Table 6. The overall population density (inh. / Km²) in areas along the administrative line.

Year	1948	1953	1961	1971	1981	1991	2002	2011
Tutin	1.8	2.0	2.2	2.1	2.0	2.0	1.5	1.5
Novi Pazar	2.1	2.4	2.5	2.2	1.6	0.9	0.6	0.4
Raška	3.3	3.7	3.9	3.5	2.7	2.2	1.8	1.3
Brus	1.8	2.0	2.3	2.1	1.7	1.4	1.2	0.9
Kuršumljija	2.3	2.5	2.3	1.7	0.7	0.6	0.4	0.3
Medveđa	3.3	3.6	3.5	2.8	2.3	1.0	1.0	0.3
Lebane	3.3	3.5	3.5	2.3	1.5	1.0	0.6	0.3
Leskovac	2.6	3.0	2.9	2.3	1.4	1.0	0.7	0.5
Vranje	3.0	3.4	3.1	2.5	1.6	1.0	0.4	0.3
Bujanovac	6.4	6.9	7.5	8.2	8.4	7.7	7.0	-
Preševo	5.1	5.3	5.7	5.1	3.7	4.3	3.2	-
Total	3.3	3.6	3.7	3.3	2.6	2.2	1.8	-

Source of data: Statistical Office of the Republic of Serbia.

The overall population density in the research area increased in the post-war period from 3.3 ft./Km² to 3.7 ft./Km². From 1961 to 2011, the population density was in steady decline. Differences in the change of population in municipalities along the administrative line towards Kosmet, have influenced the different density. The highest population density was in settlements Bujanovac (7.0%) and Presevo (3.2%) and in 7 municipalities (Kursumlija, Medvedja, Lebane, Leskovac, Vranje and Tutin) the density was less than 1 ft./Km², while Raska had 1.3 inh./km², and Bruce 1.5 ft./km².

Results of research survey of households in rural areas, as potential carriers of the future economic development

In summer 2015, we conducted research in 315 households with 512 people in 29 rural settlements of Kursumlija and Brus along the administrative line of Serbia towards province of Kosovo and Metohija. The study consists of a questionnaire containing 20 different questions to which respondents choose one of the few offered answers or gives a short responses according to their own views and opinions. The survey was conducted randomly.

In 55% of surveyed households women dominated. Most households (80%) are older people (65 and over). The largest number of respondents live in the same place where they are born, and 20% are migrants from other neighboring places. In 85% the household is composed of two members. The main occupation to all respondents is agriculture (farming, fruit growing and livestock breeding). In the settlements located on the Kopaonik, in about 10 households one member is

employed at the mine "Trepca", which is located along the administrative line. About 40% of examinee said that by agriculture can earn a decent living.

The main disadvantage to the most households in such a settlements are roads, because the connection to the town is very difficult, as well as objects of health and social care. Migration of the young and working population is constant since 80's of the last century, mostly because of education and seeking for the employment. Complete migration of the households started in 1999., after the war between the Serbs and Albanians (Rastelica, Vukojevac, Vasiljeva, Mačja Stena, Merdare, Orlovac, Tačevac).

In the research are included seasonal returnees, through an interview. Those households usually are engaged with vegetable farming and production of berries (blackberries and raspberries), what is a good opportunity for additional earnings. Many old households are revitalizing, and some of them near Blazevo and the Lukovska spa plan to have a touristic offer. In the majority of households people are aware that in rural areas money can be earned from agriculture. Dealing with the production of vegetables and berries, as well as their processing into finished products, they would be able to create a stock of healthy food in the easiest and cheapest way and to offer to the customers. The market for these products exists because along the administrative line there are many famous tourist centers (Jošanička Spa, Kopaonik-centre, Brzeće, Lukovska Spa, Kuršumlijska Spa, Devil City, Prolom Spa, Sijarinska Spa). They are all agree that they need stimulating help from competent authorities to enable them to

rebuild their households and to open a few ethnic restaurants, which would be located in attractive areas. Most households are located near Brzeća, Lukovska Spa and Devil City. The owners think that the experiences gained from the spa resorts, could be used for the development of rural tourism, with some additional advices from more experienced hosts. Reconstruction and construction of the local road network is necessary at this moment.

SWOT analysis

The word „SWOT“ is formed from the initial letters of four English words:: „Strength“, „Weaknesses“, „Opportunities“ and „Threats“. The meanings of these words are based on identifying key strengths, weaknesses and opportunities which the space along the administrative line of Serbia towards the province of Kosovo and Metohija can use, as well as the threats which can have negative influence on the future development of rural settlements in this area.

BENEFITS	INCONVINIENCES
<ul style="list-style-type: none"> • Peace in the region; • Visa liberalization; • Beginning of the EU integration process; • The consent of all political parties in Serbia on the necessity of revitalizing rural communities; • The necessity of regionalization in Serbia, which is of particular importance for the development of marginal areas; • The area is rich with natural wealths; • People are willing to be involved in the education about the modern trends for development of agriculture and tourism; • Collection and processing of medicinal herbs and forest products can improve the economic development; • Production of souvenirs and home-made products can improve the local economic development; • Expressed hospitality of the population; • Tradition; • Habits; • Infrastructure development and the big number of touristic geo-localities; • Preservation of natural environment. 	<ul style="list-style-type: none"> • Expressed centralization in Serbia; • Expressed political instability • Lack of political will for comprehensive plan for the development of marginal areas in Serbia; • That is the least developed area in Serbia; • Low-investment due to lack of funding from local governments and NIP; • The expressed population migration; • Comprehensive migration has created large empty spaces; • The negative rate of natural increase and expressed migration of young, working people, leads to aging of population; • Insufficient expertise of workers; • Uncertainty in new business investment; • Lack of interest of the local population for the reconstruction of existing rural buildings in order to develop rural tourism; • The necessity of revitalizing the infrastructure; • Insufficient access to information (Postal services, Internet ...); • Uncontrolled deforestation.
OPPORTUNITIES	THREATS
<ul style="list-style-type: none"> • Availability of funding from development programs in agriculture, rural areas and environmental protection; • Encourage the development of private entrepreneurship and handicraft production, through institutional and financial support; • Support of self-employment and employment by providing subsidies to employers to create new job positions; • Creation of adequate and sustainable conditions for agricultural development; • Processing of final agricultural products at the small family farms; • Strategic organization and association of agricultural producers through various forms of business cooperation, associations and cooperatives; • Revitalization and extension of 	<ul style="list-style-type: none"> • The current turbulence in the economic system of the country caused by the global economic crisis, the recession of the economy and political situation; • The slow process of adoption of the development programs and implementation of the inadequate measures that are not according the sustainable rural and agricultural development; • Non-sustainable sources of financial funding, technological backwardness and lack of competitiveness of agriculture; • Undeveloped and unorganized market of agricultural products; • The inconsistent policy of agricultural support (unstable and insufficient support from the state agricultural budget for investments in agriculture and processing of agricultural products); • Frequent migration of unemployed persons to urban centers in Serbia;

irrigation systems; • Improvement of agricultural advisory services and application of the good agricultural practices in land management; • Branding of agricultural products and their promotion on the market; • More rational and efficient use of available meadows and pastures in the development of animal husbandry.	• Disrepair farmland and reduced soil fertility; • A small percentage of farms ensure their crops.
--	---

5. CONCLUSION

Contemporary demographic changes, influenced by numerous factors and political instability, in correlation with low economic development had largely effected the current situation. The population in the area along the administrative line migrated to urban centers, from the higher mountain areas to the lower and developed parts of the region. In order to prevent further discharge of this area it is necessary to consider the real possibilities for economic development. Priority must be infrastructure, which is the basis of development. The higher mountain areas population should be encouraged in the development of animal husbandry, organic farming and conservation of native species. Abandoned mines, located in the villages of the municipality Kursumlija, Brus and Raska should be re-activated. Also, in towns near the highways the development of industries, based on natural resources should be achieved.

These methods (SWOT Statistical and GIS analysis) we can use for investigation of some new regions with similar thematic. The statistical approach we can complete with a geo-statistical and demographic calculation with fresh data. In that way, we can find some socio-demographic low in the territory of whole Serbia.

REFERENCES

- Bhaumik, K.S., Gang, N.I., & Myeong-Su, Y. 2006. Ethnic conflict and economic disparity: Serbians and Albanians in Kosovo. *Journal of Comparative Economics*, 34, pp. 754-773. doi:10.1016/j.jce.2006.07.002.
- Census. 2002. Households according to farm ownership and number of members: Data by settlements. In *List of Books census and other demographic publications*.
- Census. 2014. Comparative population 1948, 1953, 1961, 1971, 1981, 1991, 2002 and 2011. In *2011 Books census and other demographic publications*. Book 20, September 30.
- Census. 2014. Comparison of households and dwellings, 1948, 1953, 1961, 1971, 1981, 1991, 2002 and 2011. In *2011 Books census and other demographic publications*. Book 21, September 30.
- Coleman, D. 2015. Migrants and Migration in Europe. *International Encyclopedia of the Social & Behavioral Sciences*, 2nd ed., pp. 376-388. doi:10.1016/B978-0-08-097086-8.31122-9.
- Cvijić, J. 1922. *Balkansko poluostrvo i južnoslovenske zemlje*. Beograd. knj. 1..
- Cvijić, J. 2010. *Naučne sinteze*. Beograd: Imperija knjiga.
- Darlas, A. 1995. The earliest occupation in Europe: The Balkans. . In: W. Röhröks& T. van Kolfschoten Eds., *The Earliest Occupation of Europe. Proceedings of the European Science Foundation Workshop*, Tautavel, France. Leiden: University of Leiden., pp. 51-59.
- Heleniak, T. 2015. Population Change in the Former Communist States of Europe and Asia. In *International Encyclopedia of the Social & Behavioral Sciences*, 2nd ed., pp. 545-552. doi:10.1016/B978-0-08-097086-8.31037-6.
- Jotic, R., & Vukojicic, M. 2004. Witness of the centuries, Review of the history of blazevacki region and primary school "Vuk Karadzic". Blazovo.
- Miletic, R., Todorovic, M., & Miljanović, D. 2009. Access to undeveloped areas in regional development of Serbia. *Journal of the Geographical Institute "Jovan Cvijić"*, SASA, 59(2), pp. 149-171.
- Milincic, A.M. 2001. Settlements of municipality Brus (58 entries). In *Geographical Encyclopedia of Serbian settlements*, Scientific monography. Belgrade: Belgrade University-Department of Geography / Agena / Strucna knjiga., pp. 241-258. Volume I.
- Milincic, A.M., & Rosic, M. 2001. Settlements of municipality of Raska (61 entries). In *Geographical Encyclopedia of Serbian settlements*, Scientific monography. Belgrade: Belgrade University-Department of Geography / Agena / Strucna knjiga., pp. 429-451. Volume III.
- Milicic, D. 2003. Settlements without inhabitants in the 2002 Census: The result of depopulation in the twentieth century. *The Regional Development and Demographic Trends of the Balkan countries*. Nis: Faculty of Economics., pp. 339-344. No. 8.
- Nelles, W. 2005. Education, underdevelopment, unnecessarywar and human securityin

- Kosovo/Kosova. *International Journal of Educational Development*, 25, pp. 69-84. doi:10.1016/j.ijedudev.2004.07.001.
- Republic Institute for Statistics. . The territorial organization of the Republic of Serbia.
- Skoulikidis, N.T., Zogaris, S., Economou, A.N., & Gritzalis, K.C. 2009. Rivers of the Balkans. In *Rivers of Europe.*, pp. 421-466. Chapter 11. doi:10.1016/B978-0-12-369449-2.00011-4.
- Sacirovic, C. 2002. Settlements of Tutin municipality. *Geographical Encyclopedia of Serbian settlements*. University of Belgrade, Faculty of Geography.
- Vukoičić, D. 2014. Tourist valorization of urban, spas and rural settlements of Gornja Toplica. *Kosovska Mitrovica: University of Pristina, temporarily seated in Kosovska Mitrovica-Faculty of Science.*

* E-mail: danijela.vukoicic@pr.ac.rs

HK DISTRIBUTION MODEL FOR ATMOSPHERIC TURBULENCE CHANNEL UNDER THE INFLUENCE OF POINTING ERRORS

Marko Smilić^{1*}, Stefan Panić¹, Milan Savić¹, Petar Spalević², Dejan Milić³

¹Faculty of Natural Sciences and Mathematics, University of Priština, Kosovska Mitrovica, Serbia.

²Faculty of Technical Sciences, University of Priština, Kosovska Mitrovica, Serbia.

³Faculty of Electronic Engineering, University of Niš, Niš, Serbia.

ABSTRACT

In this paper, HK statistical model is considered. The application of HK distribution in modeling atmospheric turbulence channel under the influence of strong and weak turbulences and all irradiance fluctuations are discussed. Expression for atmospheric turbulence channel model, pointing error models and path loss are given. Probability density functions (PDF) for both pointing error models (zero boresight and nonzero

boresight) are calculated and graphically represented. Also, average bit-error-rate (BER) for zero boresight pointing error and nonzero boresight pointing error are calculated and graphically represented. Closed form expression for PDF and BER are given. Impact of zero boresight pointing error and nonzero boresight pointing error on transmission over atmospheric turbulence channel in FSO system is explained.

Key words: HK distribution model, FSO system, BER, PDF, Pointing error model.

1. INTRODUCTION

In last few years, atmospheric optical communications have become a subject of large interest. The reasons for these interests are simple because FSO system provide high security, high transmission capacity, low power and low cost characteristics in comparison with classical radio communications technologies (Heatley et al., 1998), (Jurado-Navas et al., 2012). For all of these advantages, FSO systems are the subject of bigger investigations and implementations. Atmospheric turbulence causes fluctuations in both the intensity and the phase of the received signal due to variations in the refractive index along the propagation path (Karp et al., 1988).

Many statistical models have been proposed to describe this fluctuation in both weak and strong fading regimes (Al-Habash et al., 2001). General Malaga distribution (Jurado-Navas et al., 2011) can be reduced to other distribution models such as Gamma-Gamma distribution model (Harilaos et al., 2009), K distribution model (Jakerman, 1980), Lognormal distribution model (Zhu & Kahn, 2002), HK distribution model (Destremes et al., 2013), Rice-Nakagami distribution model (Tsiftsis et al., 2009). In addition to the turbulence, there are other scenario that affect the transmission link between transmitter and

receiver such as building sway and other constructions in urban areas. Weather conditions also affect on the quality and speed of transmission link (Andrews & Philips, 1998). All of these lead to irradiance, misalignment (pointing error) between transmitter and receiver, scintillation and path loss. These scenarios affect on quality and speed of transmission link and channel capacity (Ansari et al., 2015).

In this paper, we considered influence of zero boresight pointing error and nonzero pointing error on transmission link over atmospheric channel under the strong and weak turbulences.

In addition to atmospheric channel model, we have presented pointing error models. Also, closed form expression for PDF and BER for HK model under the influence of zero boresight pointing error and nonzero boresight pointing error are calculated and graphically represented.

2. SYSTEM MODEL

Laser beams propagate along a horizontal path through a turbulence channel governed by an HK distribution in the presence of pointing errors (Peppas & Mathiopoulos, 2015). The received photocurrent signal is related to the incident optical power by the

detector responsivity R . It is assumed that the receiver integrates the photocurrent for each bit period and removes any constant bias due to background illumination (Farid & Hranilovic, 2007). The received signal y suffers from a fluctuation in signal intensity due to atmospheric turbulence and misalignment, as well as additive noise, and can be well modeled as:

$$y = I(t)RP_T + n. \quad (1)$$

where P_T is the transmitted intensity, $I(t)$ is the channel state, y is the resulting electrical signal, and n is signal-independent additive white Gaussian noise with variance.

The channel state $I(t)$ models the random attenuation of the propagation channel. In our model, $I(t)$ arises due to three factors: path loss $I_l(t)$, geometric spread and pointing errors $I_p(t)$, and atmospheric turbulence $I_a(t)$. The channel state can be formulated as:

$$I(t) = I_a(t)I_p(t)I_l(t). \quad (2)$$

The HK distribution model can be obtained as a special case of Malaga distribution model. Malaga distribution model is given in (Tsiftsis et al., 2009) as:

$$f_{I_a}(I_a) = A \sum_{k=1}^{\beta} a_k I_a^{\frac{\alpha+k}{2}-1} K_{\alpha-k} \left(2\sqrt{\frac{\alpha\beta I_a}{\gamma\beta + \Omega}} \right). \quad (3)$$

For Malaga distribution model is valid $I = |U_L + U_S^C + U_S^G| e^{2X} = YX$ where $X = e^{2Z}$ and $Y = |U_L + U_S^C + U_S^G|$ what is explained in (Jurado-Navas et al., 2012). Setting by $\rho = 0$, $X = \gamma$ and $\text{Var}[G] = 0$ we obtained HK distribution model where are

$$\gamma = 2b_0(1 - \rho). \quad \text{and}$$

$\Omega = \Omega + \rho 2b_0 + 2\sqrt{2b_0\rho\Omega} \cos(\phi_L - \phi_C)$ and $K_v(\cdot)$ is the modified Bessel function of the second kind and v order. Using this conditions, we find that the HK distribution model is given:

$$f_{I_a}(I_a) = A \sum_{k=1}^{\beta} a_k I_a^{\frac{\alpha+k}{2}-1} K_{\alpha-k} \left(2\sqrt{\frac{\alpha\beta I_a}{2b_0\beta + \Omega}} \right). \quad (4)$$

where

$$A \triangleq \frac{2\alpha^{\frac{\alpha}{2}}}{(2b_0)^{1+\frac{\alpha}{2}} \Gamma(\alpha)} \left(\frac{2b_0\beta}{2b_0\beta + \Omega} \right)^{\beta+\frac{\alpha}{2}}. \quad (4.1)$$

Information technologies

$$a_k \triangleq \frac{(\beta-1)}{(k-1)} \frac{(2b_0\beta + \Omega)^{1-\frac{k}{2}}}{\Gamma(k)} \left(\frac{\Omega}{2b_0} \right)^{k-1} \left(\frac{\alpha}{\beta} \right)^{\frac{k}{2}}. \quad (4.2)$$

We have already explained what occurs due to the pointing errors. We consider two cases. In the first case, we consider zero boresight pointing error. Zero boresight pointing error is given:

$$f_{I_p}(I_p) = \frac{g^2}{A_0^{g^2}} I_p^{g^2-1}, \quad 0 \leq I_p \leq A_0. \quad (5)$$

where $g = \omega_{zeq}/2\sigma_s$ is the ratio between the equivalent beam radius at the receiver ω_{zeq} and the pointing error displacement standard deviation at the receiver σ_s . $A_0 = (\text{erf}(v))^2$ is the fraction of the collected power where $v = \sqrt{\pi}a/\sqrt{2}\omega_z$ with $\text{erf}(\cdot)$ denoting the error function, whereas the square of the equivalent beam width is given by:

$$\omega_{zeq}^2 = \omega_z^2 \frac{\sqrt{\pi} \text{erf}(v)}{2ve^{-v^2}}. \quad (6)$$

In the second case, we consider nonzero boresight pointing error. Nonzero boresight pointing error is given:

$$f_{I_p}(I_p) = \frac{g^2 e^{-\frac{s^2}{2\sigma_s^2}}}{A_0^{g^2}} I_p^{g^2-1} I_0 \left(\frac{s}{\sigma_s^2} \sqrt{\frac{-\omega_{zeq}^2 \ln\left(\frac{I_p}{A_0}\right)}{2}} \right). \quad (7)$$

where s is the boresight displacement, σ_s^2 is the jitter variance at the receiver, $I_0(\cdot)$ is the modified Bessel function of the first kind with order zero.

I_l denotes the atmospheric attenuation, which can be described by the exponential Beers–Lambert Law as:

$$I_l(z) = e^{-\sigma z}. \quad (8)$$

where where z denotes the propagation distance and σ is the attenuation coefficient.

After defining both pointing error models, we can calculate the probability density functions. PDF is obtained by calculating the mixture of the two distributions presented above in equations (4) and (5) or equations (4) and (7).

$$f_I(I) = \int_0^\infty f_{I|I_a}(I|I_a) f_{I_a}(I_a) dI_a. \quad (9)$$

where $f_{I|I_a}(I|I_a)$ is the conditional probability given a turbulence state, I_a , and it is expressed as:

$$f_{I|I_a}(I|I_a) = \frac{g^2}{A_0 g^2 I_a} \left(\frac{I}{I_a} \right)^{g^2-1}, 0 \leq I \leq A_0 I_a. \quad (10)$$

for zero boresight pointing error and:

$$f_{I|I_a}(I|I_a) = \frac{g^2 e^{-\frac{s^2}{2\sigma_s^2}}}{A_0 g^2 I_a I_l} \left(\frac{I}{I_a I_l} \right)^{g^2-1} \times \\ \times I_0 \left(\frac{s}{\sigma_s^2} \sqrt{\frac{-\omega_{zeq}^2 \ln \left(\frac{I}{A_0 I_a I_l} \right)}{2}} \right), 0 \leq I \leq A_0 I_a I_l. \quad (11)$$

for nonzero boresight pointing error.

Substituting expression (10) in (9) we get expression for PDF for zero boresight pointing error which is represented as:

$$f_I(I) = \frac{g^2 A}{A_0 g^2} I^{g^2-1} \sum_{k=1}^{\beta} a_k \times \\ \int_{\frac{I}{A_0}}^{\infty} I_a^{\frac{\alpha+k}{2}-1-g^2} K_{\alpha-k} \left(2 \sqrt{\frac{\alpha \beta I_a}{2b_0 \beta + \Omega}} \right) dI_a. \quad (12)$$

After solving integral from equation (12) according to (Wolfram (07.34.21.0085.01)) where the modified Bessel function of the second kind, $K_\nu(\cdot)$ can be expressed as a special case of the Meijer G function, given by the following relationship (Prudnikov et al., 2003) we obtained closed form expression for PDF for zero boresight pointing error.

$$f_I(I) = \frac{g^2 A}{2} I^{-1} \sum_{k=1}^{\beta} a_k \left(\frac{\alpha \beta}{2b_0 \beta + \Omega} \right)^{-\frac{\alpha+k}{2}} \times \\ G_{1,3}^{3,0} \left(\frac{\alpha \beta}{2b_0 \beta + \Omega} \frac{I}{A_0} \middle| g^2 + 1 \right). \quad (13)$$

Substituting expression (11) in (9) we get expression for PDF for nonzero boresight pointing error which is represented as:

$$f_I(I) = \frac{g^2 A e^{-\frac{s^2}{2\sigma_s^2}}}{(A_0 I_l)^{g^2}} I^{g^2-1} \sum_{k=1}^{\beta} a_k \times \\ \int_{\frac{I}{A_0 I_l}}^{\infty} I_a^{\frac{\alpha+k}{2}-1-g^2} K_{\alpha-k} \left(2 \sqrt{\frac{\alpha \beta I_a}{2b_0 \beta + \Omega}} \right) \times \\ I_0 \left(\frac{s}{\sigma_s^2} \sqrt{\frac{-\omega_{zeq}^2 \ln \left(\frac{I}{A_0 I_a I_l} \right)}{2}} \right) dI_a. \quad (14)$$

After solving integral from equation (14) we obtained closed form expression for PDF for nonzero boresight pointing error.

$$f_I(I) = \frac{2\pi g^2 A e^{-\frac{s^2}{2\sigma_s^2}}}{\omega_{zeq}^2} I^{g^2-1} \sum_{k=1}^{\beta} \frac{a_k I^{\frac{\alpha+k}{2}-1}}{(A_0 I_l)^{\frac{\alpha+k}{2}} \sin(\pi(\alpha-k))} \times \\ \sum_{p=0}^P \left[\frac{\left(\frac{\alpha \beta I}{(2b_0 \beta + \Omega) A_0 I_l} \right)^{p+\frac{\alpha-k}{2}}}{\Gamma(p-(\alpha-k)+1) p!} \left(-\frac{\omega_{zeq}^2}{4(p+k-g^2)} e^{-\frac{\omega_{zeq}^2 s^2}{8(p+k-g^2)\sigma_s^4}} \right) - \right. \\ \left. \frac{\left(\frac{\alpha \beta I}{(2b_0 \beta + \Omega) A_0 I_l} \right)^{p+\frac{\alpha-k}{2}}}{\Gamma(p+(\alpha-k)+1) p!} \times \left(-\frac{\omega_{zeq}^2}{4(p+\alpha-g^2)} e^{-\frac{\omega_{zeq}^2 s^2}{8(p+\alpha-g^2)\sigma_s^4}} \right) \right]. \quad (15)$$

The study of the Average BER of the HK probability distribution in the presence of misalignment fading is considered. First of all, we have defined expression for ABER over BFSK modulation format (Panić et al., 2013), (Stefanović et al., 2015), (Golubović et al., 2014), (Cvetković et al., 2013).

$$P_e = \int_0^{\infty} \frac{1}{2} \operatorname{erfc} \left(\frac{P_T R}{\sigma_N} I \right) f_I(I) dI. \quad (16)$$

where $\operatorname{erfc}(\cdot)$ is related to the complementary error function. If we represented $\operatorname{erfc}(\cdot)$ as special case of MeijerG function according to (Prudnikov et al., 2003) and substituting in (16) along with expression (13), integral from (16) can be solved from relation (Wolfram (07.34.21.0013.01)). Closed form expression for zero boresight pointing error for ABER is given:

$$P_e = \frac{2^\alpha g^2 A \left(\frac{2b_0 \beta + \Omega}{\alpha \beta} \right)^{\frac{\alpha}{2}}}{32\pi \sqrt{\pi}} \sum_{k=1}^{\beta} 2^k \left(\frac{2b_0 \beta + \Omega}{\alpha \beta} \right)^{\frac{k}{2}} a_k \times \\ \times G_{7,4}^{2,6} \left(\frac{8R^2 P_T^2 A_0^2}{\sigma_N^2} \left(\frac{2b_0 \beta + \Omega}{\alpha \beta} \right)^2 \middle| \right. \\ \left. \left| \frac{1-g^2}{2}, \frac{2-g^2}{2}, \frac{1-\alpha}{2}, \frac{2-\alpha}{2}, \frac{1-k}{2}, \frac{2-k}{2}, 1 \right|, \right. \\ \left. \left| 0, \frac{1}{2}, \frac{-g^2}{2}, \frac{1-g^2}{2} \right| \right). \quad (17)$$

3. NUMERICAL RESULTS

Capitalizing on presented expressions we have efficiently evaluated and graphically presented ABER over BFSK modulation format for both zero and non-zero boresight pointing scenarios in the function of FSO propagation link parameters.

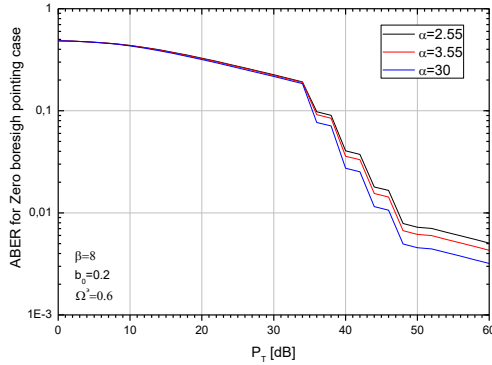


Fig. 1 ABER for Zero boresight pointing case.

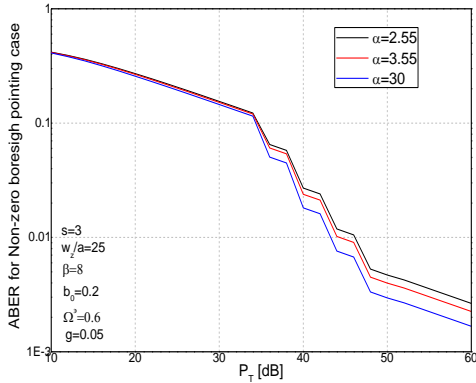


Fig. 2 ABER for Non-zero boresight pointing case.

It is visible from Figs 1-2 that better system performances are obtained for higher values of α parameter, i.e. for less severe scattering of FSO waves. α is a positive parameter related to the effective number of large-scale cells of the scattering process.

5. CONCLUSION

In this paper, two analytical closed-form representations for the ABER performance of an AOC system operating over a generalized turbulence in the presence of pointing errors are derived. Also, two analytical closed-form representations for the PDF are derived. Numerical results are graphically represented.

REFERENCES

- Al-Habash, M.A., Andrews, L.C., & Philips, R.L.. Mathematical model for the irradiance probability density function of a laser propagating through turbulent media. *Optical Engineering*, 40(8), pp. 1554-1562.
- Ansari, I.S., Yilmaz, F., & Alouini, M. 2015. Performance Analysis of Free-Space Optical Links Over Malaga (M) Turbulence Channels with Pointing Errors. *IEEE Transactions on Wireless Communications*, 15(1), pp. 91-102.
- Andrews, L.C., & Phillips, R.L. 1998. *Laser Beam Propagation Through Random Media*. SPIE.
- Cvetkovic, A., Milic, D., & Stefanovic, M. 2013. Outage Performance of Dual-Hop AF Relay Channels with Co-Channel Interferences over Rayleigh Fading. *Wireless Personal Communications*, 70(4), pp. 1993-2006.
- Destremes, F., Poree, J., & Cloutier, G. 2013. Estimation Method of the Homodyned K-Distribution Based on the Mean Intensity and Two Log-Moments. *SIAM Journal Imaging Sciences*, 6(3), pp. 1499-1530.
- Farid, A.A., & Hranilovic, S. 2007. Outage Capacity Optimization for Free-Space Optical Links With Pointing Errors. *Journal of Lightwave Technology*, 25(7), pp. 1702-1710. doi:10.1109/JLT.2007.899174.
- Golubovic, A., Sekulovic, N., Stefanovic, M., Milic, D., & Temelkovski, I. 2014. Performance Analysis of Dual-Branch Selection Diversity Receiver that Uses Desired Signal Algorithm in Correlated Weibull Fading Environment. *Technical Gazette*, 21(5), pp. 953-957.
- Heatley, D.J.T., Wisely, D.R., Neild, I., & Cochrane, P. 1998. Optical wireless: The story so far. *IEEE Communications Magazine*, 36(12), pp. 72-82. doi:10.1109/35.735881.
- Jakeman, E. 1980. On the statistics of K-distributed noise. *Journal of Physics A: Mathematical and General*, 13(1), pp. 31-48.
- Jurado-Navas, A., Garrido-Balsells, J.M., Paris, J.F., Castillo-Vázquez, M., & Puerta-Notario, A. 2012. Impact of pointing errors on the performance of generalized atmospheric optical channels. *Opt Express*, 20(11), pp. 12550-62. pmid:22714243.
- Jurado-Navas, A., Garrido-Balsells, J.M., Paris, J.F., & Puerta-Notario, A. 2011. A unifying statistical model for atmospheric optical scintillation, *Numerical Simulations of Physical and Engineering Processes*, pp. 181-206.
- Karp, S., Gagliardi, R., Moran, S., & Stotts, L. 1988. *Optical Channels*. New York: Plenum.
- Prudnikov, A.P., Brychkov, Y.A., & Marichev, O.I. 2003. *Integral and Series*, 2nd ed. Moskva: Fizmatlit.
- Panić, S., Stefanović, M., Anastasov, J., & Spalević, P. 2013. *Fading and Interference Mitigation in Wireless Communications*. CRC Press.

- Peppas, K.P., & Mathiopoulos, P.T. 2015. Free-Space Optical Communication With Spatial Modulation and Coherent Detection Over H-K Atmospheric Turbulence Channels. *Journal of Lightwave Technology*, 33(20), pp. 4221-4232.
- Sandalidis, H.G., Tsiftsis, T.A., & Karagiannidis, G.K. 2009. Optical Wireless Communications With Heterodyne Detection Over Turbulence Channels With Pointing Errors. *Journal Of Lightwave Technology*, 27(20), pp. 4440-4445.
- Stefanovic, M., Anastasov, J., Cvetkovic, A., & Djordjevic, G. 2015. Outage performance of dual-hop relaying systems over extended generalized-K fading channels. *Wireless Communications & Mobile Computing*, 15(18), pp. 2141-2149.
- Tsiftsis, T.A., Sandalidis, H.G., Karagiannidis, G.K., & Uysal, M. 2009. Optical wireless links with spatial diversity over strong atmospheric turbulence channels. *IEEE Transactions on Wireless Communications*, 8(2), pp. 951-957. doi:10.1109/TWC.2009.071318.
- Wolfram... Retrieved from: <http://functions.wolfram.com/>
- Zhu, X., & Kahn, J.M. 2002. Free-space optical communication through atmospheric turbulence channels. *IEEE Transactions on Communications*, 50(8), pp. 1293-1300. doi:10.1109/TCOMM.2002.800829.

* E-mail: marko.smilic@pr.ac.rs

THE LCR OF WIRELESS MACRODIVERSITY SSC RECEIVER IN THE PRESENCE OF GAMMA SHADOWED KAPPA-MU FADING

Časlav Stefanović¹, Danijel Došić^{1*}

¹Faculty of Natural Sciences and Mathematics, University of Priština, Kosovska Mitrovica, Serbia.

ABSTRACT

Wireless mobile macrodiversity (MaD) radio system with switch and stay (SSC) receiver and two microdiversity (MiD) selection combining (SC) branches operating over Gamma shadowed Kappa-Mu (k - μ) multipath fading environment is considered. Novel, one-folded integral expression

for average level crossing rate (LCR) of MaD SSC receiver output signal envelope is obtained. Numerical results of the proposed model are presented and discussed in relation to the system model parameters.

Key words: LCR, MaD, MiD, multipath, shadowing.

1. INTRODUCTION

Macrodiversity (MaD) system consisting of MaD receiver and two or more microdiversity (MiD) branches is often proposed in the literature ((Shankar, 2009), (Mukherjee & Avidor, 2003), (Basnayaka et al., 2013)).

Moreover, multipath fading can be mitigated by MiD receivers at single BSs (base stations) while shadowing can be mitigated by MaD receiver combining signals from two or more BSs. It is important to note that multipath fading is caused by physical phenomena such as reflection, refraction and scattering of radio waves while shadowing is caused by obstacles between transmitter and receiver.

MaD switch and stay (SSC) system with MiD selection combining (SC) as well as MaD SC system with MiD maximal ratio combining (MRC) or SC can be efficiently applied in composite fading environment to improve performances of wireless communication system as shown in ((Stefanović, 2015), (Djosic et al., 2016), (Stefanović et al., 2016), (Panić et al., 2011), (Stamenović et al., 2014)).

The Kappa-Mu (κ - μ) distribution describes signal envelope variation in line-of-sight (LoS) multipath fading channels when signals propagate in the environment with two or more clusters. Parameter k is known as Rician factor and can be calculated as the ratio of dominant components power and scattering components power while parameter μ is related to the number of clusters in the propagation environment. Moreover, kappa-mu is general distribution, which

means that for different values of κ and μ , Rayleigh, Rice and Nakagami- m distributions can be derived. Moreover, this distribution fits well with experimental data and is often applied in multipath environment ((Yacoub, 2007), (Paris, 2014), (Stefanović et al., 2015)).

Log-normal distribution and Gamma distribution are used for the purpose of describing shadowing in wireless communication channel.

In this paper, MaD system has been modeled with switch and stay (SSC) receiver at macro level and two dual branch selection combining (SC) at micro level, since its relatively low implementation complexity. Moreover, SC and SSC are often considered diversity techniques ((Zhang et al., 2014), (Milic et al., 2016), (Stefanovic et al., 2013), (Zhao et al., 2015)). Gamma distribution is proposed, with the tendency of obtaining closed form solutions due to its mathematical tractability. Moreover, the average level crossing rate (LCR) of MaD SSC receiver output signal envelope in the presence of Gamma shadowed k - μ multipath fading is efficiently calculated in the form of the sum of one-folded integral. Numerical results are presented graphically and the effect of Rician factor, multipath fading severity parameter, shadowing severity parameter, correlation coefficient and threshold of SSC on the proposed MaD model are examined.

2. SYSTEM MODEL

The MaD system with two MiD SC parts under the influence of Gamma shadowed k - μ multipath fading as shown on Fig. 1. is considered. Operation is the following: when signal envelope average power at the inputs of the first SC, Ω_1 is higher than a specified threshold, Ω_T , MaD SSC selects the first SC to process the signal to the receiver. Contrary, when Ω_1 is lower than Ω_T , SSC selects the second MiD SC to provide the signal path. At the micro level, MiD SC selects the branch with the highest signal envelope power to provide the signal to receiver.

Input signal envelopes for the first MiD path are denoted with y_{11} and y_{12} , while the second MiD input signal envelopes are denoted with y_{21} and y_{22} . Further, the output signal envelopes of the first and second MiD combiners are y_1 and y_2 , respectively, while signal envelope at the output of MaD SSC is denoted with y .

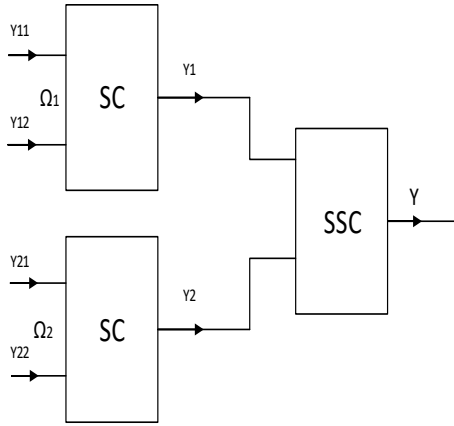


Fig. 1 The MaD system with MaD SSC structure and two MiD SC parts.

Probability density function (PDF) of κ - μ signal envelope at the inputs of the first SC are respectively (Panic et al., 2013):

$$p_{y_{li}}(y_{li}) = \frac{2\mu(k+1)^{\frac{\mu+1}{2}}}{k^{\frac{\mu-1}{2}} e^{k\mu\Omega_1^{\frac{\mu+1}{2}}} y_{li}^{\mu} I_{\mu-1} \left(2\mu \sqrt{\frac{k(k+1)}{\Omega_1}} \right) \cdot e^{-\frac{\mu(k+1)}{\Omega_1} y_{li}^2}, \quad i = 1, 2. \quad (1)$$

where, κ is Rice factor, μ is fading severity factor, Ω_1 is related to the local mean power of y_{li} and $I_{\nu}(\cdot)$ is the modified Bessel function of the first kind and order ν (Stefanovic et al., 2013). The $I_{\nu}(\cdot)$ can be transformed by utilization (Gradshteyn & Ryzhik,

2000), so that the CDF expression of k - μ signal envelope at the inputs of the first SC can be expressed as (Stüber, 1996):

$$F_{y_{li}}(y_{li}) = \int_0^{y_{li}} p_{y_{li}}(t) dt = \frac{2\mu(k+1)^{\frac{\mu+1}{2}}}{k^{\frac{\mu-1}{2}} e^{k\mu\Omega_1^{\frac{\mu+1}{2}}} \cdot \sum_{j=1}^{\infty} \left(\mu \sqrt{\frac{k(k+1)}{\Omega_1}} \right)^{2j+\mu-1} \frac{1}{2} \left(\frac{\Omega_1}{\mu(k+1)} \right)^{j+\mu} \cdot \frac{1}{j! \Gamma(j+\mu)} \gamma \left(j+\mu, \frac{\mu(k+1)}{\Omega_1} y_{li}^2 \right). \quad (2)$$

where Ω_1 is signal envelope average power at input of first micro-diversity SC and $\gamma(m, x)$ is incomplete Gamma function. CDF of the first SC output signal envelope is:

$$F_{y_1}(y_1) = F_{y_{11}}(y_1) F_{y_{12}}(y_1) = \left(\frac{2\mu(k+1)^{\frac{\mu+1}{2}}}{k^{\frac{\mu-1}{2}} e^{k\mu\Omega_1^{\frac{\mu+1}{2}}} \right)^2 \cdot \sum_{i_1=1}^{\infty} \left(\mu \sqrt{\frac{k(k+1)}{\Omega_1}} \right)^{2i_1+\mu-1} \frac{1}{2} \left(\frac{\Omega_1}{\mu(k+1)} \right)^{i_1+\mu} \frac{1}{i_1! \Gamma(i_1+\mu)} \cdot \gamma \left(i_1+\mu, \frac{\mu(k+1)}{\Omega_1} y_1^2 \right) \sum_{i_2=1}^{\infty} \left(\mu \sqrt{\frac{k(k+1)}{\Omega_1}} \right)^{2i_2+\mu-1} \cdot \frac{1}{2} \left(\frac{\Omega_1}{\mu(k+1)} \right)^{i_2+\mu} \frac{1}{i_2! \Gamma(i_2+\mu)} \gamma \left(i_2+\mu, \frac{\mu(k+1)}{\Omega_1} y_1^2 \right). \quad (3)$$

Similarly, CDF of SC output k - μ random variable y_2 is:

$$F_{y_2}(y_2) = F_{y_{21}}(y_2) F_{y_{22}}(y_2) = \left(\frac{2\mu(k+1)^{\frac{\mu+1}{2}}}{k^{\frac{\mu-1}{2}} e^{k\mu\Omega_2^{\frac{\mu+1}{2}}} \right)^2 \cdot \sum_{i_1=1}^{\infty} \left(\mu \sqrt{\frac{k(k+1)}{\Omega_2}} \right)^{2i_1+\mu-1} \frac{1}{2} \left(\frac{\Omega_2}{\mu(k+1)} \right)^{i_1+\mu} \frac{1}{i_1! \Gamma(i_1+\mu)} \cdot \gamma \left(i_1+\mu, \frac{\mu(k+1)}{\Omega_2} y_2^2 \right) \sum_{i_2=1}^{\infty} \left(\mu \sqrt{\frac{k(k+1)}{\Omega_2}} \right)^{2i_2+\mu-1} \cdot \frac{1}{2} \left(\frac{\Omega_2}{\mu(k+1)} \right)^{i_2+\mu} \frac{1}{i_2! \Gamma(i_2+\mu)} \gamma \left(i_2+\mu, \frac{\mu(k+1)}{\Omega_2} y_2^2 \right). \quad (4)$$

Signal envelope average power at inputs of two MiD SC structures, Ω_1 and Ω_2 are Gamma distributed ((Xekalaki et al, 2003), (Yue et al., 2001)):

$$\begin{aligned}
p_{\Omega_1\Omega_2}(\Omega_1, \Omega_2) &= \frac{(\Omega_1\Omega_2)^{\frac{c-1}{2}}}{\Gamma(c)(1-\rho^2)\rho^{c-1}\Omega_0^{c+1}} e^{-\frac{\Omega_1+\Omega_2}{\Omega_0(1-\rho^2)}} \\
&\cdot I_{c-1}\left(\frac{2\rho}{\Omega_0(1-\rho^2)} \Omega_1\Omega_2^{\frac{1}{2}}\right) = \\
&= \frac{1}{\Gamma(c)(1-\rho^2)\rho^{c-1}\Omega_0^{c+1}} \sum_{i=0}^{\infty} \left(\frac{\rho}{\Omega_0(1-\rho^2)}\right)^{2i+c-1} \\
&\cdot \frac{1}{i!\Gamma(i+c)} \Omega_1^{i+c-1} \Omega_2^{i+c-1} e^{-\frac{\Omega_1+\Omega_2}{\Omega_0(1-\rho^2)}}.
\end{aligned} \quad (5)$$

where ρ is correlation coefficient of the shadowing process, c is shadowing parameter and Ω_0 is mean value of Ω_1 or Ω_2 .

3. LCR OF MAD SSC RECEIVER OUTPUT SIGNAL

LCR of Kappa-Mu random variable y_{li} is (Panic et al., 2003):

$$\begin{aligned}
N_{y_{li}} &= \int_0^{\infty} \dot{y} p_{y_{li}\dot{y}_{li}}(y_{li}, \dot{y}_{li}) d\dot{y}_{li} = \\
&= \frac{\sqrt{2\pi} f_m 2\mu^{\frac{1}{2}} (k+1)^{\frac{\mu}{2}}}{k^{\frac{\mu-1}{2}} e^{k\mu} \Omega_1^{\frac{\mu}{2}}} \sum_{i_1=1}^{\infty} \left(\mu \sqrt{\frac{k(k+1)}{\Omega_1}}\right)^{2i_1+\mu-1} \\
&\cdot \frac{1}{i_1! \Gamma(i_1+\mu)} y_{li}^{2i_1+2\mu-1} e^{-\frac{\mu(k+1)}{\Omega_1} y_{li}^2}, \quad i = 1, 2.
\end{aligned} \quad (6)$$

where $p_{y_{li}\dot{y}_{li}}$ is joint probability density function (JPDF) of y_{li} and its derivative, f_m is maximal Doppler frequency.

Similarly, LCR of random variable y_{2i} is:

$$\begin{aligned}
N_{y_{2i}} &= \frac{\sqrt{2\pi} f_m 2\mu^{\frac{1}{2}} (k+1)^{\frac{\mu}{2}}}{k^{\frac{\mu-1}{2}} e^{k\mu} \Omega_2^{\frac{\mu}{2}}} \sum_{i_2=1}^{\infty} \left(\mu \sqrt{\frac{k(k+1)}{\Omega_2}}\right)^{2i_2+\mu-1} \\
&\cdot \frac{1}{i_2! \Gamma(i_2+\mu)} y_{2i}^{2i_2+2\mu-1} e^{-\frac{\mu(k+1)}{\Omega_2} y_{2i}^2}, \quad i = 1, 2.
\end{aligned} \quad (7)$$

Since the fading is identical and independent, JPDF of the MiD SC output signal envelope y_1 and its first derivative is:

$$\begin{aligned}
p_{y_1\dot{y}_1}(y_1, \dot{y}_1) &= p_{y_{11}\dot{y}_{11}}(y_1, \dot{y}_1) F_{y_{12}} + p_{y_{12}\dot{y}_{12}}(y_1, \dot{y}_1) F_{y_{11}}(y_1) = \\
&= 2p_{y_{11}\dot{y}_{11}}(y_1, \dot{y}_1) F_{y_{12}}(y_1).
\end{aligned} \quad (8)$$

The LCR of the first MiD SC output signal envelope y_1 is:

$$\begin{aligned}
N_{y_1} &= \int_0^{\infty} \dot{y}_1 p_{y_1\dot{y}_1}(y_1, \dot{y}_1) d\dot{y}_1 = 2F_{y_{12}}(y_1) N_{y_{11}} = \\
&= \frac{2\sqrt{2\pi} f_m \mu^{\frac{1}{2}} (k+1)^{\frac{\mu}{2}}}{k^{\frac{\mu-1}{2}} e^{k\mu} \Omega_1^{\frac{\mu}{2}}} \sum_{i_1=1}^{\infty} \left(\mu \sqrt{\frac{k(k+1)}{\Omega_1}}\right)^{2i_1+\mu-1} \\
&\cdot \frac{1}{i_1! \Gamma(i_1+\mu)} x_1^{2i_1+2\mu-1} e^{-\frac{\mu(k+1)}{\Omega_1} y_1^2} \frac{\mu(k+1)^{\frac{\mu+1}{2}}}{k^{\frac{\mu-1}{2}} e^{k\mu} \Omega_1^{\frac{\mu+1}{2}}} \\
&\cdot \sum_{i_2=1}^{\infty} \left(\mu \sqrt{\frac{k(k+1)}{\Omega_1}}\right)^{2i_2+\mu-1} \left(\frac{\Omega_1}{\mu(k+1)}\right)^{i_2+\mu} \\
&\cdot \frac{1}{i_2! \Gamma(i_2+\mu)} \gamma\left(i_2+\mu, \frac{\mu(k+1)}{\Omega_1} y_1^2\right).
\end{aligned} \quad (9)$$

The average level crossing rate of the second micro-diversity SC output signal is:

$$\begin{aligned}
N_{x_2} &= \frac{2\sqrt{2\pi} f_m \mu^{\frac{1}{2}} (k+1)^{\frac{\mu}{2}}}{k^{\frac{\mu-1}{2}} e^{k\mu} \Omega_2^{\frac{\mu}{2}}} \sum_{i_1=1}^{\infty} \left(\mu \sqrt{\frac{k(k+1)}{\Omega_1}}\right)^{2i_1+\mu-1} \\
&\cdot \frac{1}{i_1! \Gamma(i_1+\mu)} x_2^{2i_1+2\mu-1} e^{-\frac{\mu(k+1)}{\Omega_2} y_2^2} \frac{\mu(k+1)^{\frac{\mu+1}{2}}}{k^{\frac{\mu-1}{2}} e^{k\mu} \Omega_2^{\frac{\mu+1}{2}}} \\
&\cdot \sum_{i_2=1}^{\infty} \left(\mu \sqrt{\frac{k(k+1)}{\Omega_2}}\right)^{2i_2+\mu-1} \left(\frac{\Omega_2}{\mu(k+1)}\right)^{i_2+\mu} \\
&\cdot \frac{1}{i_2! \Gamma(i_2+\mu)} \gamma\left(i_2+\mu, \frac{\mu(k+1)}{\Omega_2} y_2^2\right).
\end{aligned} \quad (10)$$

LCR of MaD SSC output signal envelope is equal to LCR of the first MiD SC output signal envelope when the first MiD SC provides signal to mobile user and the total power at its inputs is higher than predetermined threshold or when the second MiD SC receiver provides signal to the mobile user and the total power at its inputs is lower than the threshold. On the other hand, LCR of MaD SSC output signal envelope is equal to LCR of the second MiD SC output signal envelope when the second MiD SC provides the signal to mobile user and the total power at its inputs is higher than the predetermined threshold or when the first MiD SC provides the mobile user and the total power at its input is lower than the predetermined threshold.

Accordingly, the LCR of MaD SSC output signal envelope is:

$$\begin{aligned}
N_x &= \frac{1}{2} \int_{\Omega_T} d\Omega_1 \int_0^\infty N_{y|\Omega_1} p_{\Omega_1\Omega_2}(\Omega_1\Omega_2) d\Omega_2 + \\
&+ \frac{1}{2} \int_0^{\Omega_T} d\Omega_1 \int_0^\infty N_{y|\Omega_2} p_{\Omega_1\Omega_2}(\Omega_1\Omega_2) d\Omega_2 + \\
&+ \frac{1}{2} \int_{\Omega_T} d\Omega_2 \int_0^\infty N_{y|\Omega_2} p_{\Omega_1\Omega_2}(\Omega_1\Omega_2) d\Omega_1 + \\
&+ \frac{1}{2} \int_0^{\Omega_T} d\Omega_2 \int_0^\infty N_{y|\Omega_1} p_{\Omega_1\Omega_2}(\Omega_1\Omega_2) d\Omega_1 = \\
&= \int_{\Omega_T} d\Omega_1 \int_0^\infty N_{y|\Omega_1} p_{\Omega_1\Omega_2}(\Omega_1\Omega_2) d\Omega_2 + \\
&+ \int_0^{\Omega_T} d\Omega_2 \int_0^\infty N_{y|\Omega_2} p_{\Omega_1\Omega_2}(\Omega_1\Omega_2) d\Omega_1 = I_1 + I_2.
\end{aligned} \tag{11}$$

where $N_{y|\Omega_1}$ and $N_{y|\Omega_2}$ LCR at the first and second input of SSC obtained in (9) and (10), respectively and $p_{\Omega_1\Omega_2}$ $\Omega_1\Omega_2$ is Gamma distribution already given in (5).

The LCR of MaD system with MaD SSC receiver and two MiD SC branches can be obtained by solving the following integrals (Gradshteyn & Ryzhik, 2000):

$$\begin{aligned}
I_1 &= \int_{\Omega_T} d\Omega_1 \int_0^\infty d\Omega_2 N_{y_1}(y|\Omega_1) p_{\Omega_1\Omega_2}(\Omega_1\Omega_2) = \\
&= \frac{2\sqrt{2\pi} f_m \mu^{\frac{3}{2}} (k+1)^{\mu+\frac{1}{2}}}{k^{\mu-1} e^{2k\mu}} \sum_{j_1=0}^{\infty} \mu \sqrt{k(k+1)}^{2j_1+\mu-1} \\
&\cdot \frac{1}{j_1! \Gamma(j_1+\mu)} y^{2j_1+2\mu-1} \sum_{j_2=0}^{\infty} \mu \sqrt{k(k+1)}^{2j_2+\mu-1} \\
&\cdot \frac{1}{j_2! \Gamma(j_2+\mu)} \left(\frac{1}{\mu(k+1)} \right)^{j_2+\mu} \frac{1}{\Gamma(c)(1-\rho^2)\rho^{c-1}\Omega_0^{c+1}} \cdot (12) \\
&\cdot \sum_{j_3=0}^{\infty} \left(\frac{\rho}{\Omega_0(1-\rho^2)} \right)^{2j_3+c-1} \frac{1}{j_3! \Gamma(j_3+c)} (\Omega_0(1-\rho^2))^{j_3+c} \\
&\cdot \Gamma(j_3+c) \int_{\Omega_T} \Omega_1^{j_3+c-\frac{1}{2}-\mu-j_1} \gamma \left(j_2+\mu, \frac{\mu(k+1)}{\Omega_1} y^2 \right) \\
&\cdot e^{-\frac{\mu(k+1)}{\Omega_1} y^2 - \frac{\Omega_1}{\Omega_0(1-\rho^2)}} d\Omega_1.
\end{aligned}$$

Integral I_2 is (Gradshteyn & Ryzhik, 2000):

$$\begin{aligned}
I_2 &= \int_0^{\Omega_T} d\Omega_2 \int_0^\infty d\Omega_1 N_{x_1}(x|\Omega_1) p_{\Omega_1\Omega_2}(\Omega_1\Omega_2) = \\
&= \frac{2\sqrt{2\pi} f_m \mu^{\frac{3}{2}} (k+1)^{\mu+\frac{1}{2}}}{k^{\mu-1} e^{2k\mu}} \sum_{j_1=0}^{\infty} \mu \sqrt{k(k+1)}^{2j_1+\mu-1}
\end{aligned}$$

$$\begin{aligned}
&\cdot \frac{1}{j_1! \Gamma(j_1+\mu)} y^{2j_1+2\mu-1} \sum_{j_2=0}^{\infty} \mu \sqrt{k(k+1)}^{2j_2+\mu-1} \\
&\cdot \frac{1}{j_2! \Gamma(j_2+\mu)} \left(\frac{1}{\mu(k+1)} \right)^{j_2+\mu} \frac{1}{\Gamma(c)(1-\rho^2)\rho^{c-1}\Omega_0^{c+1}} \\
&\cdot \sum_{j_3=0}^{\infty} \left(\frac{\rho}{\Omega_0(1-\rho^2)} \right)^{2j_3+c-1} \frac{1}{j_3! \Gamma(j_3+c)} (\Omega_0(1-\rho^2))^{j_3+c} \cdot (13) \\
&\cdot \gamma \left(j_3+c, \frac{\Omega_T}{\Omega_0(1-\rho^2)} \right) \int_{\Omega_T} \Omega_1^{j_3+c-\frac{1}{2}-\mu-j_1} \\
&\cdot \gamma \left(j_2+\mu, \frac{\mu(k+1)}{\Omega_1} y^2 \right) e^{-\frac{\mu(k+1)}{\Omega_1} y^2 - \frac{\Omega_1}{\Omega_0(1-\rho^2)}} d\Omega_1.
\end{aligned}$$

4. NUMERICAL RESULTS

Average level crossing rate (LCR) is important second order performance measure of wireless communication system, which determines the number of signal threshold crossings in positive going direction.

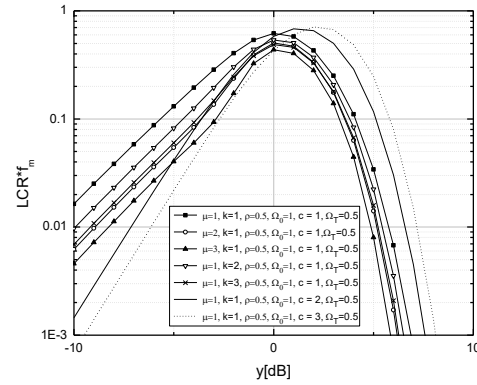


Fig. 2. Normalized LCR of MaD SSC receiver for several values of parameter μ , k and c and constant values of ρ , Ω_0 , and Ω_T .

Figure 2. presents normalized LCR of MaD SSC system for various values of fading severity parameters μ , Rice factor k shadowing severity c , and constant values of correlation parameter ρ , average power Ω_0 and threshold value Ω_T . It is evident that LCR increases for lower values of y , reaches its maximum, and then decreases for higher values of y . It can be seen that by increasing parameter μ and k , it comes to the improvement of the performances of MaD SSC system, since LCR decreases. For lower values of y , LCR decreases as parameter c increases while for higher values of y , LCR increases as parameter c increases. Moreover, parameter c has greater impact on LCR then parameter μ and k .

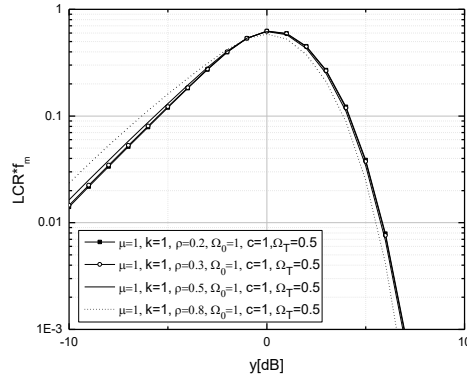


Fig. 3. Normalized LCR of MaD SSC receiver for constant values of μ , κ , c , Ω_0 and Ω_T and several values of ρ .

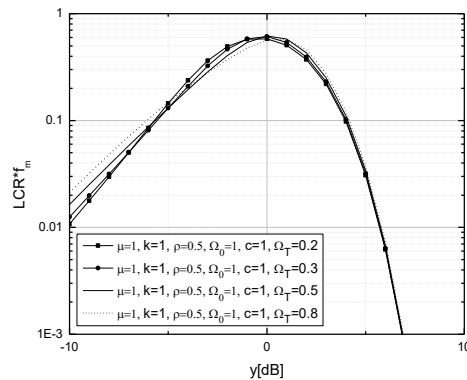


Fig. 4. Normalized LCR of MaD SSC receiver for constant values of μ , κ , c , Ω_0 and ρ and several values of Ω_T .

Fig. 3. shows normalized average level crossing rate versus y for various values of ρ and constant values of μ , κ , c , Ω_0 and Ω_T . Since there is no correlation for $\rho=0$, the impact of ρ on LCR can be noticed for higher values of ρ .

Fig. 4. shows normalized average level crossing rate versus y for various values of Ω_T and constant values of μ , κ , c , Ω_0 and ρ .

5. CONCLUSION

In this paper, MaD technique with MaD switch and stay combining reception and two MiD selection combiners in correlated Gamma shadowed Kappa-Mu multipath fading channel is considered. MaD system with MaD SSC receiver is proposed, since it has lower complexity implementation then other diversity techniques. LCR of SSC MaD receiver output signal envelope in the form the sum of one-folded integrals is

obtained and graphically presented in relation to different system model parameters.

REFERENCES

- Basnayaka, D.A., Smith, P.J., & Martin, P.A. 2013. The effect of macrodiversity on the performance of maximal ratio combining in flat Rayleigh fading. *IEEE Transactions on Communications*, 61(4), pp. 1384-1392.
- Djosic, D., Stefanovic, D., & Stefanovic, C. 2016. Level Crossing Rate of Macro-diversity System with Two Micro-diversity SC Receivers over Correlated Gamma Shadowed α - μ Multipath Fading Channels. *IETE Journal of Research*, 62(2), pp. 1-6.
- Gradshteyn, I.S., & Ryzhik, I.M. 2000. Table of Integrals, Series, and Products, 6th ed..New York: Academic.
- Milic, D., Djolic, D., Stefanovic, C., Panic, S., & Stefanovic, S.M. 2016. Second order statistics of the SC receiver over Rician fading channels in the presence of multiple Nakagami-m interferers. *International Journal of Numerical Modelling: Electronic Networks, Devices and Fields*, 29(2), pp. 222-229.
- Mukherjee, S., & Avidor, D. 2003. Effect of microdiversity and correlated macrodiversity on outages in a cellular system. *IEEE Trans. on Wireless Technol*, 2(1), pp. 50-59.
- Panić, S., Stefanovic, D., Petrović, I., Stefanović, M., Anastasov, J., & Krstic, D. 2011. Second order statistics of selection macro-diversity system operating over Gamma shadowed k - μ fading channels. *EURASIP Journal on Wireless Communications and Networking*, 2011. Oct.
- Panic, S., Stefanovic, M., Anastasov, J., & Spalevic, P. 2013. Fading and Interference Mitigation in Wireless Communications. New York: CRC Press.
- Paris, J.F. 2014. Statistical Characterization of k - μ Shadowed Fading. *IEEE Transactions on Vehicular Technology*, 63(2), pp. 518-526.
- Shankar, P.M. 2009. Macrodiversity and microdiversity in correlated shadowed fading channels. *IEEE Trans. on Vehicular Technol*, 58(5), pp. 727-732.
- Stamenović, G., Panić, S., Rančić, D., Stefanović, C., & Stefanović, M. 2014. Performance analysis of wireless communication system in general fading environment subjected to shadowing and interference. *EURASIP Journal on Wireless Communications and Networking*, 1, pp. 1-8.
- Stefanovic, Č., Jakšić, B., Spalević, P., Panić, S., & Trajčevski, Z. 2013. Performance analysis of selection combining over correlated Nakagami-m fading channels with constant correlation model for desired signal and cochannel interference. *Radioengineering*, 22(4), pp. 1176-1181. Dec.

- Stefanović, Č. 2015. Macrodiversity system with macrodiversity SSC receiver and two microdiversity receivers in the presence of composite fading environment. . In: IEEE 23rd Telecommunications forum - TELFOR 2015, Proceedings of papers, 2015-11-24, Belgrade, Serbia. , pp. 321-324.
- Stefanović, C., Petković, M., Nikolić, B., & Đorđević, G. 2015. Effect of phase noise on error performance of DE-QPSK receiver over k - μ fading channel. . In: IEEE 23rd Telecommunications forum - TELFOR 2015, Proceedings of papers, 2015-11-24, Belgrade, Serbia. , pp. 301-304.
- Stefanović, D., Stefanović, Č., Rančić, D., & Stefanović, M.. Outage probability of macrodiversity system in the presence of Gamma long term fading Rayleigh short term fading and Nakagami-m CCI. . In: Proc. IEEE Eight International Conference on Ubiquitous and Future Networks (ICUFN) 2016, Proceedings of papers, 2016-07-05, Vienna, Austria. , pp. 259-263.
- Stüber, G.L. 1996. Principles of Mobile Communications. Massachusetts, USA: Kluwer Academic Publishers.
- Xekalaki, E., Panaretos, J., & Psarakis, S. 2003. A predictive model evaluation and selection approach- the correlated gamma ratio distribution. In J. Panaretos Ed., Stochastic musings: Perspectives from the pioneers of the late 20th century. USA: Psychology Press., pp. 188-202.
- Yue, S., Ouada, T.B.M.J., & Bobee, B. 2001. A review of bivariate gamma distributions for hydrological application. J. Hydrol, 246, pp. 1-18.
- Yacoub, M.D. 2007. The k - μ distribution and the η - μ distribution. IEEE Antennas and Propagation Magazine, 49(1), pp. 68-81. doi:10.1109/MAP.2007.370983.
- Zhang, B., Zhong, Z., Ai, B., & He, R.. Impact of Shadowing Correlation on Microdiversity and Macrodiversity of Cellular System in High-speed Railway Environments. . In: Proc. Progress In Electromagnetics Research Symposium, 2014-08-25, Guangzhou, China. , pp. 2159-2163
- Zhao, J., Fan, P., Beaulieu, N.C., & Lei, X.. Switching rates of selection diversity and switch-and stay diversity on mixed high-speed train channels. . In: Proc. IEEE International Workshop on High Mobility Wireless Communications, 2015-10-21, Xi'an, China. , pp. 51-55.

* E-mail: danijel.djosic@pr.ac.rs

SOME CYCLIC FIXED POINT RESULTS FOR CONTRACTIVE MAPPINGS

Stojan Radenović¹, Sumit Chandok^{2*}, Wasfi Shatanawi³

¹Faculty of Mechanical Engineering, University of Belgrade, Serbia.

²School of Mathematics, Thapar University, Patiala, India.

³Department of Mathematics, Hashemite University, Zarqa, Jordan.

ABSTRACT

In this paper, we obtained some new cyclic type fixed point theorems using C -class functions in the framework of metric spaces. Our results extend,

generalize, improve and enrich some recent results in the existing literature.

Key words: contractive mappings, cyclic mapping, Cauchy sequence, fixed point, C -class function.

MSC: 47H10, 54H25.

1. INTRODUCTION AND PRELIMINARIES

Very recently, ((Chandok et al., 2016), Theorem 14.) proved the following result:

Theorem 1.1. ((Chandok et al., 2016), Theorem 1). Let A and B be two closed subsets of complete metric spaces (X, d) such that $A \cap B \neq \emptyset$ and let $T: A \cup B \rightarrow A \cup B$ be a mapping such that $TA \subset B$ and $TB \subset A$. Assume that:

$$\psi(d(Tx, Ty)) \leq f(\psi(d(x, y)), \phi(d(x, y))), \quad (1.1)$$

for all $x \in A$ and $y \in B$, where $f \in C, \psi \in \Psi$, and $\phi \in \Phi$. Then T has a unique fixed point in $A \cap B$.

In this paper, using C -class functions, we prove some new cyclic type fixed point theorems. Our results extend, generalize, improve and enrich recently ones in existing literature.

First, we recall some notions and properties that will be needed throughout the paper.

Definition 1.1. ((Chandok et al., 2016), Definition 5). One can say that $f: [0, +\infty)^2 \rightarrow \mathbb{R}$ is called C -class function if it is continuous and satisfies the following axioms:

- (1) $f(s, t) \leq s$ for all $s, t \geq 0$.
- (2) $f(s, t) = s$ implies that either $s = 0$ or $t = 0$ for all $s, t \geq 0$.

We denote C -class functions as C .

Example 1.1. ((Chandok et al., 2016), Example 6). The following functions $f: [0, +\infty)^2 \rightarrow \mathbb{R}$ are elements of C .

- (1) $f(s, t) = s - t$;
- (2) $f(s, t) = ks, k \in (0, 1)$;

$$(3) f(s, t) = \frac{s}{1+t};$$

$$(4) f(s, t) = \frac{\log(t+a^s)}{1+t}, a > 1;$$

$$(5) f(s, t) = \frac{\ln(1+a^s)}{2}, a > e;$$

$$(6) f(s, t) = (s + l)^{\frac{1}{1+t}} - l, l > 1.$$

Further, let ψ denote the set of all monotone increasing continuous functions $\psi: [0, +\infty) \rightarrow [0, +\infty)$, with $\psi^{-1}(\{0\}) = \{0\}$, as well as let ϕ denote the set of all continuous functions $\phi: [0, +\infty) \rightarrow [0, +\infty)$, with $\lim_{n \rightarrow \infty} \phi(t_n) = 0$ implies $\lim_{n \rightarrow \infty} t_n = 0$.

In the sequel, let X be a nonempty set, A_1, A_2, \dots, A_p be its nonempty subsets. Recall that $Y = \bigcup_{i=1}^p A_i$ is said to be a cyclic representation of Y with respect to a mapping $T: Y \rightarrow Y$ if:

$$T(A_1) \subset A_2, \dots, T(A_p) \subset A_1. \quad (1.2)$$

We will use the following auxiliary result.

Lemma 1.2. ((Radenović, 2015b), Lemma 2.1). Let (X, d) be a metric space, $T: X \rightarrow X$ be a mapping and let $X = \bigcup_{i=1}^p A_i$ be a cyclic representation of X w. r. t. T . Assume that:

$$\lim_{n \rightarrow \infty} d(x_n, x_{n+1}) = 0,$$

where $x_{n+1} = Tx_n, x_1 \in A_1, n \in \mathbb{N}$. If $\{x_n\}$ is not a Cauchy sequence, then there exist an $\varepsilon > 0$ and two sequences $\{n(k)\}$ and $\{m(k)\}$ of positive integers such that $n(k) > m(k) > k$ and the following sequences tend to ε^+ as $k \rightarrow \infty$:

$$d(x_{m(k)-j(k)}, x_{n(k)}), d(x_{m(k)-j(k)+1}, x_{n(k)}), \\ d(x_{m(k)-j(k)}, x_{n(k)+1}), d(x_{m(k)-j(k)+1}, x_{n(k)+1}), \quad (1.3)$$

where $j(k) \in \{1, 2, \dots, p\}$ is chosen so that $n(k) - (m(k) - j(k)) \equiv 1 \pmod{p}$, for each $k \in \mathbb{N}$.

If $p = 1$ we obtain very significant, important as well as useful result in the framework of metric space for standard fixed point results ((Radenović et al., 2012), Lemma 2.1.). Hence, Lemma 1.2. is its generalization.

2. MAIN RESULTS

Our main result is the following improvement of Theorem 1.1. that is, Theorem 14 from (Chandok et al., 2016). It also generalizes several enough known results in existing literature.

Theorem 2.1. Let (X, d) be a complete metric space, and let $Y = \cup_{i=1}^p A_i$ be a cyclic representation of $Y \subseteq X$ with the respect to a mapping $T: Y \rightarrow Y$, where the sets A_i are closed. Assume that:

$$\psi(d(Tx, Ty)) \leq f(\psi(d(x, y)), \phi(d(x, y))), \quad (2.1)$$

for all $x \in A_i, y \in A_{i+1}$, where $f \in \mathcal{C}$, $\psi \in \Psi$, and $\phi \in \Phi$. Then, T has a unique fixed point $z \in Y$ and $z \in \cap_{i=1}^p A_i$. Moreover, each Picard sequence $x_n = T^n x, x \in Y$ converges to z .

Proof. First of all, if T has a fixed point say $z \in Y$, using (1.2), we have $z \in \cap_{i=1}^p A_i$. (for more details see (Van Dung & Radenović, 2016), (Kadelburg et al., 2016), (Radenović et al., 2016), (Radenović, 2015a), (Radenović, 2016), (Radenović, 2015b). Further, if T has another fixed point $z_1 \neq z$, we get by (2.1)

$$\psi(d(z, z_1)) = \psi(d(Tz, Tz_1)) \leq \\ f(\psi(d(z, z_1)), \phi(d(z, z_1))) \leq \psi(d(z, z_1)). \quad (2.2)$$

Now from (2.2) follows $f(\psi(d(z, z_1)), \phi(d(z, z_1))) = \psi(d(z, z_1))$, which implies either $\psi(d(z, z_1)) = 0$ or $\phi(d(z, z_1)) = 0$. Since $z_1 \neq z$ then both cases follows a contradiction. Hence, if T has a fixed point then it is a unique as well as belongs $\cap_{i=1}^p A_i$.

Now, to prove that T has a fixed point, take arbitrary $x_0 \in Y$. It belongs to some of the subsets $A_i, i \in \{1, \dots, p\}$, for example $x_0 \in A_1$. It is clear that then the Picard sequence $x_n = T^n x_0, n \in \mathbb{N}$, is divided into the following p subsequences, each belonging to some $A_i, i \in \{1, \dots, p\}$:

$$\{x_{np}\} \subset A_1, \{x_{np+1}\} \subset A_2, \dots, \{x_{np+p-1}\} \subset A_p. \quad (2.3)$$

If $x_{k+1} = x_k$ for some $k \in \mathbb{N}$ then x_k is a unique fixed point of T and it belongs to $\cap_{i=1}^p A_i$. Therefore, suppose that $x_{n+1} \neq x_n$ for each n . Further, it can be proved in a standard way (e.g., as in the proof of (Chandok et al., 2016), Theorem 8) that $d(x_n, x_{n+1})$ is a decreasing sequence and converges to 0 as $n \rightarrow \infty$.

Further, we have to prove that $\{x_n\}$ is a Cauchy sequence. If it is not case, then, using Lemma 1.2, we have that there exist an $\varepsilon > 0$ and two sequences $\{n(k)\}$ and $\{m(k)\}$ of positive integers, with $n(k) > m(k) > k$, such that the sequences (1.3) tend to ε^+ when $k \rightarrow \infty$. Putting in (2.1), $x = x_{m(k)-j(k)}, y = x_{n(k)}$, we get:

$$\psi(d(x_{m(k)-j(k)+1}, x_{n(k)+1})) f(\psi(d(x_{m(k)-j(k)}, x_{n(k)})), \\ \phi(d(x_{m(k)-j(k)}, x_{n(k)}))). \quad (2.4)$$

Passing to the limit in (2.4) as $k \rightarrow \infty$, we get:

$$\psi(\varepsilon) \leq f(\psi(\varepsilon), \phi(\varepsilon)) \leq \psi(\varepsilon),$$

which implies that $f(\psi(\varepsilon), \phi(\varepsilon)) = \psi(\varepsilon)$. According to the property of \mathcal{C} -class function f , we get either $\psi(\varepsilon) = 0$ or $\phi(\varepsilon) = 0$. In both the cases we obtain that $\varepsilon = 0$, which is a contradiction. Therefore, we obtain that Picard sequence $\{x_n\}$ is a Cauchy. Since (X, d) is a complete then (Y, d) is also complete, that is, there exists $z \in Y = \cup_{i=1}^p A_i$ such that $x_n \rightarrow z$ as $n \rightarrow \infty$. This means that $z \in A_l$ for some $l \in \{1, \dots, p\}$ and, hence, $Tz \in A_{l+1}$. Consider the subsequence $\{x_{np+l}\} \subset A_{l+1}$ of $\{x_n\}$. Applying (2.1), we get:

$$\psi(d(x_{np+l+1}, Tz)) = \psi(d(Tx_{np+l}, Tz)) \leq \\ f(\psi(d(x_{np+l}, z)), \phi(d(x_{np+l}, z))) \leq \\ \psi(d(x_{np+l}, z)),$$

that is, $\psi(d(x_{np+l+1}, Tz)) \leq \psi(d(x_{np+l}, z))$. Since subsequences $\{x_{np+l}\}$ and $\{x_{np+l+1}\}$ converges to z also, then passing to the limit as $n \rightarrow \infty$ we get that $Tz = z$. The proof of Theorem 2.1. is complete. \square

Corollary 2.1. Let (X, d) be a complete metric space, and let $T: X \rightarrow X$ be a mapping such that:

$$\psi(d(Tx, Ty)) \leq f(\psi(d(x, y)), \phi(d(x, y))),$$

for all $x, y \in X$, where $f \in \mathcal{C}$, $\psi \in \Psi$, and $\phi \in \Phi$. Then, T has a unique fixed point $z \in X$. Moreover, each Picard sequence $x_n = T^n x, x \in X$ converges to z .

Proof. Putting in Theorem 2.1. $A_i = X$ for all $i = 1, \dots, p$ we obtain the result. \square

Similarly as in (Kadelburg et al., 2016.), (Radenović et al., 2016), (Radenović 2015a),

(Radenović 2016), (Radenović 2015b), one can easily prove that Theorem 2.1 and Corollary 2.1 are equivalent, that is, Theorem 2.1 holds if and only if Corollary 2.1 holds.

We now announce the following very significant as well as new result with new concept of C -class functions:

Theorem 2.2. Theorem 2.1 and Corollary 2.1 are equivalent.

Proof. Method as well as ideas for the proof are the same as ones in (Radenović et al., 2016), (Radenović, 2015a), (Radenović, 2016), (Radenović, 2015b).

Remarks 2.1. (a) Putting $p = 2$, $A_i = A$, $A_2 = B$ (but without assumption $A \cap B \neq \emptyset$) we get Theorem 14 from (Chandok et. al., 2016).

(b) Putting $p = 2$, $A_1 = A$, $A_2 = B$, $f(s, t)s - t$, $\psi(t) = t$, $\phi(t) = (1 - k)t$, $k \in (0, 1)$ we get Theorem 1.1 from (Kirk et. al., 2003).

For more new details regarding recent results for cyclic cases see ((Van Dung & Hang, 2016), (Van Dung & Radenović, 2016), (Kadelburg et al., 2016), (Radenović et al., 2016), (Radenović, 2015a), (Radenović, 2016), (Radenović, 2015b)).

Finally, we have the following open question: Does the following Theorem holds?

Theorem 2.3. Let (X, d) be a complete metric space, and let $Y = \cup_{i=1}^p A_i$ be a cyclic representation of $Y \subseteq X$ with the respect to a mapping $T: Y \rightarrow Y$, where the sets A_i are closed. Assume that for all $x \in A_i$, $y \in A_{i+1}$ there exists $u(x, y) \in \{d(x, y), d(x, fx), d(y, fy), \frac{d(x, fy) + d(y, fx)}{2}\}$ such that:

$$\psi(d(Tx, Ty)) \leq f(\psi(u(x, y)), \phi(u(x, y))), \quad (2.7)$$

where $f \in C$, $\psi \in \Psi$, and $\phi \in \Phi$. Then, T has a unique fixed point $z \in Y$ and $z \in \cap_{i=1}^p A_i$. Moreover, each Picard sequence $x_n = T^n x$, $x \in Y$ converges to z .

3. ACKNOWLEDGMENT

The authors are thankful to the anonymous learned referees for very careful reading and valuable suggestions.

4. CONFLICT OF INTERESTS

Authors declare that they have no any conflict of interest regarding the publication of this paper.

REFERENCES

- Chandok, S., Tas, K., & Hojat Ansari, A., 2016. Some fixed point results for TAC-type contractive mappings, *Journal of Function Spaces*, 2016, Article ID 1907676, pp. 1-6.
- Kadelburg, Z., Radenović, S., & Vujaković, J., 2016. A note on the paper "Fixed point theorems for cyclic weak contractions in compact metric spaces", *Fixed Point Theory Appl.* 2016:46, DOI 10.1186/s13663-016-0537-0.
- Kirk, W., Srinivasan P., & Veeramani, P., 2003. Fixed points for mapping satisfying cyclical contractive conditions, *Fixed Point Theory*, 4(1), pp.79-89.
- Radenović, S., Došenović, T., Aleksić Lampert, T., & Golubović, Z., 2016. A note on some recent fixed point results for cyclic contractions in b-metric spaces and an application to integral equations, *Applied Mathematics and Computation*. 273, pp. 155-164. Doi:10.1016/j.amc.2015.09.089.
- Radenović, S., Kadelburg, Z., Jandrlić, D., & Jandrlić, A., 2012. Some results on weakly contractive maps, *Bull. Iran. Math. Soc.* 38(3), pp. 625-645.
- Radenović, S., 2015a. A note on fixed point theory for cyclic weaker Meir-Keeler function in complete metric spaces, *Int. J. Anal. Appl.* 7(1), pp. 16-21.
- Radenović, S., 2015b. A note on fixed point theory for cyclic ϕ -contractions, *Fixed Point Theory Appl.*, 2015:189. DOI: 10.1186/s13663-015-0437-8.
- Radenović, S., 2016. Some remarks on mappings satisfying cyclical contractive conditions, *Afrika Matematika*. 27(1), pp. 291-295. DOI:10.1007/s13370-015-0339-2.
- Van Dung, N., & Hang, V., 2016. Remarks on cyclic contractions in b-metric spaces and applications to integral equations, *Revista de la Academia de Ciencias Exactas, Fisicas y Naturales, Serie A. Matematicas*, DOI 10.1007/s13398-016-0291-5.
- Van Dung, N., & Radenović, S., 2016, Remarks on theorems for cyclic quasi-contractions, *Kragujevac Journal of Mathematics*. 40(2), pp. 272-279.

* E-mail: chandhok.sumit@gmail.com

THE NUMBER OF ZERO SOLUTIONS FOR COMPLEX CANONICAL DIFFERENTIAL EQUATION OF SECOND ORDER WITH CONSTANT COEFFICIENTS IN THE FIRST QUADRANT

Jelena Vujaković^{1*}, Miloje Rajović²

¹Faculty of Sciences and Mathematics, University of Priština, Kosovska Mitrovica, Serbia.

²Faculty of Mechanical Engineering, University of Kragujevac, Kraljevo, Serbia.

ABSTRACT

The study of complex differential equations in recent years has opened up some of questions concerning the determination of the frequency of zero solutions, the distribution of zero, oscillation of the solution, asymptotic behavior, rank growth and so on. Besides, this is solved by only some

classes of differential equations. In this paper, our aim was to determine the number of zeros and their arrangement in the first quadrant, for the complex canonical differential equation of the second order. The accuracy of our results, we illustrate with two examples.

Key words: Differential equations, function of frequency, sine solution, cosine solution, zero solutions.

1. INTRODUCTION

The study of complex differential equations, in terms Nevanlinna theory, becomes actual again since 1982, the publication of the following works: Bank (1988), (Bank & Laine, 1982; 1983), (Bank et al., 1989).

Then are generally treated canonical complex differential equations of second order with a coefficient which is an entire function. All of these studies have focused mainly on two general issues.

The first one involved the determination of the frequency of zero solutions, while the other studied the distribution and the asymptotic behavior of zero solutions in the first quadrant i.e., in the sector

$0 \leq \varphi \leq \frac{\pi}{2}, |z| = R$. About the problem of distribution

of zero solutions of complex differential equations, the case where the coefficient $a(z)$ is polynomial

$P_n(z)$ is quite clear. When $a(z)$ is the transcendent function the situation is much more complex. Review of the scientific literature, such as (Gundersen, 1986), (Laine, 1993), (Shu Pei, 1994) and others, shows that there are mostly treated complex differential equations with transcendental coefficients e^z and coefficients derived from it: $e^z + P_n(z)$, $e^z \cdot P_n(z)$, $P_n(e^z)$,

This is because in Nevanlinna theory as a measure of transcendence and infinite growth, takes the function

e^z . Since $|e^z| = e^x, x \in \mathbb{R}$, as $x \rightarrow \infty$ function e^z tends to complex infinity of transcendent type.

Unlike classical Nevanlinna theory, we are using the the idea of (Dimitrovski & Mijatović, 1998), (Lekić et. al., 2012), (Vujaković et al., 2011), (Vujaković, 2012) developed a new approach in determining the location and number of zero solutions. This method looked better in the applications for us.

In this paper, the subject of our considerations is complex canonical differential equations of second order with constant coefficients.

2. PRELIMINARIES

For complex canonical differential equation of the second order :

$$\frac{d^2 w}{dz^2} + a(z)w(z) = 0 \quad (1)$$

with an analytical coefficient $a(z) = \alpha(x, y) + i\beta(x, y)$, where $\alpha(x, y)$ and $\beta(x, y)$ are harmonic functions, by series-iterations method which are described in detail in the works (Dimitrovski & Mijatović, 1998), (Lekić et al., 2012), (Vujaković, 2012), we get two fundamental solutions:

$$\begin{aligned}
w_1(z) &= \cos_{a(z)} z \\
&= 1 - \int_0^z \int_0^z a(z) dz^2 + \int_0^z \int_0^z a(z) dz^2 \int_0^z \int_0^z a(z) dz^2 - \dots \approx \\
&\approx \cos\left(z\sqrt{a(z)}\right), \tag{2}
\end{aligned}$$

$$\begin{aligned}
w_2(z) &= \sin_{a(z)} z \\
&= \frac{1}{\sqrt{a(z)}} \left[z - \int_0^z \int_0^z za(z) dz^2 + \int_0^z \int_0^z a(z) dz^2 \int_0^z \int_0^z za(z) dz^2 - \dots \right] \\
&\approx \frac{\sin\left(z\sqrt{a(z)}\right)}{\sqrt{a(z)}}. \tag{3}
\end{aligned}$$

Function $w_1(z)$ and $w_2(z)$ we called oscillatory complex functions with base $a(z)$. Mark them with (2) and (3), respectively. Further, let

$$F(z) = z\sqrt{a(z)}. \tag{4}$$

denotes a function of the frequency. We have seen in the papers (Vujaković et al., 2011; 2016), (Vujaković, 2012) that the zero solutions (2) and (3) are approximately in the solutions of equations

$$\left. \begin{aligned} w_1 : z\sqrt{a(z)} &= (2n-1)\frac{\pi}{2}, n=1,2,3,\dots \\ w_2 : z\sqrt{a(z)} &= n\pi, n=0,1,2,\dots \end{aligned} \right\}. \tag{5}$$

Therefore, it is important to know the behavior of $\sqrt{a(z)}$ for the analytical functions $a(z) = \alpha(x, y) + i\beta(x, y)$.

Theorem 1. For analytic function $a(z) = \alpha(x, y) + i\beta(x, y)$, in complex canonical second-order differential equation (1), it is possible to determine the equation of zero cosine and sine solutions.

Proof. Putting $z = x + iy$ and $a(z) = \alpha(x, y) + i\beta(x, y)$, for example in the second equation of the system (5), after the elementary calculation (i.e., squaring, multiplying complex numbers and on the basis of equality of complex numbers), we obtain the following system of equations for $\alpha(x, y)$ and $\beta(x, y)$.

$$\begin{aligned}
(x^2 - y^2)\alpha(x, y) - 2xy\beta(x, y) &= n^2\pi^2 \\
(x^2 - y^2)\beta(x, y) + 2xy\alpha(x, y) &= 0.
\end{aligned}$$

Elimination $\beta(x, y)$ from the second equation of the last system and substituting them in the first

equation of the same system we get the equation for $\alpha(x, y)$. We got the system of equations

$$\left. \begin{aligned} \alpha(x, y) &= n^2\pi^2 \frac{x^2 - y^2}{(x^2 + y^2)^2}, \\ \beta(x, y) &= -n^2\pi^2 \frac{2xy}{(x^2 + y^2)^2}. \end{aligned} \right\} \tag{6}$$

If $\alpha(x, y)$ and $\beta(x, y)$ are given, that is, if known coefficient $a(z)$, from (6) we find the zero (x_n, y_n) of sine solutions $w_2(z)$ of complex differential equations of the second order (1). This means that (6) is a system of biquadratic equations. From (6), dividing $\alpha(x, y)$ and $\beta(x, y)$, we get

$$\frac{x^2 - y^2}{2xy} = -\frac{\alpha(x, y)}{\beta(x, y)}.$$

This equation is easy to solve only for the constant $a(z) = c_1 + ic_2$.

Zero of cosine solutions for the canonical complex differential equations of the second order (1) can be found in a similar manner. Namely, from the first equation of the system (5) we have

$$(x + iy)\sqrt{\alpha(x, y) + i\beta(x, y)} = (2n-1)\frac{\pi}{2}, n=1,2,3,\dots$$

From here, similarly as moment ago, we obtain a system of equations

$$\left. \begin{aligned} \alpha(x, y) &= \left(n - \frac{1}{2}\right)^2 \pi^2 \frac{x^2 - y^2}{(x^2 + y^2)^2}, \\ \beta(x, y) &= -\left(n - \frac{1}{2}\right)^2 \pi^2 \frac{2xy}{(x^2 + y^2)^2}. \end{aligned} \right\} \tag{7}$$

Solving the system (5) is not a trivial task for all forms of the coefficient $a(z) = \alpha(x, y) + i\beta(x, y)$.

The best and easiest way is if you have zero solutions of $w_1(z) = \cos\left(z\sqrt{a(z)}\right)$ and $w_2(z) = \sin\left(z\sqrt{a(z)}\right)$ at a proper geometric line, so there is some law of their schedule. ■

Theorem 2. Zeros solutions for $w_1(z) = \cos \lambda z$ (and similar to $w_2(z) = \sin \lambda z$) exists if a module of the function $a(z)$ is right proportional to the order of

$\left(n - \frac{1}{2}\right)^2$ zero (respectively n^2) and inversely proportional to the square of the module ρ .

Proof. Using the polar form $z = \rho e^{i\varphi}$ of a complex number, for example, from the system (7), we obtain the system

$$\begin{cases} \alpha = \alpha(\rho, \varphi) = \left(n - \frac{1}{2}\right)^2 \pi^2 \frac{\cos 2\varphi}{\rho^2}, \\ \beta = \beta(\rho, \varphi) = -\left(n - \frac{1}{2}\right)^2 \pi^2 \frac{\sin 2\varphi}{\rho^2}. \end{cases} \quad (8)$$

From here we have $\alpha^2 + \beta^2 = \left(n - \frac{1}{2}\right)^4 \frac{\pi^4}{\rho^2}$, that is we obtain the connection between the α and β , which does not depend on the argument 2φ . If we write $a(z)$ in polar form $a(z) = \alpha(x, y) + i\beta(x, y) = Re^{i\theta}$, we have $R = \left(n - \frac{1}{2}\right)^2 \frac{\pi^2}{\rho^2}$. Besides, from $\tan \theta = \frac{\beta}{\alpha}$ follows $\tan \theta = -\tan 2\varphi = \tan(-2\varphi)$, or equivalent $\theta = -2\varphi + k\pi$.

By the same reasoning from the system (6) we prove the assertion for $w_2(z) = \sin \lambda z$. ■

3. MAIN RESULTS

For starters, it is important to determine the number of zeros solutions of complex second order differential equation (1) for a constant $a(z) = c_1 + ic_2$, or to try to evaluate zeros better. Because of the multifaceted analytic functions it is best first to observe the characteristic examples of differential equations with constant coefficients

$$\frac{d^2 w}{dz^2} + a(z)w(z) = 0, a(z) = c_1 + ic_2. \quad (9)$$

The problem is that we must know in advance for which $a(z)$, the value of $\sqrt{a(z)} = \sqrt{c_1 + ic_2}$, which is ambiguous, it remains in the first quadrant, and when he leaves. Therefore, consider the four basic equations.

1. Assume first that $a(z) = 1$, is pure real constant coefficient. Follows, $c_1 = 1 > 0, c_2 = 0$. Then $\sqrt{a(z)} = \pm 1$ and a function of frequency is $z\sqrt{a(z)} = \pm z$. The solutions of the canonical

complex differential equation of the second order $\frac{d^2 w}{dz^2} + w(z) = 0$ are $w_1(z) = \cos z, w_2(z) = \sin z$.

Zeros of sine solutions $z = n\pi, n = 0, 1, 2, \dots$ are on the real axis (limit of the first quadrant).

2. For real constant coefficient $a(z) = -1$ we have $c_1 = -1 < 0, c_2 = 0$. Then $\sqrt{a(z)} = \sqrt{-1} = \pm i$, and $z\sqrt{a(z)} = \pm iz$. The solutions of canonical complex differential equations of the second order $\frac{d^2 w}{dz^2} - w(z) = 0$ are $w_1(z) = \cos(iz)$ and $w_2(z) = \sin(iz)$. Zeros of sine solutions are in the solutions of equations $z = -n\pi, n = 0, 1, 2, \dots$. They are on the imaginary axis and not in the first quadrant, except solution $z = 0$.

3. Consider now the complex canonical second-order differential equation $\frac{d^2 w}{dz^2} + iw(z) = 0$, with the imaginary constant coefficient $a(z) = i$, where $c_1 = 0, c_2 = 1 > 0$. Then $\sqrt{a(z)} = \sqrt{i} = \pm \frac{1+i}{\sqrt{2}}$, and a function of frequency is $z\sqrt{a(z)} = z\left(\pm \frac{1+i}{\sqrt{2}}\right)$.

Solutions of complex differential equations are $w_1(z) = \cos\left(\pm \frac{1+i}{\sqrt{2}} z\right)$ and $w_2(z) = \sin\left(\pm \frac{1+i}{\sqrt{2}} z\right)$.

Zeros of sine solutions $z = \pm(1-i)\frac{n\pi}{\sqrt{2}}, n = 0, 1, 2, \dots$ are in the second or fourth quadrant. So, there is no zero in the first quadrant.

For complex canonical second-order differential equation $\frac{d^2 w}{dz^2} - iw(z) = 0$, with the imaginary constant coefficient $a(z) = -i$, are $c_1 = 0, c_2 = -1 < 0$ and $\sqrt{a(z)} = \sqrt{-i} = \pm \frac{1-i}{\sqrt{2}}$. Zeros of sine solutions are

$z = \pm(1+i)\frac{n\pi}{\sqrt{2}}, n = 0, 1, 2, \dots$. From this, we conclude that there are zeros in the first and third quadrant.

By this elementary examination, we find out that only if $\text{Im } a(z) = \text{Im}(c_1 + ic_2) < 0$, is likely to be zeros of sine solutions in the first quadrant. However, we need a more general and more secure approach to solving this problem, but not elementary examples.

Theorem 3. For complex canonical second-order differential equation (9), with constant coefficients $a(z) = c_1 + ic_2$, sine solution has zero in the first quadrant if $c_2 < 0$.

Proof. For a constant $a(z) = c_1 + ic_2$, $z = x + iy$, zeros of sine solutions are in the roots of the equations $z\sqrt{a(z)} = n\pi, n = 0, 1, 2, \dots$. Hence, according to the formula (6), we obtain the system:

$$\left. \begin{aligned} c_1 &= n^2 \pi^2 \frac{x^2 - y^2}{(x^2 + y^2)^2}, \\ c_2 &= -n^2 \pi^2 \frac{2xy}{(x^2 + y^2)^2}. \end{aligned} \right\} \quad (10)$$

Because we want that $z = x + iy$ be in the first quadrant, therefore that $x > 0, y > 0$ holds, it must be $c_2 < 0$ in the $a(z) = c_1 + ic_2$. If this holds yet for $x > y$ then $c_1 > 0$. In case $x < y$ we have that $c_1 < 0$. ■

Let us now return to solving the system of equations (10). By switching to polar form $z = \rho e^{i\varphi}$, from $c_1 = n^2 \pi^2 \frac{\cos 2\varphi}{\rho^2}$ and $c_2 = -n^2 \pi^2 \frac{\sin 2\varphi}{\rho^2}$, we find $\varphi = -\frac{1}{2} \arctan \frac{c_2}{c_1}$. Now, from $c_1 = n^2 \pi^2 \frac{\cos 2\varphi}{\rho^2}$ following $\rho = \frac{n\pi}{\sqrt[4]{c_1^2 + c_2^2}}$. Substituting these values in $x = \rho \cos \varphi$ and $y = \rho \sin \varphi$ respectively, after the well-known trigonometric identities for the sine and cosine, we get the coordinates for the zeros of sine solutions of the complex canonical differential equations of the second order:

$$x = x(n) = \frac{n\pi}{\sqrt[4]{c_1^2 + c_2^2}} \sqrt{\frac{\sqrt{c_1^2 + c_2^2} + c_1}{2\sqrt{c_1^2 + c_2^2}}}, \quad (11)$$

$$y = y(n) = -\frac{n\pi}{\sqrt[4]{c_1^2 + c_2^2}} \sqrt{\frac{\sqrt{c_1^2 + c_2^2} - c_1}{2\sqrt{c_1^2 + c_2^2}}}, \quad (12)$$

for $n = 0, 1, 2, \dots$

From equations (12) it is evident that $y < 0$, and comparing equations (11) with (12) we see that $|x| > |y|$. Dividing the (12) with (11) we obtain the

equation $y = -\sqrt{\frac{\sqrt{c_1^2 + c_2^2} - c_1}{\sqrt{c_1^2 + c_2^2} + c_1}} x$ of the straight line

through the second and fourth quadrant.

We still need to determine how many zeros have a sine i.e., cosine solution of canonical complex differential equations of second order in the sector

$$|z| < R, 0 \leq \arg z < \frac{\pi}{2}.$$

Theorem 4. In canonical complex second-order differential equation (9), with constant coefficients, the number of zeros of sine solutions is determined by

the formula $N(z_k) = kE \left[\frac{\pi}{\sqrt[4]{\alpha^2 + \beta^2}} \right]$, where E is a

whole part of the above argument, and k is an integer

unit in the $|z| < R, 0 \leq \arg z < \frac{\pi}{2}$. Cosine solution has one less zero.

Proof. For complex canonical differential equation of second order

$$\frac{d^2 w}{dz^2} + (\alpha + i\beta)w(z) = 0$$

with constant coefficients $a(z) = \alpha + i\beta$, according to Theorem 3, it follows that zeros of sine solutions do not exist for all α, β , but only for those values $\alpha = c_1, \beta = c_2$, that satisfy equations (11) and (12). Then we get the points $z_n = x_n + iy_n$ of region

$$|z| < R, 0 \leq \arg z < \frac{\pi}{2}.$$

From a function of frequency $z\sqrt{a(z)} = n\pi, n = 0, 1, 2, \dots$ we have

$z_n = \frac{n\pi}{\sqrt[4]{\alpha^2 + \beta^2}}, n = 0, 1, 2, \dots$. We see that this is a

series of zeros per the length $|z_n| = \frac{n\pi}{\sqrt[4]{\alpha^2 + \beta^2}}$ of some

direction, which runs from $z = 0$ to a point on a circle of radius R . The number of zeros is the number of slices on a circle of R and has a length $\frac{n\pi}{\sqrt[4]{\alpha^2 + \beta^2}}$.

If we introduce the function $E(x) = [x]$ (the whole part of the argument x), based on the properties $E[nr] = nE[r]$, where n is a positive integer, we have for the number of zeros:

$$N(z_n) = E \left[\frac{n\pi}{\sqrt[4]{\alpha^2 + \beta^2}} \right] = nE \left[\frac{\pi}{\sqrt[4]{\alpha^2 + \beta^2}} \right].$$

Notice that the sine zeros are equidistant because for two consecutive n and $n+1$ is valid

$$\begin{aligned} |N(z_{n+1}) - N(z_n)| &= \\ &= \left| (n+1)E \left[\frac{n\pi}{\sqrt[4]{\alpha^2 + \beta^2}} \right] - nE \left[\frac{n\pi}{\sqrt[4]{\alpha^2 + \beta^2}} \right] \right| \\ &= E \left[\frac{\pi}{\sqrt[4]{\alpha^2 + \beta^2}} \right] \end{aligned}$$

Concerning the property that the sine function within a period 2π has three zeros $0, \pi, 2\pi$ and the cosine function in the same period has only two zeros $\frac{\pi}{2}, \frac{3\pi}{2}$, we conclude that the cosine solution has one less zero than sine. ■

4. EXAMPLES

Let us illustrate the validity of our results in the examples.

Example 1. Sine solution of canonical complex differential equations of second order

$\frac{d^2 w}{dz^2} + (2-i)w(z) = 0$, with constant coefficients $a(z) = 2-i$, for which are $c_2 < 0$ and $|c_1| > |c_2|$, has a zero in the sector $|z| < R, 0 \leq \arg z < \frac{\pi}{2}$. Number of zeros will be equal:

$$\begin{aligned} E \left[\frac{n\pi}{\sqrt[4]{2^2 + (-1)^2}} \right] &= nE \left[\frac{\pi}{\sqrt[4]{5}} \right] = nE \left[\frac{3,14}{1,5} \right] = \\ &= nE[2,1] = 2n. \end{aligned}$$

For example, if $R=10$, then from $2n=10$ follows that there are $n=5$ sine zeros.

Example 2. Let were given complex canonical second-order differential equations

$\frac{d^2 w}{dz^2} + (3-2i)w(z) = 0$ with constant coefficient $a(z) = 3-2i$. Here are $c_1 = 3, c_2 = -2$, so the conditions $c_2 < 0$ and $|c_1| > |c_2|$ are fulfilled. Sine solution is in the circle. For example, in circle of radius $|z| = R = 100$ there are 50 zeros because:

$$\begin{aligned} N(\sin_{(3-2i)} z) &= E \left[\frac{n\pi}{\sqrt[4]{3^2 + (-2)^2}} \right] = nE \left[\frac{\pi}{\sqrt[4]{13}} \right] = \\ &= 2n = 100 \end{aligned}$$

ACKNOWLEDGMENT

Financial support for this study was granted by the Ministry of Education, Science and Technology Development of the Republic of Serbia (Project Number TR 35030).

REFERENCES

- Bank S., 1988. On determining the location of complex zeros of solutions of certain linear differential equations, *Annali di Matematica Pura ed Applicata*, 151(1), pp. 67-96. DOI:10.1007/BF01762788
- Bank S., & Laine I., 1982. On the oscillation theory of $f'' + Af = 0$ where A is entire, *Transactions of the American Mathematical Society*, 273(1), pp. 351-363.
- Bank S., & Laine I., 1983. On the zeros of meromorphic solutions of second order linear differential equations, *Commentarii Mathematici Helvetici*, 58, pp. 656-677.
- Bank S., Laine I., & Langley K., 1989. Oscillation results for solutions of linear differential equations in the complex domain, *Results in Mathematics*, 16, pp. 3-15.
- Dimitrovski D., & Mijatović M., 1998. A series-Iteration Method in the Theory of Ordinary Differential Equations, Hadronic Press.
- Gundersen G., 1986. On the real zeros of solutions of $f'' + A(z)f = 0$ where $A(z)$ is entire, *Annales Academiae Scientiarum Fennicae Mathematica*, 11, pp. 275-294.
- Laine I. 1993, Nevanlinna theory and complex differential equations, de Gruyter Studies in Mathematics 15, Walter de Gruyter, Berlin/New York 1993.
- Lekić M., Cvejić S., & Dimitrovski D., 2012. Sturm theorems through iteration, Monography, University of Priština, Faculty of Sciences and Mathematics, Kosovska Mitrovica, (in Serbian).
- Shu Pei W., 1994. On the sectorial oscillation theory of $f'' + A(z)f = 0$, *Annales Academiae Scientiarum Fennicae*, Helsinki.
- Vujaković J., Rajović M., & Dimitrovski D. 2011. Some new results on a linear equation of the second order, *Computers and Mathematics with Applications* 61, pp. 1837-1843, doi: 10.1016/j.camwa.2011.02.012.
- Vujaković J., 2012. Zeros solution of complex differential equations, Dissertation, University of

Priština, Faculty of Sciences and Mathematics,
Kosovska Mitrovica, (in Serbian)
Vujaković J., Lalović Lj., & Rajović M., 2016.
Equation of oscillations with one common cause of
oscillations and with variable amplitudes, Journal of

Advanced Mathematical Studies Bucharest, Vol.
9(2), pp.259-265,
http://journal.fairpartners.ro/volume-92016-no-2-_17.html, Article in Press.

* E-mail: jelena.vujakovic@pr.ac.rs

CAN THE TRANSFORMATION OF INSTRUCTION PROCESS INTO A VIRTUAL PLACE INDUCE A SHIFT IN BEHAVIORAL PATTERNS OF TEACHERS AND STUDENTS?

Eugen Ljajko^{1*}, Vladica Stojanović¹, Dragana Valjarević¹, Tanja Jovanović¹

¹Faculty of Sciences and Mathematics, University of Priština, Kosovska Mitrovica, Serbia.

ABSTRACT

The goal of this study is to reveal possible influence that the participants' age and Information and Communications Technologies (ICT) usage in the instruction process can have on behavior that defines whether students and teachers belong to one of the Digital Native/Immigrant or Visitor/Resident groups. We collected data through two surveys that covered a total of 1273 students and 382 teachers from southern regions of Serbia. The surveys consisted of questions about availability of computers and internet, ICT use in the instruction process, and communication habits in the ICT-empowered instruction process. The first survey covered both, students and teachers that were involved in the

instruction process mostly deprived of the ICT usage. The second survey covered participants of an instruction process that was successfully improved by an ICT usage. Data analysis shows a shift in communication patterns of teachers and a sharp improvement in computer use for educational purposes for both groups included in the surveys. The change is induced by a proper ICT usage in the instruction process. Conclusions that followed the data analysis lead us to better approaches in organizing ICT usage in the instruction process that enable participants fully employ their resources in order to improve teaching techniques and learning.

Key words: Digital natives/immigrants, Visitors/residents, Behavioral patterns, ICT-enriched instruction, Virtual places.

1. INTRODUCTION

With Information and Communications Technologies (ICT) introduced in the instruction process, inquiries of new relations between teachers and students, as well as ways participants of the instruction process relate to the technologies and use them, come to the focus. Though the differences in the ways the generations of teachers and students understood and experienced concepts and procedures were observable earlier, it was not clear were they sharper or alleviated after ICT introduction. The differences mostly refer to the way an individual approaches acquisition, understanding and application of the knowledge and skills in the new environment. Therefore, generations of students born after substantial ICT introduction in the instruction process are considered to be different than those born before it.

The mission of equipping Serbian schools with ICT has been carried out partly through the "Digital school" (Digitalna škola) programme of Serbian Ministry of Telecommunications. The program was very successful, and around 95% (2808) of

participating schools were supplied with at least one computer classroom, (Strategija, 2013). Other sources ((Ibro, 2011), (Herceg, 2007)) portray a similar image of ICT availability in Serbian schools.

There are more opinions among the authors concerning the connection between the knowledge, skills and habits to use ICT in instruction process and the group (mostly defined by age) the person belongs to. The opinions could roughly be divided into two streams. Some of them ((Prensky, 2001 a), (Zur, & Zur, 2011), (Tapscott 2009), (Jukes, McCain, & Crockett 2010), (Cunningham 2007)) attribute higher skills to younger participants, while others ((Bullen ET al., 2011), (White & Le Cornu, 2011), (Bennett & Maton, 2010), (Oblinger, & Oblinger, 2005)) hold that the level of skills and habits depends on context instead. Therefore, questions arise:

Do the students and teachers of our schools actually belong to different groups concerning the ICT usage, and, if yes, what are the criteria that define a person's belonging to a group or another?

Answers to these questions are needed to define better ways to organize an ICT-enriched instruction that would be more effective in terms of knowledge transmission/acquisition and quality of knowledge obtained by students.

Digital natives/digital immigrants dichotomy

(Prensky, 2001a) proposed a sharp social division concerning a person's relation to the ICT usage. According to him, there are two groups diametrically opposed concerning their relation to the ICT usage: Digital Immigrants and Digital Natives. The division is mostly based on habits different generations have in interactions with ICT in different aspects of their lives, which unsurprisingly leads to a conclusion that most, if not all of today's students, are Digital Natives and, similarly, majority of today's teachers are Digital Immigrants. This, further, reflects on their interrelations within schools. Discussions by other researchers diverged in different directions.

Some of them discuss stratification within each of these two groups. The groups, according to them, are not as homogenous as Prensky tried to present them. (Zur & Zur, 2011) offer a stratification within each of them in terms of a person's attitudes and capacities in regard to digital technologies.

Regardless on the way the division is described, there is still a generational clash between groups of teachers (parents, employers, etc.) on one side, and students (children, employees, etc.) on the other side at school, home or work (Zur & Zur 2011). In regard with relations between the generations, the stratification proposed by Zur & Zur does not offer a different point of view than the Prensky's one.

The Digital Natives/Digital Immigrants dichotomy and its variations imply differences between the groups concerning ways they think or build knowledge ((Prensky 2001 b), (Tapscott, 2009), (Kelly et al., 2009), (Cunningham 2007)). As a result of Digital Natives' way of thinking and knowledge building, many authors and researchers ((Prensky, 2001 b), (Tapscott 2009), (Kelly et al., 2009), (McNierney, 2004), Howell, 2012)) propose a new way of teaching Digital Natives. According to them, it should be implemented mostly through Digital Immigrants adaptation to youngsters' behavior built by Digital Natives' life-long "immersion into ICT world". However, concerns arise whether parts of knowledge built by Digital Immigrants without ICT will be lost in such a process?

Some researchers consider similar stratifications regardless on a person's age – and therefore not complying with Digital Native/Digital Immigrant dichotomy. (Toledo, 2007) proposed a stratification that is more a *continuum* than a dichotomy.

Since this stratification is not based on age, it does not necessarily lead to different thinking, knowledge building and transmission patterns between the different generations. It rather means that the patterns are distinctive to specific groups within both generations.

Other authors ((McKenzie, 2007), (Bennet & Maton, 2010), (Helsper & Eynon, 2010)) even argue the very way Prensky has set the dichotomy. (McKenzie, 2007), for instance, not only disagrees with Prensky's division among generations, but also questions the grounds of logic that led to the Digital Immigrants/Digital Natives divide.

(Even Prensky, 2009) himself, influenced by development of human – technology relations and results of other researches ((Gardner, 2000), (VanSlyke, 2003), (McKenzie, 2007), (Carr, 2008)), has changed the way he described the divide. Since he found the Digital Immigrants/Digital Natives dichotomy less relevant in new circumstances, he moved the accent of his interest from the divide to thinking of more efficient ways to enhance human abilities by an appropriate use of new technologies.

Visitors/ residents continuum

The Digital Native/Digital Immigrant dichotomy can be considered in terms different than those of the generational gap. The gap is narrowing as Digital Immigrants get integrated into the digital society, and more Digital Natives take positions (like educator, employer, etc.) earlier widely attributed to Digital Immigrants exclusively. (VanSlyke, 2003) notes "that we should conceive of the cultural assimilation between Digital Natives and Immigrants as a mutual process of adaptation rather than a one-way street." Based on this notion, he concludes that "The native/immigrant analogy can help us understand the differences between those who are comfortable with technology and those who are not". There are more evidences suggesting that the divide is more due to the context than to the age ((Bullen et al., 2011), (White & Le Cornu, 2011), (Bennett & Maton, 2010), (Oblinger & Oblinger, 2005)). The same technology can have different level of influence under different circumstances. The level of influence depends on the person's need for the technology to understand or

solve a problem under given conditions. Similarly, a person can behave in different ways using the same technology in various contexts.

Having in mind that the modern ICT usage means using Web services mostly, it is reasonable to consider a new typology that describes a persons' habits and relation with Web and ICT regardless on his/her age. The first step toward it is defining the use of place metaphor in order to describe "being in a virtual place" ((Johnston, 2009), (Wenger et al., 2009). (White & Le Cornu, 2011) propose that "place is primarily a *sense of being present with others*". In accordance with the time spent in "Web places", activities conducted during that time, quality of interactions between the person and technology and, to some degree, results achieved by the person, there are two types of approach to technology use: Visitors and Residents (White & Le Cornu, 2011).

It is clear that the Visitors/Residents typology is not meant to replace the Immigrant/Native dichotomy. We can use the Visitors/Residents typology to describe patterns of behavior of a person achieving a goal within more or less "computerized" environment. It has nothing to do with the person's age. Even more, the same person may not belong to the same Visitor/Resident type all the time, as he/she can behave as a Visitor in one situation and as a Resident in another. The key issue that determines the behavioral pattern is context. Individuals may be able to place themselves at a particular point along this continuum rather than in one of two boxes (White & Le Cornu, 2011). A very small number of individuals can, therefore, be described as 'total' Residents or Visitors.

2. METHOD

The aim of this study is to determine whether the Digital Natives/Immigrants dichotomy and/or Residents/Visitors continuum can be applied to our students and teachers groups. If yes, it is important to disclose factors that shift an individual's or group's behavior toward one or another end of the classification. We paid special attention to permanency or inconstancy of the classification. Finally, answers to these questions would help us find more efficient ways to organize an ICT-enriched instruction that would successfully employ resources of all its participants, regardless on their age or position.

Mathematics

For these reasons we conducted a survey about:

1. Availability of ICT to our teachers and students at home and school,
2. Ways they use available ICT in teaching/learning process, and
3. Habits they have in communication and interactions with each other in an ICT-enriched environment.

2.1. Research design

We used quantitative data to compare behavioral patterns of students and teachers in an ICT-empowered instruction environment. Answers to the survey questions were coded in "0 – 1" form. Series of Wilcoxon Rank Sum (WRS) tests were conducted in order to determine if the groups of students and teachers come from the same population, i.e. whether they belong to different groups in Digital Natives/Immigrants dichotomy or Visitors/ Residents analogy.

2.2. Sampling

The survey was divided into two parts – two separate surveys. The first survey covered 1239 students aged from 7 to 18 (with average 12.88 years and $SD = 3.42$), and 371 teachers from 21 primary and secondary schools in southern regions of Serbia, mostly from rural background. Teachers' age ranged from 26 to 62, with average 43.42 years and $SD = 10.76$. The sample for the second survey was comprised of 11 Mathematics and Informatics teachers and 34 students from "Nikola Tesla" Engineering School in Leposavić, Serbia. They had the same cultural background as the participants to the first survey. The only difference between the samples was the way Mathematics instruction process was organized. The students and teachers included in the second survey had successfully taken part in an ICT-enriched Mathematics instruction including GeoGebra usage in Mathematics lessons ((Ljajko et al., 2010), (Ljajko & Maksić, 2011), (Ljajko & Ibro, 2013)).

3. DATA COLLECTION AND ANALYSIS

All participants in both surveys were asked to fill in a simple form containing questions referring to their access to computers and internet at home, their habits in using basic and educational software, and communication habits in ICT environment.

Data we gathered in the first survey show that the schools were poorly equipped with ICT, as opposed to majority of schools in Serbia. This could be expected, since the least developed regions of Serbia are its southern ones. Namely, there were 3 schools out of 21 without a computer classroom and additional four had no internet access. Even despite such a low ICT access in schools, a well scheduled instruction with properly prepared instruction by skillful teachers would show

improvement in terms of quality and results achieved by students. (Ljajko et al. 2010; Ljajko & Ibro 2013).

Both teachers and students included in the first survey had much higher accessibility to computers and internet at home, table 1. The same table presents the ways students and teachers use computers and Internet for learning/instructing purposes and in communication in the instruction process.

Table 1. The first survey – distribution of students' ($n_1 = 1239$) and teachers' ($n_2 = 371$) answers.

	Students		Teachers	
	Count	%	Count	%
Q1. Have access to a computer at home?	1079	87	345	93
Q2. Have access to Internet at home?	1067	86	343	92
Q3. Use basic Office programs?	678	55	217	58
Q4. Use computers to learn/prepare instruction?	644	52	190	51
Q5. Use e-mail to communicate teachers/students?	905	73	136	37
Q6. Have social network account/s?	1018	82	107	29

The reason why participants of the second survey were separated was that most of the Mathematics lessons in the school were conducted in an ICT-enriched environment using GeoGebra software ((Ljajko & Ibro, 2013), (Ljajko & Maksić, 2011), (Ljajko et al., 2010)). As a result, the teaching/learning process was not restricted to school only, but the students and teachers could invest their resources into

The data about the indicators are shown in Table 2.

the process at any time and place they found appropriate. (Ljajko & Ibro, 2013). This means the instruction process was reshaped into a “virtual place”. Thus, taking part in the instruction process was, in fact, their presence at a “virtual place”, as some authors propose, ((Johnston, 2009), (Wenger et al., 2009), (White & Le Cornu, 2011)).

Table 2. The second survey – distribution of students' ($n_1 = 34$) and teachers ($n_2 = 11$) answers.

	Students		Teachers	
	Count	%	Count	%
Q1. Have access to a computer at home?	34	100	11	100
Q2. Have access to Internet at home?	32	94	11	100
Q3. Use basic Office programs?	31	91	11	100
Q4. Use computers to learn/prepare instruction?	33	97	10	91
Q5. Use e-mail to communicate teachers/students?	34	100	10	91
Q6. Have social network account/s?	34	100	9	82

Our idea with the separate survey was to find out if there is a possible influence of such a computer usage in the instruction process to behavioral patterns of students and teachers in an ICT-enriched environment.

Therefore, our aims were to:

1. Find out if the groups of students and teachers within the school are significantly different to each other concerning behavior in ICT-enriched environment.
2. Compare their accessibility to ICT at home, the ways and habits they show in ICT usage in the instruction process to the corresponding indicators of the overall population in the first survey.

4. RESULTS

Every question in the tables 1 and 2 was used as a criterion to a WRS test. In every of the WRS tests the null hypothesis was:

H_0 : The two samples come from the same population, i.e. there is no statistical difference between the groups.

Therefore, the alternate hypothesis would be:

H_1 : The two samples do not come from the same population.

4.1. The first survey

1. First two questions were meant to reveal the degree of availability of ICT to teachers and students at home.
As a result to the WRS test for the first question data, we obtained the z-value

$$z = 1.7498 < 1.96 = z_{0.025}.$$

The WRS test for the second question gave the z-value

$$z = 1.8535 < 1.96 = z_{0.025}.$$

Having in mind the z-values we obtained, we can accept the null hypothesis at 95% confidence level for both cases. In other words, there is no difference between teachers and students, meaning they do not belong to different social groups that would be defined by having access to a computer or Internet respectively.

2. The purpose of the third and fourth questions was to find out if there was a difference

between the samples concerning the ways the participants use ICT in instruction process.

The results of the third WRS test show that the z-value is

$$z = 1.1027 < 1.96 = z_{0.025}.$$

The z-value in the fourth case was

$$z = -0.2237 \Rightarrow |z| < 1.96 = z_{0.025}.$$

Both z-values show that the null hypothesis can be accepted at 95% confidence level, i.e. both samples come from the same population defined by ICT usage in the instruction process. Apart of that, it is evident that relatively small shares of both groups use ICT for educational purposes.

3. Answers to the last two questions were used to reveal information about the habits the participants have in communication with each other in an ICT-enriched environment.

The z-value we obtained through a WRS test for the fifth question was

$$z = -10.6453 \Rightarrow |z| > 1.96 = z_{0.025}.$$

Concerning the social network accounts, the difference is even sharper and the corresponding z-value we obtained through a WRS test was

$$z = -15.5938 \Rightarrow |z| > 1.96 = z_{0.025}.$$

Both z-values show that the null hypothesis can be rejected in favor of the alternate one at 95% confidence level, i.e. the samples come from the different populations defined by participants' habits in ICT usage to communicate each other in the instruction process.

All these show that the difference between students and their teachers is statistically significant only concerning their habits in ICT usage for communication purposes. Further research would be needed to reveal if these habits are restraints or can be helpful for the teaching/learning process.

4.2. The second survey

We applied the same type of WRS tests to the data gathered in the second survey. Series of WRS tests gave following results:

1. According to answers to the first question, we learnt that all of the students and teachers covered with the second survey had access to computers at home. Only two students had no internet access at home. Clearly, the corresponding z-values were

$$z = 0 < 1.96 = z_{0.025}$$

for the first question, and

$$z = 0.2905 < 1.96 = z_{0.025}$$

for the second one.

2. For the third question we obtained z-value

$$z = 0.4358 < 1.96 = z_{0.025},$$

and for the fourth one the z-value was

$$z = -0.3037 \Rightarrow |z| < 1.96 = z_{0.025}.$$

Though the difference between the groups was not statistically significant concerning these two criteria in the first survey, too, comparing results of the first survey to the results of the second survey, one can notice a sharp increase in percentage for both groups – from 54.72% to 97.06% for students, and from 54.89% to 90.91% for teachers.

3. Participants' habits in communication related to the instruction process in an ICT environment were judged according to their answers to the last two questions. The WRS test applied on data gathered in the fifth question gave z-value

$$z = -0.4490 \Rightarrow |z| < 1.96 = z_{0.025}.$$

The resulting z-value for the sixth question was

$$z = -0.8980 \Rightarrow |z| < 1.96 = z_{0.025}.$$

In this case, the increase in percentage was much sharper for the group of teachers – from 28.57% to 81.82%.

The results of the second survey show that the null hypothesis can be accepted at 95% confidence level, which means there is no statistically significant difference between the groups of students and teachers within this school concerning any of the criteria.

5. DISCUSSION AND CONCLUSION

The data analysis shows that the groups in the first survey were different only concerning the habits participants showed in communication using ICT tools. Students tend to use ICT in communication between each other and with their teachers far more frequently than their teachers do. Still, a closer look at percentages in the Table 1 reveals that the same group of participants shows different behavioral patterns at different aspects of their activities. Both groups confirmed very seldom ICT usage for instruction purposes. For these reasons, we characterized both groups as one of the groups within Digital Native/Immigrant (N/I) or Resident/Visitor (R/V) divisions, as Table 3 shows:

Table 3. Characterization of groups according to their behavior in the ICT environment.

	Sample 1		Sample 2	
	Students	Teachers	Students	Teachers
Q1	N(R)	N(R)	N(R)	N(R)
Q2	N(R)	N(R)	N(R)	N(R)
Q3	I(V)	I(V)	N(R)	N(R)
Q4	I(V)	I(V)	N(R)	N(R)
Q5	N(R)	I(V)	N(R)	N(R)
Q6	N(R)	I(V)	N(R)	N(R)

On the other hand, the groups in the second survey were very similar to each other concerning this criterion. Both surveys covered population with the same cultural background. The main difference between the populations was the way they did Mathematics instruction in the same period. Namely, the second survey covered students and teachers that were included in an ICT-empowered

Mathematics teaching/learning process using GeoGebra software.

In the first sample, students are mostly identified as Digital Natives (Residents) and teachers mostly as Digital Immigrants (Visitors), while in the second sample, both groups behave as Digital Natives (Residents). Though it looks like the main result of the ICT-empowered instruction was making the groups equal concerning communication habits in

the instruction process, the real advancement can be noticed in ICT usage for educational purposes for both groups.

Having in mind participants' answers, their behavioural patterns and the results we obtained through WRS tests, we can draw several conclusions:

1. By an appropriate introduction of ICT into the instruction process, it is being transformed into a "virtual place" for both students and teachers. Apart of school classes, both students and teachers feel to be at their common "virtual place", i.e. instruction process at any place or time they find suitable, which is in accordance with the notion of "virtual place" introduced by Johnston (2009), Wenger, et al. (2009) or White & Le Cornu (2011). Of course, in this way all participants of the instruction process employ their resources at much higher level than they did at school only.
2. Behavior of social groups and individuals in particular highly depends on the context. Two groups – teachers and students, apparently very different in age, showed two different communication habits in one case (the first survey – no ICT included in the instruction process), but in another case (the second survey – ICT included in the instruction process) the habits were almost identical for both groups. On the other hand, two groups of the same age or with same predispositions behave in one way when the lessons were held in an ICT-empowered environment, and in another way when the instruction process was deprived of ICT usage.
3. Comparing results of both surveys, we see that the group of teachers showed a shift in a segment of their behavior (communication habits) towards the way students did regardless on the context. This may suggest that the instruction process in an ICT-empowered environment should be organized through teachers' adaptation to students' behavior. However, conclusions should be drawn only if the situation as a whole is observed, and not by taking into consideration isolated parts of information.

This will be discussed in the next conclusion.

4. Finally, answers to the second set of questions in both surveys reveal a sharp increase in ICT usage for educational purposes for both groups simultaneously, which supports the idea of "conceiving of the cultural assimilation between Digital Natives and Immigrants as a mutual process of adaptation rather than a one-way street.", (VanSlyke, 2003). Therefore, a proper ICT usage in the instruction process can help in integration of groups of teachers and students different in age into a single group, defined by the very ICT environment, successful in accomplishing the task of building new knowledge by students.

Further researches are needed to define most effective ways to arrange relations between participants, technology and subject material in the ICT-empowered instruction process in order to achieve better results.

REFERENCES

- Bennett, S., & Maton, K. 2010. Beyond the 'digital natives' debate: Towards a more nuanced understanding of students' technology experiences. *Journal of Computer Assisted Learning*, 26, pp. 321-331.
- Bullen, M., Morgan, T., & Qayyum, A. 2011. Digital Learners in Higher Education: Generation is Not the Issue. *Canadian Journal of Learning Technology*, 37(1), pp. 1-24.
- Carr, N. 2008. Is Google making us stupid?, What the internet is doing to our brains. *The Atlantic*, 301(6), pp. 56-63.
- Cunningham, B. 2007. Digital Native or Digital Immigrant, Which Language Do You Speak?. NACADA Clearinghouse of Academic Advising Resources. Retrieved from <http://www.nacada.ksu.edu/Resources/Clearinghouse/View-Articles/Digital-natives-and-digital-immigrants.aspx#sthash.GhqjNVgH.dpuf>
- Gardner, H. 2000. *Intelligence reframed: Multiple intelligences for the 21st century*. New York: Basic Books.
- Helsper, E.J., & Eynon, R. 2010. Digital natives: Where is the evidence?. *British Educational Research Journal*, 36, pp. 503-520.
- Herceg, D. 2007. Matematika i računari u školi. In *Tehnologija, informatika i obrazovanje za društvo učenja i znanja - Zbornik radova.*, pp. 470-475.

- Howell, J. 2012. Teaching with ICT: Digital pedagogies for collaboration and creativity. Melbourne: Oxford University Press.
- Ibro, V.D. 2011. Didakticko-metodické mogućnosti unapređenja nastave matematike u osnovnoj školi. Leposavić: Faculty of Teacher Education.
- Johnston, R. 2009. Salvation or destruction: Metaphors of the Internet. First Monday, 14, pp. 4-6.
- Jukes, I., McCain, T., & Crockett, L. 2010. Understanding the Digital Generation: Teaching and Learning in the New Digital Landscape. Melbourne, Vic: Hawker Brownlow Education.
- Kelly, F.S., McCain, T., & Jukes, I. 2009. Teaching the digital generation: No more cookie-cutter high schools. Melbourne, Vic: Hawker Brownlow Education.
- Ljajko, E., Mihajlović, M., & Pavličić, Z. 2010. The hyperbola and GeoGebra in high - school instruction. Teaching Mathematics and Computer Science, 8(2), pp. 277-285.
- Ljajko, E., & Maksić, J. 2011. Proučavanje elipse pomoću GeoGebra. Osječki matematički list, 11(1), pp. 39-44.
- Ljajko, E., & Ibro, V. 2013. Development of ideas in a GeoGebra - aided mathematics instruction. Mevlana International Journal of Education, 3(3), pp. 1-7.
- Mckenzie, J. 2007. Digital nativism, digital delusions, and digital deprivation. The Educational Technology Journal, 17(2). From Now On.
- Mcnierney, D.J. 2004. Case study: One teacher's odyssey through resistance and fear. TechTrends, 48(5), pp. 64-69. doi:10.1007/BF02763533
- Oblinger, D., & Oblinger, J. 2005. Is it Age or IT: First steps towards understanding the net generation?. In D. Oblinger & J. Oblinger Eds., Educating the Net Generation. Boulder, CO: EDUCAUSE.. pp. 2.1-2.20.
- Prensky, M. 2001. Digital Natives, Digital Immigrants Part 1. On the Horizon, 9(5), pp. 1-6.
- Prensky, M. 2001. Digital Natives, Digital Immigrants Part 2: Do they really think differently. On the Horizon, 9(6), pp. 1-6.
- Prensky, M. 2009. H. sapiens digital: From digital immigrants and digital natives to digital wisdom. Innovate, 5(3).
- Strategija razvoja obrazovanja u Srbiji do 2020 godine 2013. Government of the Republic of Serbia. Retrieved from http://www.srbija.gov.rs/vesti/dokumenti_sekcija.php?id=45678
- Tapscott, D. 2009. Grown up digital: How the Net Generation is Changing Your World. New York: McGraw-Hill.
- Toledo, C.A. 2007. Digital Culture: Immigrants and Tourists Responding to the Natives' Drumbeat. International Journal of Teaching and Learning in Higher Education, 19(1), pp. 84-92.
- Vanslyke, T. 2003. Digital natives, digital immigrants: Some thoughts from the generation gap. The Technology Source, Commentary.
- Wenger, E., White, N., & Smith, J.N. 2009. Digital Habitats - Stewarding Technology for Communities. Portland, OR: CPsquare.
- White, D.S., & Le Cornu, A. 2011. Visitors and Residents: A new typology for online engagement. First Monday, 16(9-5).
- Zur, O., & Zur, A. 2011. On Digital Immigrants and Digital Natives: How the Digital Divide Affects Families, Educational Institutions, and the Workplace. Zur Institute. Online Publication. Retrieved from http://www.zurinstitute.com/digital_divide.html

* E-mail: eugen.ljajko@pr.ac.rs

MODIFICATION OF TRANSITION'S FACTOR IN THE COMPACT SURFACE-POTENTIAL- BASED MOSFET MODEL

Tijana Kevkić^{1*}, Vladica Stojanović¹, Dragan Petković¹

¹Faculty of Sciences and Mathematics, University of Priština, Kosovska Mitrovica, Serbia.

ABSTRACT

The modification of an important transition's factor which enables continual behavior of the surface potential in entire useful range of MOSFET operation is presented. The various modifications have been made in order to obtain an accurate and computationally efficient compact MOSFET model. The best results have been achieved by introducing the generalized logistic function (GL) in fitting of considered factor. The smoothness and speed of the transition of the

surface potential from the depletion to the strong inversion region can be controlled in this way. The results of the explicit model with this GL functional form for transition's factor have been verified extensively with the numerical data. A great agreement was found for a wide range of substrate doping and oxide thickness. Moreover, the proposed approach can be also applied on the case where quantum mechanical effects play important role in inversion mode.

Key words: MOSFET modeling, generalized logistic functions, surface potential, quantum mechanical effects.

1. INTRODUCTION

The various compact MOSFET models which satisfy basic requirements such as continuity, accuracy, scalability, and simulation performance have been developed over the years. The most accurate among them are the surface-potential-based MOSFET models (henceforth referred to as SPBMs). These inherently single-piece models are essentially short-channel adaptations of the physically based charge sheet model (Eftimie et al., 2007). Although SPBMs continually describe current and its derivatives in all regions of MOSFET operation, they need an iterative solution of a well-known implicit equation (Cunha et al., 1998). The iterative procedure requires expensive times and represents a significant detriment to implement SPB models in popular circuit simulators.

To overcome these difficulties an explicit approximate solution of the mentioned implicit equation has been proposed in (van Langevelde & Klaassen, 2000). This solution, in its present form, introduces a pure empirical fitting factor to control the smoothness of the surface potential behavior. However, the empirical nature of that factor causes the significant deviations of results of approximate SPBM (van Langevelde & Klaassen, 2000) from the implicit ones, especially in regions near and below the threshold (Chen & Gildenblat, 2001).

The purpose of this work is to replace empirical transition's factor with a function that can be precisely determined for given technological characteristics of the MOSFET devices. The first two proposed functions incorporated in the original SPB model (van Langevelde & Klaassen, 2000) have given excellent results for the surface potential of MOS transistors only for certain technological generation. Then, in order to obtain the model that will be applicable to any MOSFET devices, i.e., which will be technologically mapped, we have introduced GL function in fitting of the observed transition's factor. In this way, control of the smoothness as well as the speed of the surface potential transition from the depletion region to the strong inversion region is enabled. Implementation of proposed GL functional form of mentioned factor in original SPB model removes limits in computational efficiency of the model and also increases its accuracy and continuity.

Moreover, the surface potential values obtained from the resulting model have been verified extensively with the numerical data, and a great agreement was found for a wide range of substrate doping and oxide thickness. Finally, the proposed GL approach can be broaden on the compact MOSFET modeling based on surface potential terms, which

takes into account quantum mechanical effects ((Chaudhry et al., 2010), (Pregaldini et al., 2004)).

2. THE BASIC EXPLICIT SPB MODEL

Consider an n-MOS transistor with gate oxide thickness t_{ox} , and the channel homogenously doped with an acceptor concentration of N_A . Under the gradual channel and charge sheet approximation, for the usual range of the n-MOS operation, the surface potential is related to the terminal voltage V_G through the implicit equation (Arora, 1993):

$$V_G - V_{FB} - \psi_s = \gamma \cdot \sqrt{\psi_s + u_T \cdot \exp\left(\frac{\psi_s - 2\phi_F - V_{ch}}{u_T}\right)} \quad (1)$$

Here, we denoted:

- V_{FB} is the flat band voltage,
- $\gamma = \sqrt{2qN_A\epsilon_0\epsilon_{si}/C_{ox}}$ is the body effect coefficient, where $C_{ox} = \epsilon_{ox}/t_{ox}$ is the oxide capacitance per unit area, ϵ_{ox} is the oxide permittivity,
- $u_T = kT/q$ is the thermal voltage,
- $\phi_F = u_T \ln(N_A/n_i)$ is Fermi potential,
- V_{ch} is the channel potential defined by the difference between the quasi-Fermi potentials of the carriers forming the channel (ϕ_n) and that of the majority carriers (ϕ_p).

The Eq. (1) can be solved only numerically. The explicit approximate solution of Eq. (1) has been developed in (van Langevelde & Klaassen, 2000) and is expressed as:

$$\psi_s^*(V_G) = f + u_T \ln \left[\frac{1}{\gamma^2 u_T} \left(V_G - V_{FB} - f - \frac{\psi_{s_{wi}} - f}{\sqrt{1 + \left(\frac{\psi_{s_{wi}} - f}{4u_T}\right)^2}} - \frac{f}{u_T} + 1 \right) \right] \quad (2)$$

Here, $\psi_{s_{wi}}$ is the surface potential in the weak inversion regions and is approximately given by (van Langevelde & Klaassen, 2000):

$$\psi_{s_{ei}}(V_G) = \left(-\frac{\gamma}{2} + \sqrt{V_G - V_{FB} + \frac{\gamma^2}{4}} \right)^2 \quad (3)$$

In Eq. (2), f is the empirical function which changes smoothly from $\psi_{s_{wi}}$ to $2\phi_F + V_{ch}$, and is given by:

$$f(\psi_{s_{ei}}, \epsilon) = \frac{2\phi_F + V_{ch} + \psi_{s_{ei}}}{2} - \frac{1}{2} \sqrt{(\psi_{s_{ei}} - 2\phi_F - V_{ch})^2 + 4\epsilon^2}, \quad (4)$$

where ϵ is the fitting factor which controls the smoothness of the transition of the function f from weak inversion region to the onset of the strong inversion region and it is fixed at a value of 0.02V (van Langevelde & Klaassen, 2000).

3. MODIFICATION OF THE FITTING PARAMETER

Below the threshold, i.e. for $V_G < V_T$, the expected equality $f = \psi_{s_{wi}}$ can be fulfill only by reducing the value of fitting factor ϵ . However, the simple annulment the value of ϵ would make the transition of the function f abrupt at the threshold voltage. This would jeopardize the smoothness of the behavior both of f and ψ_s^* , as functions of the so-called effective voltage $V_E = V_G - V_T$. Instead that, the constant value of parameter ϵ can be replaced by a function which varies from a value close to zero in the depletion region, to a value close to 0.02V as the threshold voltage V_T is approached. In that purpose, the next form for parameter ϵ as the function of effective bias V_E is proposed in (Basu & Dutta, 2006):

$$\epsilon_m(V_E) = 0.01 \left(1 + \frac{V_E + 8u_T}{\sqrt{(V_E + 8u_T)^2 + 0.02}} \right) \quad (5)$$

Values of ψ_s^* , obtained from Eq. (2), with ϵ_m given by Eq. (5), show better match with results of the implicit Eq. (1) than ones with 0.02V, as proposed in (van Langevelde & Klaassen, 2000).

On the other side, the application of explicit SPB model with a constant ϵ as well as with ϵ_m on the scaled MOSFET devices with thinner gate oxides and higher doping concentrations gives results that differ substantially from the results of implicit SPB model. In order to reduce this difference we have proposed following functional form for transition's factor (Kevkić & Petković, 2009):

$$\varepsilon = 0.02 \cdot \left[1 - \exp\left(-\frac{V_G - V_T + 16u_T}{8u_T}\right) \right]. \quad (6)$$

The results for the surface potential obtained from explicit SPB model with ε given by Eq. (6) are accurate particularly in the case of submicron scaled MOSFET devices. The function (6) increases slower than (5) as we can see from Fig. 1.

However, as CMOS technology scales down aggressively, it approaches a point where quantum mechanical effects become significant. In this case ε must be very quickly approached to the value of 0.02V, so we suggest the next function for transition's smoothing factor (Kevkić & Petković, 2010):

$$\varepsilon = 0.02 \cdot \left[1 - \frac{1}{2} \cdot \exp\left(-\frac{V_G - V_T + 8u_T}{4u_T}\right) \right]. \quad (7)$$

The transition's factor ε versus gate voltage V_G calculated according to the relations (5), (6) and (7) are shown in Fig.1.

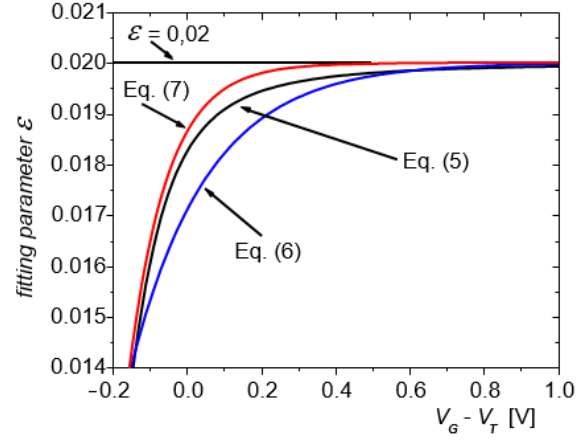


Fig. 1. Fitting parameter ε versus gate voltage V_G , calculated according relations (5), (6) and (7).

Based on the above it is clear that different technological characteristics of MOSFETs require changes of factor ε from 0 to 0.02 with various speeds. In the other words, the manner and speed of continual transition of the function f , and consequently of ψ_s^* between weak and strong inversion determine different

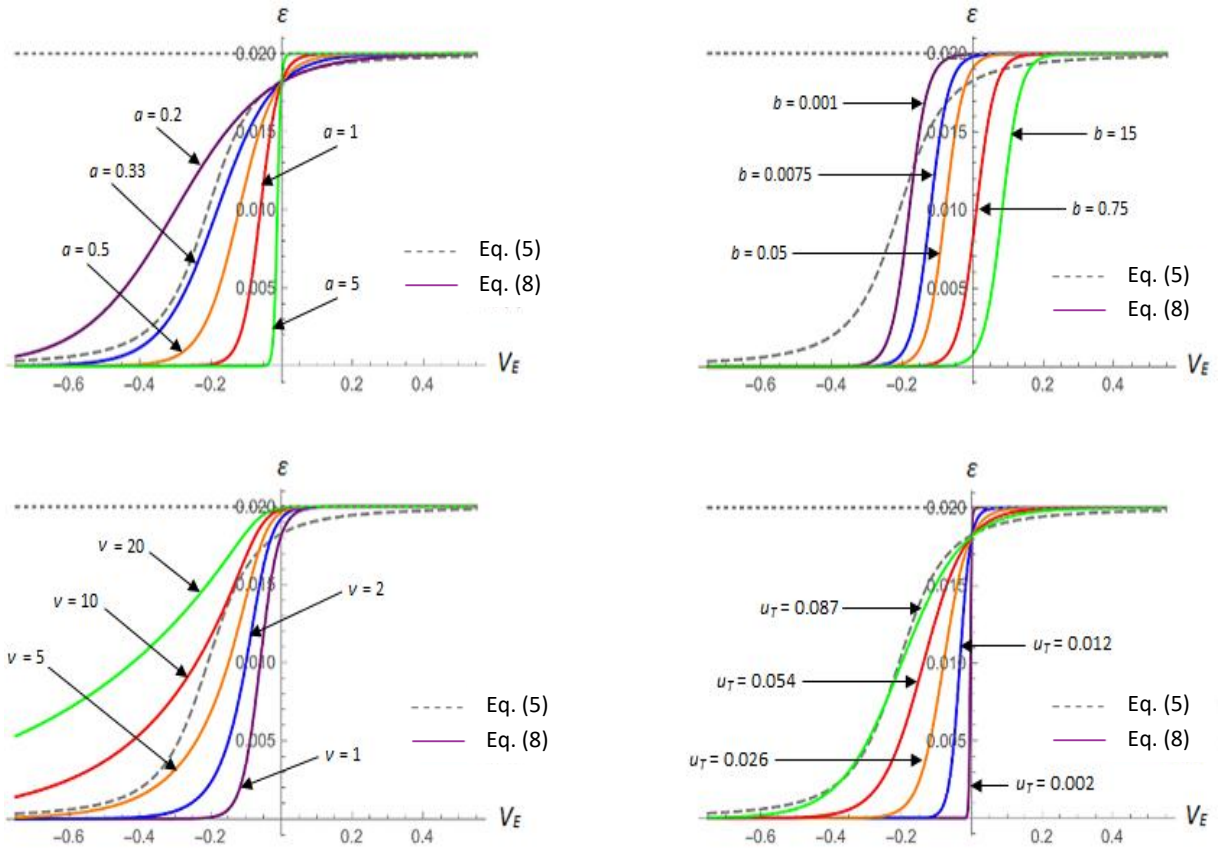


Fig. 2. Graphs of the GL-fitting parameter ε vs. effective voltage $V_E = V_G - V_T$, by using the Eq. (8) (solid lines), compared to the fitting model proposed in Eq. (5) (dashed line). Above left diagram: Varying of the parameter a ($b = 0.1$, $v = 1$, $u_T = 0.026$). Above right diagram: Varying of the parameter b ($a = v = 1$, $u_T = 0.026$). Lower left diagram: Varying of the parameter v ($a = 1$, $b = 0.1$, $u_T = 0.026$). Lower right diagram: Varying of the parameter u_T ($a = v = 1$, $b = 0.1$).

combinations of gate oxide thickness t_{ox} and dopant concentration N_A of device. Especially, thinner gate oxides and higher dopant concentration of the modern MOSFET devices require faster and smoother transitions. It is clear that technologically mapped SPB model can be obtained if sensitivity of the speed and also the way of the transition of ε on changes in the technological characteristics of MOSFETs are taken into account. Several simulations have shown that it can be achieved by introducing new the *Generalized Logistic (GL)* functional form for ε (Kevkić et al., 2015):

$$\varepsilon_{GL}(V_E) = \frac{0.02}{\left(1 + b \exp\left(-a \frac{V_E}{u_T}\right)\right)^{1/\nu}}. \quad (8)$$

Here, $a, \nu > 0$ are the growth parameters, and $b > 0$ is parameter which determines the shift of the GL curve, related to the value.

$$\varepsilon_{GL}(0) = 0.02(1+b)^{-1/\nu} \lesssim 0.02. \quad (9)$$

The parameters a, b can be obtained by using a fitting procedure in accordance to MOSFETs technical characteristics (Kevkić et al., 2015). Unlike them, the parameter $\nu > 0$ will be determined in advance, according to the condition of the asymptotic linear growth of the following, the *Logit-function*:

$$L(V_E/u_T) := \ln \frac{\varepsilon_{GL}^\nu(V_E)}{0.02^\nu - \varepsilon_{GL}^\nu(V_E)} = a \frac{V_E}{u_T} - \ln b.$$

The linear form of function $L(V_E/u_T)$ provides easily obtaining the GL-fitted factor ε_{GL} , given by Eq. (8), by using some of the standard fitting techniques (Jukić & Scitovski, 2003). The graphs of $\varepsilon_{GL}(V_E)$, for varying values of a, b, ν , as well as the thermal voltage u_T , are shown in Fig. 2. The graphs of $\varepsilon_m(V_E)$ are also shown in this figure for comparison. As can be readily seen, the diverse and adapted transitions of ε_{GL} from 0 to 0.02 have been realized with simple changes in values of the parameters a, b, ν .

4. VALIDATION OF THE GL-FITTING

The advantages of introducing the GL function in the original explicit SPB model (van Langevelde & Klaassen, 2000) are shown in Table 1 via the mean values of some typical error functions for the

transition's factor ε obtained by using Eq. (5) and Eq. (8), and accordingly for the approximate surface potential ψ_s^* . The first two rows of the table show the average values of the *Absolute Error (AE)* which is defined as the absolute value of the difference between fitted and reference values of the factor ε , as well as between the corresponding approximate surface potential ψ_s^* , and ψ_s obtained from implicit Eq. (1).

The average values of *Fractional Error (FE)* are shown in third and fourth rows of the Table 1. The FE presents the percentage value of the ratio of AE to the reference values of ε and ψ_s . Finally, the last two rows contain average values of the typical statistics error labeled as the *Squared Error (SE)*, which is commonly used in approximation theory. As we can see, all the estimated errors are obviously smaller in the case of GL-fitted factor ε_{GL} , and it is particularly pronounced in the weak inversion region.

Table 1. Estimated errors obtained by various types of the ε -fitting. Device parameters are: $t_{ox} = 2.3\text{nm}$, $N_A = 10^{18}\text{cm}^{-3}$, $V_{FB} = -1\text{V}$, $V_{ch} = 0\text{V}$, $u_T = 0.026\text{V}$.

Errors	Region	ε -fitting		Surface potential approximation (ψ_s^*)	
		Eq.(5)	Eq.(8)	Eq.(5)	Eq.(8)
AE	w.i.	8.62E-04	1.00E-04	5.21E-05	2.71E-06
	s.i.	1.75E-02	1.73E-02	2.23E-03	2.21E-03
FE	w.i.	8.947	0.930	5.74E-03	3.08E-04
	s.i.	46.60	46.01	2.09E-01	2.08E-01
SE	w.i.	1.10E-06	1.40E-08	1.38E-08	2.02E-11
	s.i.	3.17E-04	3.10E-04	5.01E-06	4.92E-06

The absolute errors, defined as $AE = |\psi_s - \psi_s^*|$, are plotted versus V_G in logarithmic scales in Fig. 3. The values of the explicit surface potential ψ_s^* are obtained from Eq. (2) with ε_m , then with ε_{GL} as well as with the constant value of 0.02V, respectively. The both diagrams show that the best matches with reference values are achieved by using the GL-fitted transition's factor.

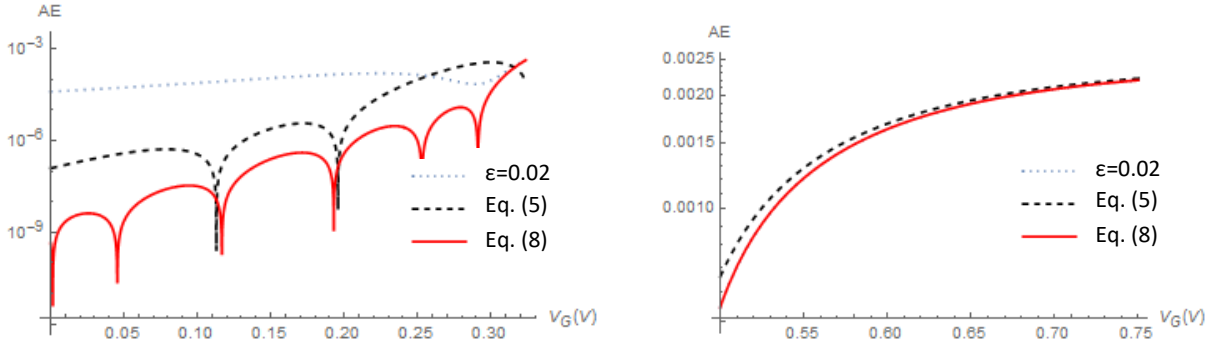


Fig. 3. Absolute errors of the surface potential, $AE = |\psi_s - \psi_s^*|$, vs. V_G in the weak inversion region (left diagrams) and in the strong inversion region (right diagrams). Device parameters are: $t_{ox}=2.3\text{nm}$, $N_A = 10^{18}\text{cm}^{-3}$, $V_{FB} = -1\text{V}$, $V_{ch} = 0\text{V}$, $u_T = 0.026\text{V}$.

5. MODELING THE INCREASE IN SURFACE POTENTIAL DUE TO THE QUANTUM MECHANICAL EFFECTS

The developed GL approach can be applied in the case where severe band bending on the Si side of the Si-SiO₂ interface confines the carriers in a narrow potential well. The energy levels of the carriers are grouped in sub-bands what results in increasing of threshold voltage and surface potential compared to the classical case where the energy band is not split. The decreasing of the inversion charge density and other quantum mechanical effects (QME) are also observed in that case.

The SPB models which include QME require the solution of the Schrödinger's and Poisson's equations which gives the correction of the surface potentials caused by the energy quantization process in the substrate. Under the assumption that only the lowest subband is occupied by the electrons, the variational approach gives a good estimation of the eigen energy of the lowest subband (Stern, 1972):

$$E_0 = (3\hbar^2 b^2)/(8m_{zz}).$$

Here, b is the variational parameter and is obtained by minimizing the ground state energy of the lowest subband with respect to it ((Stern, 1972), (Sho et al., 2016)), m_{zz} is the longitudinal effective mass of electrons, and \hbar is reduced Planck's constant.

The QM correction of the surface potential is equal to the ratio of the energy E_0 and the elementary charge of the electron q :

$$\delta\psi_s = E_0 / q.$$

that the weak inversion approximation gives inaccurate results in the strong inversion region.

Thus, the main task is reduced to finding $\delta\psi_s$ as a function of the applied terminal voltages, and its adequate inclusion in the original SPB model (van Langevelde & Klaassen, 2000). A good way to do that is modification of the function f given by Eq. (4), so that it varies from $\psi_{s_{wi}}$ in weak inversion to $2\phi_F + V_{ch} + \delta\psi_s$ from the onset of strong inversion. The modified smoothing function has the following form:

$$f_{GL} = \frac{\psi_{s_{wi}}}{2} + \frac{2\phi_F + V_{ch} + \delta\psi_s}{2} - \frac{1}{2} \sqrt{(\psi_{s_{wi}} - 2\phi_F - V_{ch} - \delta\psi_s)^2 + 4\epsilon_{GL}^2}, \quad (11)$$

where ϵ_{GL} is given by Eq. (8). To get an explicit QME incorporated SPB model, we only need to use the function f_{GL} in place of f in Eq. (2).

The results of explicit QME incorporated SPB model as a function of the gate voltage $V_G - V_{FB}$ are shown in Fig. 4. The results of implicit SPB model and weak inversion approximation, given by Eq. (3), are also depicted in this figure. As we can see, the deviation between quantum and classical results is the most obvious in the strong inversion region. This deviation will become much more significant with increasing of dopant concentration and decreasing the thickness of gate oxides, i.e. with greater influence of quantum mechanical effects on the MOSFET's operation. Additionally, from Fig. 4 is quite evident

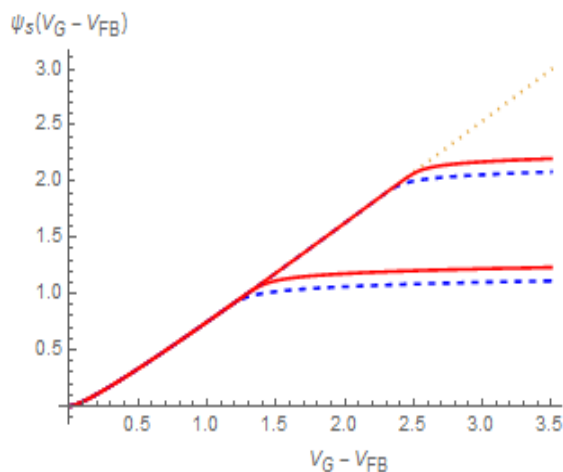


Fig. 4. The electrostatic surface potential ψ_s vs. gate voltage $V_G - V_{FB}$ obtained from the QM incorporated explicit SPB model with ε_{GL} (solid line). The results of the weak inversion approximation (3) (dotted line), and the classical implicit ψ_s model (dashed line) are also shown.

5. CONCLUSION

The explicit surface-potential-based MOSFET model has been modified in order to increase its accuracy, continuity and simulation performances. The modifications consist in new functional forms for important smoothing factor which controls continuity of the surface potential transition from depletion to strong inversion region. Pure empirical parameter has been avoided and an accurate as well as technology mapped model has been obtained by introducing the generalized logistic function in fitting of mentioned smoothing factor. Very important is that the complexity of calculations increases only marginally over the similar advanced models reported in the literature. The results of the surface potential values obtained from the proposed model have been verified extensively with the numerical results of classical implicit equation on which are based all known SPB models, and a great agreement was found. Moreover, the application of GL-fitted model can be broadened to the case where quantum mechanical effects become important. Finally, the validity of the model was proven by comparisons with full numerical solutions data from different advanced CMOS technologies.

REFERENCES

- Arora, N. D. 1993. MOSFET models for VLSI circuit simulation. Springer-Verlag, New York.
- Basu, D., & Dutta, A. 2006. An explicit surface-potential-based MOSFET model incorporating the Quantum mechanical effects. *Solid-State Electronics*, 50, pp. 1299-1309.
- Chaudhry, A., & et al., 2010. Mosfet Models, Quantum Mechanical Effects and Modeling Approaches: A Review. *Journal of Semiconductor Technology and Science*, 1(10), pp. 20-27.
- Chen, T.L., & Gildenblat, G. 2001. Analytical approximation for the MOSFET surface potential. *Solid-State Electronics*, 45, pp. 335-339.
- Cunha, A. & et al. 1998. An MOS transistor model for analog circuit design. *IEEE Journal of solid-state circuits*, 33, 1510-1519.
- Eftimie, S., & et al., 2007. MOSFET Model with Simple Extraction Procedures, Suitable for Sensitive Analog Simulations. *Romanian Journal of Information Science and Technology*, 10, pp. 189-197.
- Jukić, D., & Scitovski, R. 2003. Solution of the least-squares problem for logistic function. *J. Comput. Appl. Math.*, 156, pp. 159-177.
- Kevkić, T., & Petković, D. 2009. Klasični i kvantnomehanički modeli za površinski potencijal i kapacitivnost MOS strukture u uslovima jake inverzije. . In: *Proc. of 53rd ETRAN Conference*, V. Banja, Serbia.
- Kevkić, T., & Petković, D. 2010. A Quantum Mechanical Correction of Classical Surface Potential Model of MOS Inversion Layer. . In: *Proc. Of 27th International Conference on Microelectronics*, Niš, Serbia. , pp. 115-118 1.
- Kevkić, T., Stojanović, V., & Petković, D. 2015. An analytical surface potential model of MOS inversion layer incorporating the quantum mechanical correction. . In: *Proc. of the International Conference of Contemporary materials*, Banja Luka.
- Kumar, M., & et al., 2007. Approaches to nanoscale MOSFET compact modeling using surface potential based models. . In: *14th International Workshop on the Physics of Semiconductor Devices*, Mumbai, India.
- Pregaldini, F., & et al., 2004. An advanced explicit surface potential model physically accounting for the quantization effect in deep-submicron MOSFETs. *Solid-State Electronics*, 48, pp. 427-435.
- Stern, F. 1972. Self-Consistent Results for n-Type Si Inversion Layer. *Physical Review B*, 5(12), pp. 4891-4899.
- van Langevelde, R., & Klaassen, F. 2000. An explicit surface-potential-based MOSFET model for circuit simulation. *Solid-State Electronics*, 44, pp. 409-418.

* E-mail: tijana.kevkic@pr.ac.rs

THE INFLUENCE OF NONLINEAR AND LINEAR DEFECTS ON THE LIGHT PROPAGATION THROUGH LINEAR ONE-DIMENSIONAL PHOTONIC LATTICE

Slavica Kuzmanović^{1*}, Marija Stojanović Krasić², Ana Mančić³, Branko Drljača¹ and Milutin Stepić⁴

¹Faculty of Natural Sciences and Mathematics, University of Priština, Kosovska Mitrovica, Serbia.

²Faculty of Technology, University of Niš, Leskovac, Serbia.

³Faculty of Natural Sciences and Mathematics, University of Niš, Niš, Serbia.

⁴Vinča Institute of Nuclear Sciences, University of Belgrade, Belgrade, Serbia.

ABSTRACT

In this paper, the light beam propagation through one-dimensional photonic lattice, possessing one nonlinear defect and one linear defect, has been investigated numerically. Different dynamical regimes have been identified in terms of the distance between the two defects, position of the incident light beam, the width of linear defect, the values of nonlinearity and presence of the transverse kick. Strong localized modes on the defects, breathing and zig-zag modes in the area between defects have been observed. It has been concluded that the width of the linear defect placed

next to the nonlinear one influences localization of the beam at the nonlinear waveguide. On the other hand, the nonlinear defect, regardless of the values of nonlinearity, have a small influence on the beam propagation in photonic lattice. It has been observed that the transverse kick of the initial beam leads to the distortion of localized structures. By launching the light beam towards defects, the reflection of light has been noticed. Presented results can be useful for different applications, such as blocking, filtering and routing of light beam through optical media.

Key words: waveguide array, nonlinear defect, linear defect, light localization, control of light propagation.

1. INTRODUCTION

Photonic lattices (PL) represent special kind of photonic crystals which consist of periodic arrays of waveguides (WGs) closely spaced to provide weak coupling between neighboring WGs through their evanescent fields. PLs offer the possibility to control the light beam by changing the system parameters, such as refractive index and period of the lattice. Due to their properties and structure, they represent suitable systems for investigation of the wave propagation in periodic systems (Denz et al., 2010) and visualization of different effects such as discrete diffraction (Christodoulides et al., 1988), Fano resonance ((Miroshnichenko et al., 2010), (Naether et al., 2009)), Anderson localization ((Lahini et al., 2008), (Schwartz et al., 2007)), etc. In PLs, different defects can appear in the process of their fabrication, but nowadays, they can be made intentionally and used in attempts to control the light beam propagation ((Noda et al., 2007), (Tran, 1997)). Defects in PL can be formed by changing the value of refractive index in

certain WG or by changing the width of the WG or the distance between WGs ((Meier et al., 2005), (Morandotti et al., 2003)). These defects destroy the translation symmetry of the system but, at the same time, they enable the existence of different stable, localized modes ((Beličev et al., 2010), (Fedele et al., 2005), (Molina et al., 2008)). Recently, the influence of nonlinear defect (ND) on the light beam propagation in one-dimensional (1D) linear uniformed lattice has been investigated (Kuzmanović et al., 2015a) as well as the influence of linear defect (LD) and interface defect on the beam dynamics (Stojanović Krasić et al., 2016).

In this work, we investigate numerically light beam propagation through uniform, 1D PL possessing one linear and one nonlinear defect. The paper is organized in the following way. Mathematical model of wave propagation through the system is formulated in Section 2. By changing the initial position of the beam with respect to the position of the ND and LD,

the width of LD and incident angle of the light beam, different regimes have been obtained and these numerical results are presented and discussed in Section 3. In Section 4, the conclusions have been briefly summarized.

2. MODEL EQUATIONS

We consider the PL which consists of the linear WG arrays with embedded one nonlinear WG (i. e. nonlinear defect) and one linear defect (Figure 1).

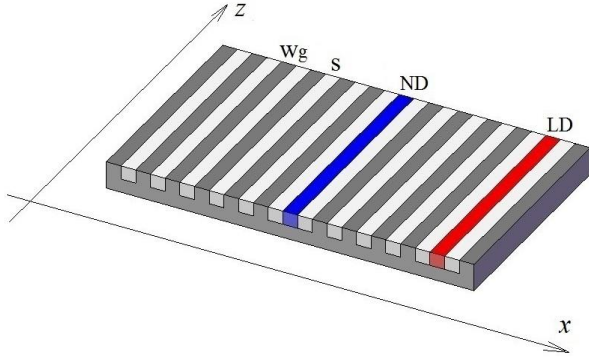


Figure 1. Schematic representation of the system. Blue line shows the position of the nonlinear defect, while the red line denotes the position of the linear defect.

Light propagation in the lattice has been modelled by the paraxial time-independent Helmholtz equation (Kuzmanović et al., 2015a):

$$i \frac{\partial E}{\partial z} + \frac{1}{2k_0 n_0} \frac{\partial^2 E}{\partial x^2} + k_0 n_0 n(x) E = 0, \quad (1)$$

where z is the propagation amplitude, $E(x, z)$ represents the component of the light electric field in the z -direction, $k_0 = 2\pi/\lambda$ is the wave number, n_0 is the refractive index of the substrate, whereas λ marks the wavelength of the incident beam. The lattice contains 49 WGs on the left and 49 WGs on the right of ND in the x (transverse) direction. The stationary profile of refractive index of the lattice is given by the following equation:

$$n(x) = n_l(x) + n_{nl}(x), \quad (2)$$

where $n_l(x)$ represents the linear part of the refractive index and $n_{nl}(x)$ is local nonlinear term. Linear part of the refractive index is defined in a form:

$$n_l(x) = \Delta n \left[\sum_{j=1}^{k-1} G_j(w_g, s, x) + G_k(w_{gk}, s_k, x) + \sum_{j=k+1}^N G_j(w_g, s, x) \right], \quad (3)$$

where Δn is the value of lattice potential, k is the position of the LD which is arbitrary placed in the lattice, N is the total number of WGs in the lattice. Parameter w_g marks the width of the WGs, whereas w_{gk} represents the width of the LD. Functions $G_j(w_g, s, x)$ represent Gaussians corresponding to the lattice WGs, whereas function $G_k(w_{gk}, s_k, x)$ corresponds to the LD.

Nonlinear part of the refractive index locally induced at one WG is defined in a form:

$$n_{nl}(x) = -\frac{1}{2} n_0^2 r E_{pv} \frac{|E|^2}{I_d + |E|^2} \delta, \quad (4)$$

where E_{pv} is component of the light electric field, r is electro-optic coefficient, δ is the Kronecker delta symbol and I_d is dark irradiance ((Chen et al., 2005), (Smirnov et al., 2006)). Dark irradiance is the parameter of the material proportional to the number of thermally generated photons in non-lighted material.

Introducing dimensionless variables $\zeta = k_0 x$ and $\eta = k_0 z$, the equation (1) can be written in the following dimensionless form:

$$i \frac{\partial E}{\partial \eta} + \frac{1}{2n_0} \frac{\partial^2 E}{\partial \zeta^2} + n_0 n(\zeta) E = 0. \quad (5)$$

The light propagation across the lattice is initiated by the Gaussian shaped incident beam with the FWHM of the order of the width of the lattice WGs, and simulated numerically by the split – step Fourier method (Radosavljević et al., 2014). The intensity of the incident light beam, with a wavelength $\lambda = 514.5 \text{ nm}$ is kept at fixed value, whereas the position of the injection with respect to the defect position, its transverse tilt α and the nonlinearity and the width of LD are changeable parameters.

3. RESULTS AND DISCUSSION

In the PL with ND and LD, qualitatively different dynamical behaviour has been observed in comparison to the previously investigated cases with one ND located in the uniform lattice (Kuzmanović et al., 2015a) or with one geometrical defect and LD in the composite system (Kuzmanović et al., 2015b). The width of the LD is either 2 or 6 μm and further in the paper they will be marked as narrow and wide defect, respectively. The width of the WG within the lattice is $w_g = 4 \mu\text{m}$ and the distance between neighboring WGs is $s = 4 \mu\text{m}$. ND is fixed in the middle of the lattice and its position does not change, whereas the position of LD is changeable. The nonlinearity strength of ND has been taken to be $\Gamma = 1.3$ or 10.

Since the aim of this research is to investigate the common influence of the LD and ND on the beam propagation, we will start with analyzing the case in which the LD is placed next to the ND, in the first WG to the right of it. The width of LD has been varied as well as the values of nonlinearity of the ND. If regime possesses 10% of the amplitude value we have claimed that regime existed. In Figs. 2-7. amplitude of refractive index of modulation has larger values on narrow LD than in the case of wider. Linear part of refractive index of modulation is highly dependent of geometry of the system. Hence, changing of the width of WGs or the width of the separation between WGs, will lead to the formation of different amplitude of refractive index. It is shown, by number of numerical simulations, that narrow LD forms larger value of amplitude of refractive index of modulation than wider one.

It can be seen that in this case when the light beam is launched into the ND, the width of LD influences the localization of the light on the ND, Figure 2a. Namely, the narrow LD is better potential barrier than the wide one and the light beam is localized completely on the ND. The efficiency of capturing the beam depends on the values of nonlinearity and in the case of higher nonlinearity, capturing effect is very weak, almost not noticeable (Fig.2c). In the case when the LD 6 μm wide is placed next to the ND in which the beam is initiated breathing mode between two neighbouring WGs is formed. One component of the breathing mode is placed at the nonlinear WG whereas the other is located at the adjacent LD, Fig.2b. For higher nonlinearity strength one can observe light scattering and absence of energy localization, Fig.2d.

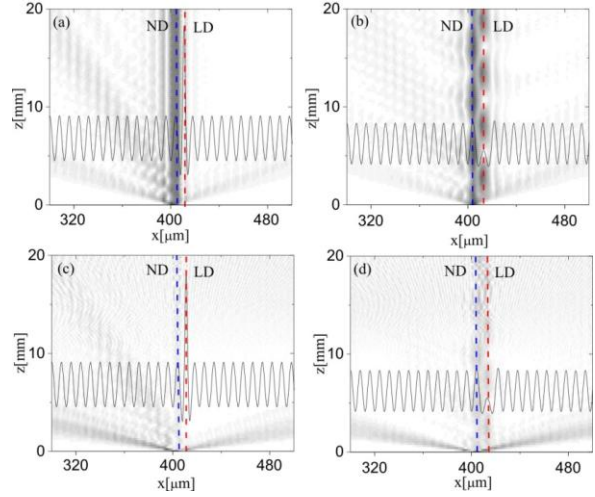


Fig. 2. 2D plot of the average beam intensity profiles, LD is located at the 1st wg on the right of the ND, incident beam enters the ND: (a) nonlinearity strength of ND is $\Gamma=1.3$, width of LD is 2 μm ; (b) $\Gamma=1.3$, width of LD is 6 μm ; (c) $\Gamma=10$, width of LD is 2 μm ; (d) $\Gamma=10$, width of LD is 6 μm . Blue line shows the position of the nonlinear defect, while the red line denotes the position of the linear defect.

If the beam is inserted into the LD which is next to the ND, one can observe that the strength of nonlinearity have a small influence on the beam propagation in the LD, Fig. 3. The width of LD has the dominant influence on the beam propagation. When the beam enters the narrow LD positioned next to the ND, the beam is strongly localized at the position of LD regardless of the strength of ND, (Figs. 3a,c).

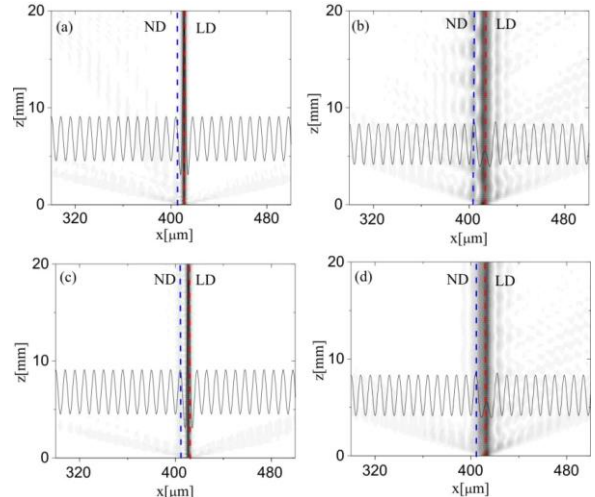


Fig. 3. 2D plot of the average beam intensity profiles, LD is located at the 1st wg on the right of the ND, incident beam enters the LD: (a) $\Gamma=1.3$, LD is 2 μm wide; (b) $\Gamma=1.3$, width of LD is 6 μm ; (c) $\Gamma=10$, width of LD is 2 μm ; (d) $\Gamma=10$, width of LD is 6 μm . Blue line shows the position of the nonlinear defect, while the red line denotes the position of the linear defect.

If the beam is launched into the wide LD (Fig. 3b), localized mode has a smaller amplitude than in the case when the light has been inserted into the narrow LD. Here, one can see that higher nonlinearity strength of the ND (Fig. 3d) will slightly improve localization on LD.

We have investigated the influence of the transverse kick of the input beam on its propagation through the system. For lower values of the kick ($\alpha \leq 2\pi/30$), if the beam is launched from the left towards the ND ($\Gamma=1.3$) with LD 2 μm wide placed next to it, on the side opposite to the input beam, it is possible to obtain mild capturing of the beam at the position of ND and partial reflection from it (Figure 4a). For a wide LD, this capturing at the ND has not been observed, Figure 4b. For narrow LD and higher nonlinearity ($\Gamma = 10$) beam launching at same position (left towards ND) leads towards beam capturing at ND position. However, for wide LD and same nonlinearity ($\Gamma = 10$) reflection of the light at position left of ND is dominant process. Light reflection becomes dominant process no matter from which side (left from ND or right from LD) the input beam is launched into the lattice.

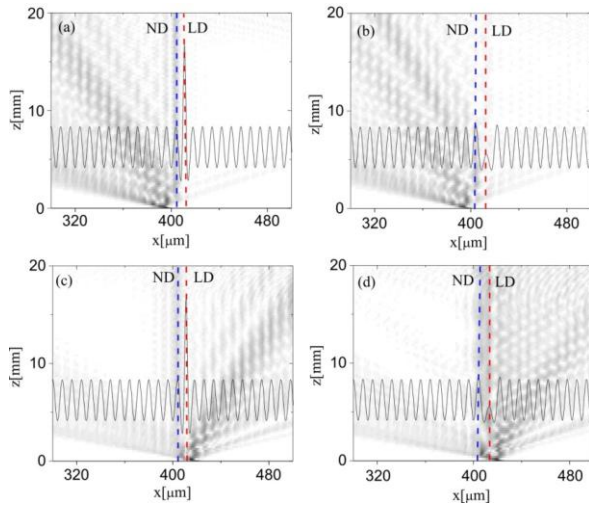


Fig.4 2D plot of the average beam intensity profiles, LD is located at the 1st wg on the right of the ND, $\alpha=2\pi/30$: (a) incident beam enters the 1st wg on the left of the ND, $\Gamma=1.3$, width of LD is 2 μm ; (b) width of LD is 6 μm , $\Gamma=1.3$; (c) incident beam enters the 1st wg on the right of the LD, $\Gamma=10$, width of LD is 2 μm ; (d) width of LD is 6 μm , $\Gamma=10$. Vertical blue dashed line denotes the ND, while vertical red line shows LD.

For nonlinearity strength $\Gamma=10$ and the same low values of the kick when the beam is launched towards the narrow LD, weak capturing at the position of the LD has been obtained, Figure 4c. Greater width of LD

contributes to more efficient trapping of the beam at the LD, Figure 4d. Partial reflection is visible here as well. The higher value of the transverse kick leads to the decrease of the reflection and mild capturing of energy at the ND, transmission begins to appear as well. Transmission, in the presence of the kicks that are big enough ($2\pi/6$ to $2\pi/12$), becomes the only effect which appears for the given values of the parameters. When defects are more distant and with beam launched in the cavity that's placed between ND and LD, incidence angle of the beam affects its capturing and its zig-zag modes. Cavity is the formed area between ND and LD, when they are separated by at least one WG. If the beam is launched outside the cavity, light reflection becomes dominant process.

The increase of the distance between the defects leads to the cavity formation in which the localization of energy can appear. This is illustrated in Figures 5a, b, c where the LD is located at the second WG on right of the ND. Trapping of the light is observed when the light is launched into the ND, Fig. 5a. When the beam is launched in the wg between the two defects, i. e. in the cavity, it becomes captured in it and this is due to potential barriers which appear as a consequence of defects' presence on the right and left side, it can capture the light efficiently now, Figures 5b, c. By comparing these two figures it can be concluded that the width of the LD has no impact on the efficiency of capturing the light in the cavity. Efficiency of capturing means the ratio between the amplitude of the light, captured within the region between the defects or at the positions of the defects, and amplitude of the input light beam. Since the effects of only linear and only ND on the beam propagation through the lattice have already been investigated (Kuzmanović et al. 2015a), by comparing those results with ones obtained here, it can be seen that capturing of the light in the LD located at the second WG from nonlinear one is equivalent to the one obtained when only LD has been investigated, Figure 5d, e. The light of capturing in the LD has been observed for narrow and wide LD, when the light beam has been launched into the LD. ND has a small influence on the formation of localized mode.

For greater distances between the ND and LD, it is possible to obtain multicomponent breathing modes in the cavity. In Figure 6, two-component breathing modes and the influence of the closeness of either of the two defects on these modes have been shown. There are no significant qualitative nor quantitative differences on the light beam propagation whether the light beam is launched near the narrow LD or near the wide LD within the cavity, Figures 6a and

6c. In both cases, two-component breathing mode is formed in the cavity between the defects. However, if we replace the narrow LD with the wide one, the two cases will be slightly different, Figures 6b and 6d. In this case, the breathing-mode component closer to the wide LD (the beam is launched in the cavity, in the WG adjacent to the LD) will be more pronounced than the one adjacent to the ND.

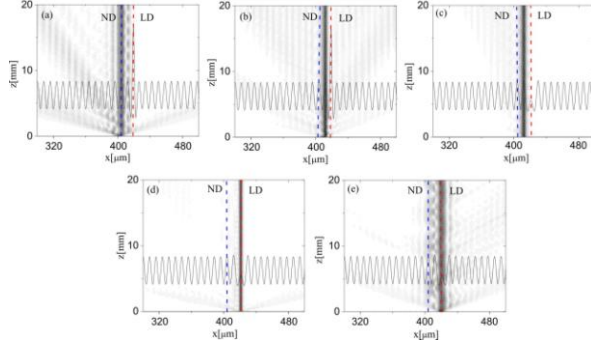


Fig. 5. 2D plot of the average beam intensity profiles, LD is located at the 2nd wg on the right of the ND: (a) $\Gamma=1.3$, incident beam enters the ND, width of LD is 2 μm ; (b) $\Gamma=10$, incident beam enters the 1st on the right of the ND, width of LD is 2 μm (c) $\Gamma=10$, incident beam enters the 1st on the right of the ND, width of LD is 6 μm , (d) $\Gamma=10$, incident beam enters the LD 2 μm wide; (e) $\Gamma=10$, incident beam enters the LD 6 μm wide. Vertical blue dashed line denotes the ND, while vertical red line shows LD.

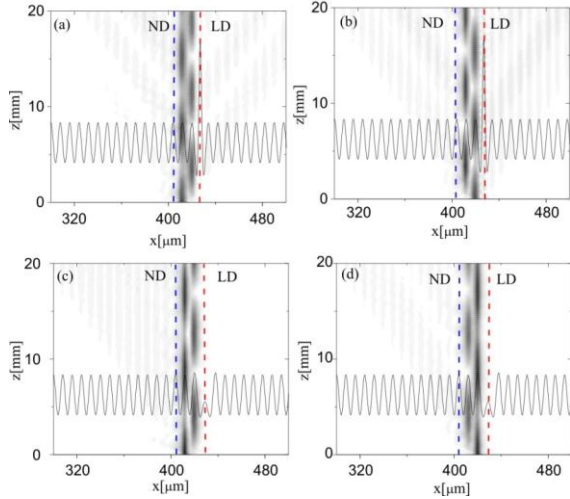


Fig. 6. 2D plot of the average beam intensity profiles, $\Gamma=10$, LD is located at the 3rd wg on the right of the ND: (a) incident beam enters the 1st wg on the right of the ND, width of LD is 2 μm ; (b) incident beam enters the 2nd wg on the right of the ND, width of LD is 2 μm ; (c) incident beam enters the 1st wg on the right of the ND, width of LD is 6 μm ; (d) incident beam enters the 2nd wg on the right of the ND, width of LD is 6 μm . Vertical blue dashed line denotes the ND, while vertical red line shows LD.

In the area between the ND and narrow LD, if the light is launched in the middle of the cavity it is possible to obtain symmetric – like structures because at the first sight they look symmetric but further analysis shows that they not, Figures 7, a, b. For smaller distances between the defects (three WGs or 28 μm) (Figure 7a), there is a dominant central mode whereas for greater distances, this central mode is no longer dominant (Figure 7b, d). Central mode is the one located at the center of the distance between the LD and ND. In the case of the LD 6 μm wide, it is not possible to obtain symmetrical structures irrespective of the distance between defects, Figure 7e. This means that the potential of the wide LD cannot balance the potential of ND, thus enabling the formation of symmetrical structure. It is possible to obtain zig-zag modes as well, when the beam is launched at the WG near the one or the other defect, Figure 7c.

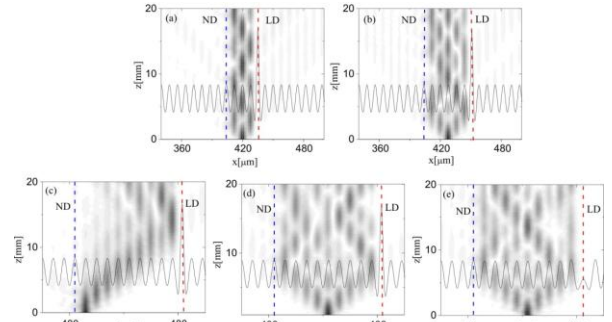


Fig. 7. 2D plot of the average beam intensity profiles, $\Gamma=10$, width of LD is 2 μm : (a) incident beam enters the 2nd wg, LD is located at the 4th wg; (b) incident beam enters the 3rd wg, LD is located at the 6th wg; (c) incident beam enters the 1st wg, LD is located at the 10th wg; (d) incident beam enters the 5th wg, LD is located at the 10th wg; (e) incident beam enters the 5th wg, LD 6 μm wide is located at the 10th wg on the right of the ND. Vertical blue dashed line denotes the ND, while vertical red line shows LD.

5. CONCLUSION

The influence of ND and LD on the light beam propagation through 1D PL is investigated numerically. LD represents a WG which is narrower or wider than the rest of the WGs in the array. For narrow LD, when the beam is launched without the transverse kick, the total localization of the light on either of the defects has been observed. The narrow LD is more efficient in the localization of the light at the ND when they are located next to each other. On the other hand, the significant influence of ND on the beam

propagation in this system is not observed. The localization of the light is stronger at the narrow LD and for smaller nonlinearity strength. The influence of ND and LD on the light propagation in the area between them has also been investigated. Changing the initial parameters such as the initial position of the light beam, incident angle, strength of ND and the width of LD, different regimes of light propagation have been identified: localized modes, symmetrical breathing structures and symmetric – like zig-zag modes. The results presented here can be useful for all-optical control of the wave transmission in interferometry.

REFERENCES

- Beličev, P., Ilić, I., Stepić, M., Maluckov, A., Tan, Y., & Chen, F. 2010. Observation of linear and nonlinear strongly localized modes at phase-slip defects in one-dimensional photonic lattices. *Opt. Letters*, 35, pp. 3099-3101.
- Chen, F., Stepić, M., Rüter, C., Runde, D., Kip, D., Shandarov, V., . . . Segev, M. 2005. Discrete diffraction and spatial gap solitons in photovoltaic LiNbO₃ waveguide arrays. *Opt Express*, 13(11), pp. 4314-24. pmid:19495346. doi:10.1364/OPEX.13.004314.
- Christodoulides, D.N., & Joseph, R.I. 1988. Discrete self-focusing in nonlinear arrays of coupled waveguides. *Opt. Letters*, 13, pp. 794-796.
- Denz, C., Flach, S., & Kivshar, Y.S. 2010. Nonlinearities in periodic structures and metamaterials. Springer Series In Optical Sciences, Springer-Verlag Berlin Heidelberg, 150.
- Fedele, F., Yang, J.K., & Chen, Z.G. 2005. Defect modes in one-dimensional photonic lattices. *Opt. Letters*, 30, pp. 1506-1508.
- Kuzmanović, S., Stojanović-Krasić M., Milović, D., Radosavljević, A., Gligorić, G., Maluckov, A., & Stepić, M. 2015. Defect induced wave-packet dynamics in linear one-dimensional photonic lattices. *Phys. Scripta*, 90, p. 25505.
- Kuzmanović, S., Stojanović-Krasić, M., Milović, D., Miletić, M., Radosavljević, A., Gligorić, G., . . . Stepić, M. 2015. Light propagation inside 'cavity' formed between nonlinear defect and interface of two dissimilar one-dimensional linear photonic lattices. *Eur. Phys. J. D*, 69, p. 207.
- Lahini, Y., Avidan, A., Pozzi, F., Sorel, M., Morandotti, R., Christodoulides, D.N., & Silberberg, Y. 2008. Anderson localization and nonlinearity in one-dimensional disordered photonic lattices. *Phys. Rev. Letters*, 100, p. 13906.
- Meier, J., Stegeman, I.G., Christodoulides, D.N., Silberberg, Y., Morandotti, R., Yang, H., . . . Aitchison, J.S. 2005. Beam interactions with a blocker soliton in one-dimensional arrays. *Opt. Letters*, 30, pp. 1027-1029.
- Miroshnichenko, A.E., Flach, S., & Kivshar, S.(. 2010. Fano resonances in nanoscale structure,. *Rev. Mod. Phys.*, 82, pp. 2257-2298.
- Morandotti, R., Eisenberg, H.S., Mandelik, D., Silberberg, Y., Modotto, D., Sorel, D., . . . Aitchison, J.S. 2003. Interactions of discrete solitons with structural defects. *Opt. Letters*, 28, pp. 834-836.
- Molina, M., & Kivshar, S.(. 2008. Nonlinear localized modes at phase-slip defects in waveguide arrays. *Opt. Letters*, 33, pp. 917-919.
- Noda, S., Fujita, M., & Asano, T. 2007. Spontaneous-emission control by photonic crystals and nanocavities. *Nature Photonics*, 1(8), pp. 449-458. doi:10.1038/nphoton.2007.141
- Naether, U., Rivas, D.E., Larenas, M.A., Molina, M.I., & Vicencio, R.A. 2009. Fano resonances in waveguide arrays with saturable nonlinearity. *Opt. Letters*, 34(2721).
- Radosavljević, A., Gligorić, G., Maluckov, A., & Stepić, M. 2014. Control of light propagation in one-dimensional quasi-periodic nonlinear photonic lattices. *J. Optics*, 16(025201).
- Schwartz, T., Bartal, G., Fishman, S., & Segev, M. 2007. Transport and Anderson localization in disordered two-dimensional photonic lattices. *Nature*, 446(7131), pp. 52-5. pmid:17330037. doi:10.1038/nature05623.
- Smirnov, E., Stepić, M., Rüter, C.E., Kip, D., & Shandarov, V. 2006. Observation of staggered surface solitary waves in one-dimensional waveguide arrays. *Opt. Letters*, 31, pp. 2338-2340.
- Stojanović-Krasić, M., Mančić, A., Kuzmanović, S., Veljković-Đorić, S., & Stepić, M. 2016. Linear and interface defects in composite linear photonic lattice. submitted to *Optics Communications*.
- Tran, P. 1997. Optical limiting and switching of short pulses by use of a nonlinear photonic bandgap structure with a defect. *J. Opt. Soc. Am. B*, 14, pp. 2589-2595.

* E-mail: slavica.kuzmanović@pr.ac.rs

CALCULATION OF THE FREQUENCY RESPONSE AND BANDWIDTH IN LOW NUMERICAL APERTURE STEP-INDEX PLASTIC OPTICAL FIBER USING TIME-DEPENDENT POWER FLOW EQUATION

Branko Drljača^{1*}, Slavica Jovanović¹, Svetislav Savović²

¹Faculty of Natural Sciences, University of Priština, Kosovska Mitrovica, Serbia.

²Faculty of Science, University of Kragujevac, Kragujevac, Serbia.

ABSTRACT

Time-dependent power flow equation is employed to calculate frequency response and bandwidth of low numerical aperture step-index optical fiber excited with Gaussian-like light source with large width. Both, frequency response and

bandwidth, are specified as function of the fiber length measured from the input end of the fiber. Analytical and numerical solutions are compared and good agreement between results is obtained.

Key words: Plastic optical fiber, Frequency response, Bandwidth.

1. INTRODUCTION

In recent decades there has been significant growth in the amount of transferred data both in long-distance and short-distance communication. For high-performance short-distance communication, such as local-area networks (LANs), multi-node bus networks plastic or digital car networks, industrial control, plastic optical fibers (POFs) are often considered as best choice ((Golowich et al., 2003), (Ishigure et al., 2000), (Green, 1996), (Koeppen et al., 1998)). This is based upon their low cost, ease of manipulation and high bandwidth.

In comparison to systems based upon glass optical fiber or copper wire, systems based upon POFs are much more affordable in total. With a fiber diameter of 1 millimeter, and a core diameter of 980 μm (for most applications) cutting and treating of POF's ends is done without much effort. Nonetheless large core diameter allows POFs to be paired with light sources of higher NA, such as LED sources, using low-precision plastic couplers. This, in total, results in inexpensive but robust systems that are easy to interconnect. Bandwidth of typical step-index optical fiber (SI POF) is higher than with copper wire systems and approximately is 100 MHz over 100 m (Koike, 2015). Bit rates of about 200 Mbit/s over 50 m can be obtained without any additional measures, and bit rates of over 1000 Mbit/s over 50 m have been realized with special transmission schemes (equalizing, OFDM) over the last years.

From the previous statements it is clear that transmission properties of SI POF, such as bandwidth and frequency response, have most significant role in their further development. Frequency response and consequently bandwidth of multimode SI POFs depend strongly on the mode-dependent attenuation, modal dispersion and the rate of mode coupling (power transfer from lower to higher order modes). In order to examine influence of the width of launch beam to frequency response and bandwidth we calculated it for tested SI POF and compared with available results for the same fiber (Savovic et al., 2014a).

This paper is organized as follows. In chapter 2 mathematical model based upon time-dependent power flow equation, developed by Gloge (Gloge, 1973), is presented. Using the time-dependent power flow equation we have determined frequency response and bandwidth of SI POF with low numerical aperture in addition to mode coupling and mode-dependent attenuation. Comparison of results obtained by analytical and numerical solution is presented in chapter 3. Finally conclusion is presented in chapter 4.

2. TIME-DEPENDENT POWER FLOW EQUATION

2.1. Analytical solution

Gloge's time-dependent power flow equation can be written as (Gloge, 1973):

$$\frac{\partial P(\theta, z, t)}{\partial z} + \frac{\partial t}{\partial z} \frac{\partial P(\theta, z, t)}{\partial t} = -\alpha(\theta)P(\theta, z, t) + \frac{1}{\theta} \frac{\partial}{\partial \theta} \left[\theta D(\theta) \frac{\partial P(\theta, z, t)}{\partial \theta} \right] \quad (1)$$

where $P(\theta, z, t)$ is power distribution over angle θ measured with respect to fiber axis, space z and time t ; $\alpha(\theta)$ is mode-dependent attenuation; $\partial t/\partial z$ is mode delay per unit length; and $D(\theta)$ is the mode-dependent coupling coefficient. Mode-dependent attenuation can be written in the form $\alpha(\theta) = \alpha_0 + A\theta^2 + \dots$. Term α_0 represents loss common to all modes and it can be accounted for by multiplying the end-solution by $e^{-\alpha_0 z}$ (Gloge, 1973). More important is the term $A\theta^2$ which describes the losses at core-cladding boundary and for that reason, in solving (1), one needs to consider only the term $A\theta^2$ as the most dominant of the higher order modes (Gloge, 1972). Coupling coefficient $D(\theta)$ is, as it is stated, also mode-dependent (Olshansky, 1975), but mode-independent coupling constant D has been used frequently by other authors ((Gloge, 1973), (Drljaca et al., 2009), (Drljaca et al., 2012)). If coupling constant D is used equation (1) can be written as (Gloge, 1973):

$$\frac{\partial P(\theta, z, t)}{\partial z} = -A\theta^2 P(\theta, z, t) - \frac{n}{2c} \theta^2 \frac{\partial P(\theta, z, t)}{\partial t} + \frac{D}{\theta} \frac{\partial}{\partial \theta} \left(\theta \frac{\partial P(\theta, z, t)}{\partial \theta} \right). \quad (2)$$

In order to solve time-dependent equation (2) analytically it is transformed into time-independent equation (Gloge, 1973):

$$\frac{\partial p}{\partial z} = -A\theta^2 p + \frac{D}{\theta} \frac{\partial}{\partial \theta} \left(\theta \frac{\partial p}{\partial \theta} \right). \quad (3)$$

Using time-independent power flow equation (3) analytical solution for impulse response can be obtained (Gloge, 1973). For short fibres ($z < 1/(2(AD)^{1/2})$), impulse response is:

$$Q(z, t) = \frac{2c\pi}{nz(1 + \gamma_\infty z)} \exp(-2ct/n\Theta_0^2 z), \quad (4)$$

while in case of long fibers ($(z \gg 1/(2(AD)^{1/2}))$), it has the form:

$$Q(z, t) = \Theta_0^2 \sqrt{\frac{\pi}{Tt}} \left(\frac{t}{\gamma_\infty z T} + \frac{1}{2} \right)^{-1} \exp \left(-\frac{\gamma_\infty^2 z^2 T}{4t} - \frac{t}{T} \right). \quad (5)$$

After obtaining impulse response, frequency response can be obtained easily by applying Fourier transform to the impulse response:

$$H(f) = \int_{-\infty}^{\infty} Q(t) \exp(2\pi i f t) dt. \quad (6)$$

After obtaining frequency response, -3dB bandwidth, for different lengths, is easily obtained by selecting frequencies for which frequency response has 50% drop for given length.

2.2. Numerical solution

In order to solve time-dependent power flow equation numerically we start from equation (1). In the same manner, as with analytical solution, for mode-dependent attenuation term $A\theta^2$ is used and coupling coefficient is once more assumed to be constant – D . If so, equation (1) can be written as (2). After applying the Fourier transform to (2):

$$p(\theta, z, \omega) = \int_{-\infty}^{\infty} P(\theta, z, t) e^{-j\omega t} dt \quad (7)$$

the time-dependent equation (2) transforms into (8):

$$\frac{\partial p(\theta, z, \omega)}{\partial z} = - \left[A\theta^2 + j\omega \frac{n}{2c} \theta^2 \right] p(\theta, z, \omega) + \frac{D}{\theta} \frac{\partial p(\theta, z, \omega)}{\partial \theta} + D \left(\theta \frac{\partial^2 p(\theta, z, \omega)}{\partial \theta^2} \right) \quad (8)$$

where $\omega = 2\pi f$ is the angular frequency.

The boundary conditions are:

$$p(\theta_c, z, \omega) = 0, \quad D \frac{\partial p(\theta, z, \omega)}{\partial \theta} \bigg|_{\theta=0} = 0, \quad (9)$$

where θ_c is the critical angle. The first condition implies that modes with infinitely large loss do not transfer any power; the second condition implies that mode coupling is limited to modes travelling with the angle $\theta > 0$.

Since $p(\theta, z, \omega)$ is complex we can therefore separate $p(\theta, z, \omega)$ into its real and imaginary parts, $p = p^r + jp^i$. Equation (8) can now be rewritten as the following system of simultaneous differential equations:

$$\frac{\partial p^r}{\partial z} = -A\theta^2 p^r + \frac{D}{\theta} \frac{\partial p^r}{\partial \theta} + D \frac{\partial^2 p^r}{\partial \theta^2} + \omega \frac{n}{2c} \theta^2 p^i \quad (10)$$

$$\frac{\partial p^i}{\partial z} = -A\theta^2 p^i + \frac{D}{\theta} \frac{\partial p^i}{\partial \theta} + D \frac{\partial^2 p^i}{\partial \theta^2} - \omega \frac{n}{2c} \theta^2 p^r$$

After obtaining p^r and p^i by solving equations (10), frequency response at distance z from input end of the fiber is calculated as:

$$H(z, \omega) = \frac{2\pi \int_{\theta_c}^{\theta_c} [p^r(\theta, z, \omega) + jp^i(\theta, z, \omega)] d\theta}{2\pi \int_{\theta_c}^{\theta_c} \theta [p^r(\theta, 0, \omega) + jp^i(\theta, 0, \omega)] d\theta} \quad (11)$$

After separating the power flow equation (8) into two simultaneous equations (10), we solved the latter (10) by explicit finite difference method (EFDM). Using central difference scheme for derivatives $\partial p(\theta, z, \omega) / \partial \theta$ and $\partial^2 p(\theta, z, \omega) / \partial \theta^2$ (Savovic et al. 2004), (Djordjevic et al. 2000), (Anderson 1995):

$$\left(\frac{\partial p(\theta, z, \omega)}{\partial \theta} \right)_{k,l} = \frac{p_{k+1,l} - p_{k-1,l}}{2\Delta\theta} + O(\Delta\theta)^2 \quad (12)$$

$$\left(\frac{\partial^2 p(\theta, z, \omega)}{\partial \theta^2} \right)_{k,l} = \frac{p_{k+1,l} - 2p_{k,l} + p_{k-1,l}}{(\Delta\theta)^2} + O(\Delta\theta)^2$$

and using the forward difference scheme for the derivative $\partial p(\theta, z, \omega) / \partial z$:

$$\left(\frac{\partial p(\theta, z, \omega)}{\partial z} \right)_{k,l} = \frac{p_{k,l+1} - p_{k,l}}{\Delta z} + O(\Delta z) \quad (13)$$

equations (10) can be written in the form:

$$p_{k,l+1}^r = \left(\frac{\Delta z D}{\Delta \theta^2} - \frac{\Delta z D}{2\theta_k \Delta \theta} \right) p_{k-1,l}^r + \left(1 - \frac{2\Delta z D}{\Delta \theta^2} - \Delta z A \theta_k^2 \right) p_{k,l}^r + \left(\frac{\Delta z D}{2\theta_k \Delta \theta} + \frac{\Delta z D}{\Delta \theta^2} \right) p_{k+1,l}^r + \frac{\omega n \Delta z}{2c} \theta_k^2 p_{k,l}^i \quad (14)$$

and

$$p_{k,l+1}^i = \left(\frac{\Delta z D}{\Delta \theta^2} - \frac{\Delta z D}{2\theta_k \Delta \theta} \right) p_{k-1,l}^i + \left(1 - \frac{2\Delta z D}{\Delta \theta^2} - \Delta z A \theta_k^2 \right) p_{k,l}^i +$$

$$+ \left(\frac{\Delta z D}{2\theta_k \Delta \theta} + \frac{\Delta z D}{\Delta \theta^2} \right) p_{k+1,l}^i - \frac{\omega n \Delta z}{2c} \theta_k^2 p_{k,l}^r. \quad (15)$$

Boundary conditions (9) now become:

$$p_{N,l}^r = 0, \quad p_{N,l}^i = 0 \quad \text{and} \quad (16)$$

$$p_{0,l}^r = p_{1,l}^r, \quad p_{0,l}^i = p_{1,l}^i$$

where $N = \theta_c / \Delta\theta$ is the grid size in the θ direction. In order to prevent the problem of singularity at grid points $\theta = 0$, the following relation is used (Anderson 1995):

$$\lim_{\theta \rightarrow 0} \frac{1}{\theta} \frac{\partial}{\partial \theta} \left(\theta \frac{\partial p}{\partial \theta} \right) = 2 \frac{\partial^2 p}{\partial \theta^2} \Big|_{\theta=0} \quad (17)$$

In our previous work (Savovic et al. 2014a), we have determined frequency response and bandwidth of the low numerical aperture (NA=0.3) SI POF for a Dirac impulse in time and a laser mode distribution with the $\theta_0 = 0^\circ$ (central launch) and FWHM = 7.5° in the parallel plane. In this work, using Gloge's analytical solution of (2) and our numerical results for (2) we calculate the frequency response and bandwidth of same SI POFs for a Dirac impulse in time and a laser mode distribution with the $\theta_0 = 0^\circ$ and FWHM = 16° in the parallel plane and compare obtained analytical to numerical results.

3. ANALYTICAL AND NUMERICAL RESULTS

In this section we present results for frequency response and bandwidth of the tested MH4001 ESKA Mitsubishi Rayon fiber (MH fiber). The fiber's dimensions are typical for this kind of fiber. Core and clad diameters are $d_{core} = 980 \mu\text{m}$ and $d_{clad} = 1000 \mu\text{m}$, respectively. Numerical aperture is NA=0.3, core refractive index is $n=1.49$, and critical angle is $\theta_c = 11.7^\circ$ (measured inside the fiber) or $\theta_c = 17.6^\circ$ (measured in air). The number of modes in this step-index multimode plastic optical fiber at $\lambda = 660 \text{ nm}$ is $N = 2\pi^2 a^2 (\text{NA})^2 / \lambda^2 \approx 1.02 \times 10^6$, where a is radius of the fiber core. This large number of modes may be represented by a continuum as required for application of equation (2).

In recently published works (Savovic et al. 2014a), (Savovic et al. 2014b), coupling coefficient D and loss coefficient $\alpha(\theta)$ ($\alpha(\theta) \approx \alpha_0 + A\theta^2$) for this fiber were calculated as $D = 1.62 \times 10^{-3} \text{ rad}^2/\text{m}$ and $\alpha_0 = 0.10793$

1/m and $A=0.29166 \text{ (rad}^2 \text{ m)}^{-1}$. The lengths of the MH4001 fiber that we used in our calculations were 3 m, 5 m, 10 m, 15 m, 25 m, 50 m and 100 m. A Dirac impulse in time and mode distribution with the $\theta_0 = 0^\circ$ (central launch) and FWHM=16° in the parallel plane were used for the input. Analytical and numerical results for the frequency response for different fiber lengths of the MH fiber are shown in Figure 1. Analytical and numerical results match well. A pronounced drop at low frequencies is apparent for long fiber lengths. Fig. 2 shows analytically and numerically obtained bandwidth for MH4001 fiber. Bandwidth is shown in log-log scale versus length of the fiber. Slightly lower values of bandwidth are observed than in the case of the narrower beam with FWHM=7.5° previously investigated by (Savovic et al. 2014a). This is more pronounced for shorter fiber lengths and it is due to the excitation of higher order modes when fiber is excited with wider input light beam. Higher modes experience higher loss since at shorter fiber lengths dominant process is mode-dependent attenuation. With increasing fiber length mode coupling begins to significantly influence fibers frequency response and bandwidth. In that case influence of the width of the launched beam on the fiber bandwidth becomes negligible since process of mode coupling at those lengths is either finished or came near end.

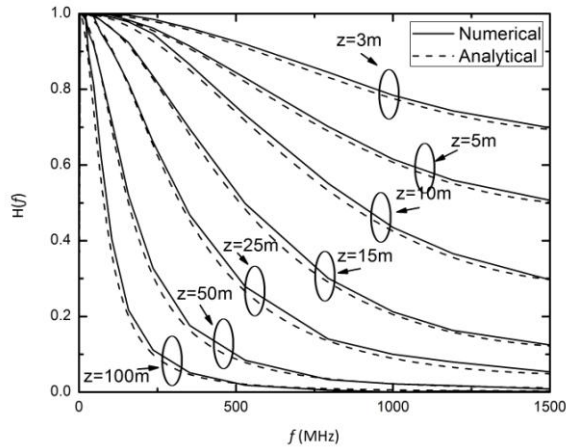


Fig. 1 Analytical (dashed line) and numerical (solid line) results for the frequency response for MH fiber, for different fiber lengths.

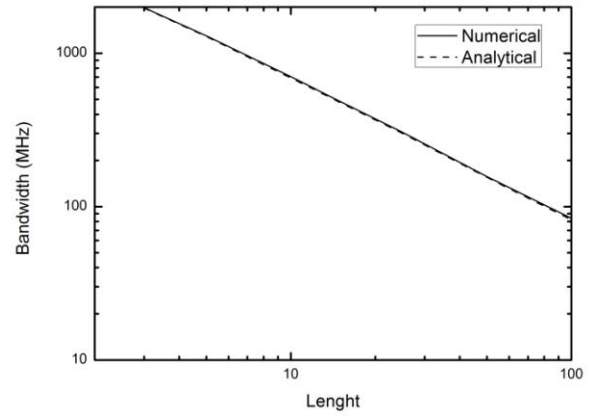


Fig. 2 Analytical (dashed line) and numerical (solid line) results for the bandwidth for MH fiber, for different fiber lengths.

4. CONCLUSION

Analytical and numerical solution of time-dependent power flow equation were employed to calculate frequency response and bandwidth of MH4001 step-index optical fiber. Obtained results show good match. Moreover if our results are compared to previously obtained results for the same fiber, but different input conditions (narrower width of input light beam) (Savovic et al., 2014a), expected results are obtained. Namely, frequency response (and consequently bandwidth) obtained for the input light beam with FWHM=16° (this paper) show slightly lower values than in the case of the narrower beam with FWHM=7.5° previously investigated by (Savovic et al. 2014a). This is more pronounced for shorter fiber lengths where mode-dependent attenuation is dominant process. With increasing fiber length mode coupling begins to significantly influence fibers transfer characteristics, that is frequency response and bandwidth. Namely, influence of the width of the launched beam on the fiber's frequency response and bandwidth, is more pronounced at shorter fiber lengths (Savovic et al., 2010), leading to lower values of frequency response and bandwidth and becomes negligible at longer fiber lengths.

ACKNOWLEDGMENT

The work described in this paper was supported by a grant from Serbian Ministry of Science and Technological Development (project no. 171011).

REFERENCES

- Anderson, J.D. 1995. Computational Fluid Dynamics. New York, USA: McGraw-Hill.
- Djordjević, A., & Savović, S. 2000. Investigation of mode coupling in step index plastic optical fibers using the power flow equation. *IEEE Photon. Technol. Lett.*, 12, pp. 1489-1491.
- Drljača, B., Savović, S., & Djordjević, A. 2009. Calculation of the Impulse Response of Step-Index Plastic Optical Fibers Using the Time-Dependent Power Flow Equation. *Acta Phys. Pol. A*, 116, pp. 658-660.
- Drljača, B., Djordjević, A., & Savović, S. 2012. Frequency response in step-index plastic optical fibers obtained by numerical solution of the time-dependent power flow equation. *Optics and Laser Technology*, 44(6), pp. 1808-1812.
- Gloge, D. 1973. Impulse Response of Clad Optical Multimode Fibers. *Bell Syst. Tech. J.*, 52, pp. 801-816.
- Gloge, D. 1972. Optical power flow in multimode fibers. *Bell Syst. Tech. J.*, 51, pp. 1767-1783.
- Golowich, S.E., White, W., Reed, W.A., & Knudsen, E. 2003. Quantitative estimates of mode coupling and differential modal attenuation in perfluorinated graded-index plastic optical fiber. *Journal of Lightwave Technology*, 21(1), pp. 111-121. doi:10.1109/JLT.2003.808668.
- Green, P.E. 1996. Optical networking update. *IEEE Journal on Selected Areas in Communications*, 14(5), pp. 764-779. doi:10.1109/49.510902.
- Ishigure, T., Kano, M., & Koike, Y. 2000. *J. Lightwave Technol.*, 18, pp. 959-965.
- Koeppen, C., Shi, R.F., Chen, W.D., & Garito, A.F. 1998. *J. Opt. Soc. Am. B*, 15, pp. 727-739.
- Koike, Y. 2015. *Fundamentals of Plastic Optical Fibers*. Weinheim, Germany: Wiley-VCH.
- Olshansky, R. 1975. Mode Coupling Effects in Graded-index Optical Fibers. *Appl Opt*, 14(4), pp. 935-45. pmid:20135002.
- Savović, S., & Djordjević, A. 2004. Influence of numerical aperture on mode coupling in step-index plastic optical fibers. *Appl Opt*, 43(29), pp. 5542-6. pmid:15508612.
- Savović, S., Djordjević, A., Tse, P.W., Zubia, J., Mateo, J., & Losada, M.A. 2010. Determination of the width of the output angular power distribution in step index multimode optical fibers. *J. Opt.*, 12(115405), p. 5.
- Savović, S., Drljača, B., Kovačević, M.S., Djordjević, A., Bajić, J.S., Stupar, D.Z., & Stepniak, G. 2014. Frequency response and bandwidth in low-numerical-aperture step-index plastic optical fibers. *Appl Opt*, 53(30), pp. 6999-7003. pmid:25402786.
- Savović, S., Kovačević, M.S., Djordjević, A., Bajić, J.S., Stupar, D.Z., & Stepniak, G. 2014. Mode coupling in low NA plastic optical fibers. *Opt. Laser Technol*, 60, pp. 85-89.

* E-mail: branko.drljaca@pr.ac.rs

CIP - Каталогизација у публикацији
Народна библиотека Србије, Београд

5

The UNIVERSITY thought. Publication in natural sciences / editor in chief Nebojša Živić. - Vol. 3, no. 1 (1996)- . - Kosovska Mitrovica : University of Priština, 1996- (Kosovska Mitrovica : Art studio KM). - 29 cm

Polugodišnje. - Prekid u izlaženju od 1999-2015. god. - Je наставак: Универзитетска мисао. Природне науке = ISSN 0354-3951
ISSN 1450-7226 = The University thought. Publication in natural sciences
COBISS.SR-ID 138095623

Available Online

This journal is available online. Please visit <http://www.utnsjournal.pr.ac.rs> to search and download published articles.